INTRINSIC CONNECTIVITY OF IDENTIFIED PROJECTION NEURONS IN CAT VISUAL CORTEX BRAIN SLICES

Thesis by

Lawrence Charles Katz

In Partial Fulfillment of the Requirements

for the Degree of

Doctor of Philosophy

California Institute of Technology

Pasadena, California

1984

(Submitted April 27, 1984)

"Nel mezzo del cammin di nostra vita
mi ritrovai per una selva oscura,
che la diratta era smarrita."

("Midway in the journey of our life
I found myself in a deep forest,
for the right way had been lost.")

Dante Alighieri, The Divine Comedy

"...the full-grown forest turns out to be impenetrable and indefinable..."

S. Ramon y Cajal, Recollections of My Life

ACKNOWLEDGEMENTS

Overall, my years at Caltech have been extraordinarily exciting, challenging and rewarding. For this, I wish to extend my deepest thanks to my thesis advisor, Mark Konishi. His office door, and his mind, were always open to discussions, and he has generously supplied a rare commodity: the freedom to explore new areas. And, at the times when I needed it most, he simply said, "It will work," and I believed him.

I also wish to thank David Van Essen, who consistently provided thoughtful, critical input into much of my work here, and encouraged me to think things through more carefully.

My collaboration with Mark Gurney profoundly influenced the course of my subsequent research. A subsequent collaboration with Andreas Burkhalter was enlightening and enjoyable, and I thank Andreas for his role both as a collaborator, and a great friend.

Rich Lewis has been the most extraordinary of friends, a fellow traveller though the complexities of graduate school, and a deeply thoughtful, insightful colleague.

I wish to thank Carol Newsom, a very special kind of friend, for introducing me to entirely new worlds and perspectives outside the realm of the sciences, and for her overall support.

I have been helped on numerous occasions by Andy Moiseff to deal with computers, by Dan Felleman to deal with cats (at some very crucial stages), by Jeanne Nerbonne to deal with the world, and by Daniela Bonafede. I thank them all. Takuji Kasamatsu provided animals, equipment, and advice.

Herb Adams brought his consummate skill to the design and fabrication of critical pieces of equipment. For immeasurable assistance over the years I thank

Nancy Gill and Kathy O'Loughlin. Candace Hochenedel has been similarly helpful, and I wish to thank her and Caren Oto for typing this manuscript. Bill Lease has both my admiration and gratitude (and no questions asked) for his ability to locate and procure almost anything.

I thank my many sources of financial support during my graduate education, including an NSF Pre-Doctoral Fellowship, an NIH training grant fellowship (#5 T32 GM07737-05), and grants from the Caltech President's Venture Fund, the NIH Biomedical Research Support Grant Program (#RR07003) and the Weigle Memorial Fund (for thesis preparation).

Finally, there are two people whom I can never adequately thank--my parents, Margot and Leonard Katz. Their strong belief that the pursuit of knowledge, in all areas of human endeavor, is an important contribution of the individual to society, has always been my most constant and basic support.

ABSTRACT

The mammalian primary visual cortex is a structure of remarkable physiological and morphological heterogeneity. Despite quite intensive efforts, using a variety of approaches, the relationships between neuronal form and neuronal function have remained obscure. Most previous attempts proceeded on the assumption that a cell's physiological responses to particular stimuli were the best indication of its function. In this study a different assumption was made: that since different efferent targets of area 17 neurons were presumably engaged in different sorts of neural processing, area 17 cells that project to those targets should be engaged in different intrinsic circuits. This in turn might be reflected in distinctive patterns of intrinsic axons and dendrites. This hypothesis was tested by comparing the morphology of two groups of neurons within layer VI of cat area 17: those that project to the claustrum and those that project to the lateral geniculate nucleus. Since both projections occupy the same laminar position, and therefore have potential access to the same environmental and lamina-specific influences, this projection was an excellent system to examine the role of different efferent projections in defining neuronal form, not confounded by differences in laminar position.

This study was carried out by retrogradely labeling, in vivo, one or the other of the projections with a newly developed fluorescent tracer, latex microspheres. Subsequently, in vitro brain slices were prepared from area 17, and the retrogradely labeled neurons were visualized, impaled, and intracellularly stained with a second fluorescent dye, lucifer yellow.

Comparisons of the two efferent projection classes revealed non-overlapping patterns of distributions of intrinsic axons and dendrites between the two groups, and a remarkable degree of homogeneity within each group.

Particularly dramatic was the difference in intrinsic axons: claustrum projecting cells had long, horizontally directed collaterals restricted to layer VI, whereas LGN projecting neurons had few if any collaterals within layer VI, possessing instead thick, ascending collaterals which arborized in layer IV. Additionally, claustrum projecting cells had significantly fewer, yet more extensive, basal dendritic arms than LGN projecting cells. The apical dendrites of the two groups arborized within different overlying laminae, suggesting that the two classes receive different inputs. These differences in axons and dendrites demonstrate that the two cell classes participate in different intrinsic circuits within area 17.

In addition to the two efferent projection classes, a considerable number of pyramidal cells lacking an efferent axon were observed. They resembled either one or the other of the projection classes, and may represent a substantial population of neurons that, during development, were unable to maintain an efferent projection.

These results suggest that, independent of laminar differences, at least some of the cellular heterogeneity observed in cortex may be attributed to the different informational needs of various efferent targets.

TABLE OF CONTENTS

CHAPTER I

Intrinsic Connectivity of Identified Projection Neurons

INTRODUCTION

The visual systems of the more primitive vertebrates--such as the frog--are highly specialized, via hard-wired neural circuits, to detect a certain limited category of objects (such as a fly) within the organism's visual field (Ewert 1980).

Higher animals have achieved increasingly sophisticated visual abilities not by enlarging the repertoire of hard wired feature detectors, but rather by elaborating a more generalized approach to representing the visual world. Thus mammals, and in particular primates, are capable of an enormous range of visual perceptions and tasks.

Beginning at the level of the retina, the mammalian visual system is organized around a collection of separate, parallel informational pathways, or channels. In higher mammals such as cats and monkeys, these parallel systems contain within them the information necessary for all attributes of form vision, depth perception, color detection, and movement detection. Unlike organisms such as the frog, or even mammals such as the rabbit, in which some such information can be analyzed and extracted at the level of the retina (Barlow et al. 1964, Levick 1967), the extensive processing of retinal signals in the higher mammals begins within the primary visual cortex. It is at this level that information is integrated both within each individual channel, and between channels. The result of this is a remarkable series of transformations of incoming sensory data, as shown by Hubel and Wiesel (1962).

Whereas cells in the retina and lateral geniculate nucleus have a simple concentric "center-surround" organization and respond to spots or annuli of light (Hubel and Wiesel 1961, Kuffler 1953), cells within the cortex respond most vigorously to bars of light oriented in particular directions. In addition, cells within the cortex are excited to varying degrees by stimuli to both eyes, whereas

the inputs from the lateral geniculate are monocular. Cells in cortical layers outside the zone of primary afferent termination tend to have even more selective properties; in addition to requiring stimuli of particular orientation, many cells have strong preferences for stimuli of a particular length, or those moving at a particular velocity (Hubel and Wiesel 1962).

These combined attributes of cortex are striking in that it is difficult, a priori, to predict them. The construction of properties such as orientation selectivity must therefore be reflected in the elaboration of specific patterns of connections between afferent fibers and cortical neurons, and between the neurons within cortex itself.

Cells with similar eye preference and cells with similar orientation preference are grouped together in columns spanning the thickness or cortex (Hubel and Wiesel 1963). Columns are not, however, as their name might imply, uniform structures. Each kind of vertical column (e.g. ocular dominance, orientation) is composed of (in the cat) six laminae, which differ markedly in regards to which channels they receive connections from, or whether they receive direct input at all. The columnar organization provides a vertical framework in which different channels can combine to varying degrees, or remain separate. Such groupings strongly suggest that many of the neuronal interactions underlying the generation of response properties take place within the vertical dimension in restricted regions of primary visual cortex. Primary visual cortex has been modeled as a network of modules, each consisting of two ocular dominance column and a set of orientation columns representing all stimulus orientations (Hubel and Wiesel 1972). Each module receives input from a restricted portion of the visual field and provides specific kinds of output to other cortical and subcortical areas. Modules are presumably connected in an orderly fashion in the horizontal dimension of cortex, allowing formation of a

visual map. This map, however, contains distinctly different information than a strict point-to-point representation of the retina. It is, in several respects, an interpretive map: areas of presumed greater interest, such as the fovea, are expanded at the expense of the periphery, most cells are interested in lines, not points, and in moving, rather than stationary stimuli. The problem of relating the response properties of individual neurons to their structure and connections thus becomes one of understanding the cellular constituents and circuitry of an individual module, their relationship to particular informational channels, and the manner in which modules are linked together to form a coherent representation of the visual world. Understanding the input-output relationships of a module relies on an understanding the input-output characteristics of the neurons that comprise it (Gilbert 1983).

The discovery of the physiological complexity of cortical cells gave a strong rationale for relating the structure of cells to their function. Hubel and Wiesel's physiological work revealed that cells within visual cortex showed three apparently distinct classes of response properties--"simple," "complex," and "hypercomplex" ("hypercomplex" cells are now generally regarded as complex cells with end-stop inhibition) (Hubel and Wiesel, 1962). The occurrence of simple cells primarily in layer IV of cortex, which is composed mostly of stellate cells, and complex cells in the supra- and infragranular layers, which are populated primarily by pyramidal cells, suggested that the morphology and laminar position of cortical neurons might be somehow related to their physiology.

A number of studies directly addressed the question of the relationship between laminar position and receptive field properties (Henry et al. 1979, Gilbert 1977, Leventhal and Hirsh 1978). In general, all these studies found that certain receptive field characteristics were found in greater proportions in some

laminae than in others. For instance, the "special hypercomplex" cell (Palmer and Rosenquist 1974) seems to be located exclusively in layers V and at the III/IV border. Gilbert (1975) and Henry et al. (1979) concluded that the most significant determinant of the receptive field types in a given lamina was the relationship of the lamina to afferent input from the LGN. Thus simple cells, presumably representing the first stage of cortical processing, are found concentrated in layers IV and VI.

A logical extension of this approach were attempts to directly correlate receptive field properties with specific morphological cell classes. Before this was actually done, it seems that there was a strong implicit belief that the various types of receptive field properties would be strongly correlated with the apparent morphological complexity revealed by over 70 years of Golgi studies.

Kelly and Van Essen (1974), using intracellular recording and staining of cortical cells, disproved at least the simplest version of the structure/receptive field hypothesis. Although simple cells tended to be of the stellate morphology, and complex cells tended to be pyramidal, these receptive field properties again seemed more a property of where the cells basal dendrites lay in reference to geniculate input. Using better staining techniques (HRP), and larger samples, Gilbert and Wiesel (1979, 1983) have made this particular relationship clear. However, it is still impossible to explain, on a morphological basis, the structure of a given cell's receptive field.

Especially in early studies, a cells "function" was considered to be primarily reflected in the type of response (e.g. simple, complex, or hypercomplex) that it showed to visual stimulation. The search for correlations of neuronal form and function in visual cortex has been rather narrowly defined in terms of the features of cells that generate a limited set of response properties. Neurons in cortex participate in a variety of circuits, related, not

only to their receptive field type, but also to their laminar position, and their interaction with various afferent channels. Probably the best example of this comes from work on the parallel X, Y, and W pathways (see, for example, Rodiek 1979). These distinct afferent systems terminate at different horizontal levels within area 17; thus the striate recipient cells from the outset have differential access to this input. In cortical layers outside layer IV, cells appear to be dominated by one form of input or another, although some mixing apparently does take place (Malpeli et al. 1981). Other sorts of parallel inputs may likewise be differentially distributed: the association of particular geniculate inputs with the "blobs" of monkey striate cortex may preferentially endow them with the ability to process stimulus color related information (Livingstone and Hubel 1984).

The introduction of retrograde (HRP) and autoradiographic anterograde tracing methods (LaVail 1975, Cowan et al. 1972) has permitted a rather complete description (in the cat) of the areas to which pyramidal cells in area 17 project. Several important "rules" of cortical organization have emerged: 1) although there are exceptions, in most cases a neuron projects to a single efferent target, and 2) neurons that project to the same type of targets occupy specific laminae; layers II and III, for instance, send their output to other cortical areas (e.g. areas 18, 19, STS, see Toyama et al. 1974, Maciewicz 1974, Gilbert and Kelly 1975, Kawamura and Naito 1980) whereas cells in the lower layers (V an VI) send their outputs primarily to subcortical structures (e.g. superior colliculus, pons, lateral geniculate nucleus; see Toyama et al. 1974, Palmer and Rosenquist 1974, Gilbert and Kelly 1975, Magelhaes-Castro et al. 1975, Kawamura and Konno 1979, Albus and Donate-Oliver 1977, Kawamura and Chiba 1979).

The various extrastriate cortical targets are likely to be concerned with specialized features of the visual world, and serve as processing areas for these features (Van Essen 1979). Probably the best studied example of this is the primate area MT, which shows a marked functional specialization for processing movement related parameters of visual stimuli (Zeki 1974, Baker et al. 1981, Maunsell and Van Essen 1983a,b).

The neurons in area 17, therefore, that project to different efferent targets, must be specialized in some manner to extract different sorts of information about the visual world, and send this to a specific efferent target. An implicit assumption is that different efferent targets require different sorts of incoming information. Thus, the various neurons of origin may serve to integrate several different sorts of input in order to generate a more complex output, related to a particular feature, or set of features, of interest in the next stage of cortical processing.

Several investigators have in fact attempted to look for specific features of receptive fields that correlate with a particular efferent projection. The general approach has been to implant electrodes in various target areas (e.g. superior colliculus, LGN) and attempt to antidromically stimulate a cell in area 17 whose receptive field properties have been analyzed. This approach has produced only limited success: these responses of "identified" efferent projection cells have shown no obvious differences in receptive field properties that distinguish them from other neurons in the same lamina, although neurons in different laminae show clear differences (Palmer and Rosenquist 1974, Gilbert 1977, Ferster and Lindström 1983, Singer et al. 1975). However, these studies have a number of limitations: first, it is difficult to obtain large samples, and perhaps more serious, it is very difficult to tell whether a cell which fails to show antidromic stimulation in fact doesn't project to a given area, or simply

cannot be easily antidromically activated. Thus Gilbert (1977) was only able to activate a few cells in layer VI via stimulating electrodes in the LGN, while anatomical work showed that over half the cells in the lamina project to the LGN (Gilbert and Kelly 1975). Second, these sorts of studies, by technical necessity, are restricted to comparing one projection to all other cells in the lamina, rather than comparing two distinct efferent populations occupying the same lamina.

The equivalent experiment in terms of cell morphology, i.e., comparing the morphology of cells that share the same laminar position, but project to different sites, has not been done. If cells that project to different efferent targets are in fact specialized to extract certain features from incoming sensory information, then cells that share the same position in a cortical lamina, but project to distinct efferent targets, should show different patterns of dendritic and intrinsic axonal arborizations. Is projection site, therefore, perhaps a more obvious link between a cells structure and its physiological function than specific receptive field characteristics?

This sort of experiment is exceedingly difficult in vivo. Such an investigation requires a) a method to identify cells projecting to a given efferent site, b) a method for visualizing the dendrites and axons of such cells, and c) the ability to obtain sufficient numbers of cells so as to make comparisons between efferent populations meaningful. In vivo, the only method for doing this is to combine antidromic stimulation from a specific target site with intracellular recording and staining. In practice, the difficulty of positioning an electrode in the correct layer, and the slim chance of penetrating, holding, and successfully intracellularly staining an identified cell, makes it virtually impossible to obtain a representative sample of identified projection neurons.

There have been several attempts to correlate projection patterns with specific cell types seen in Golgi preparations (Lund and Boothe 1975, Tombol et al. 1975). These studies rely on characteristics such as cell soma size, or the position of the cell body within a given lamina, to identify classes of projection neurons. Neither of these characteristics can be considered absolute criteria; cells projecting to different sites are often not distinguishable on the basis of cell size, and there can be varying degrees of intermingling of projection cells within a given lamina. These sorts of indirect studies show, at best, that it is likely that a certain cell type projects to a given efferent site. However, the vagaries of the Golgi technique may significantly influence the types of cells seen, and, especially in the case of axons in adult animals, may severely compromise the completeness of the morphological picture.

In the work described here, a new approach to this problem is used. A retrogradely transported fluorescent tracer is injected, in vivo, into a specific efferent target of neurons in area 17 (A17) of the cat. Several days later A17 is surgically removed, and thin (400 μm) brain slices are prepared and maintained in vitro. An epifluorescence equipped microscope is then used to locate retrogradely labeled cell bodies; these are subsequently impaled under microscopic control and intracellularly injected with the fluorescent dye lucifer yellow (Stewart 1978), which visualizes the dendrites and axons of the retrogradely labeled neuron. Because this can all be performed under visual control, locating retrogradely labeled neurons in specific laminae is greatly simplified. In addition, the vastly greater stability of the in vitro situation (compared to in vivo) markedly facilitates the ease with which high quality intracellular recordings and dye fills can be obtained.

The question of whether cells in the same lamina projecting to different targets show distinct patterns of axons and dendrites within A17 has been studied

by comparing the efferent projections of layer VI in the cat. Layer VI has two distinct efferent projections: a massive recurrent projection back to the lateral geniculate (Gilbert and Kelly 1975) and a considerably smaller projection to the visual claustrum (LeVay and Sherk 1981a). This system has a number of features which make it attractive for this sort of study. First, both projections originate exclusively from layer VI (except for a very few cells in layers II/III that project to the claustrum). Second, the efferent target areas are physically well separated, relatively large, and have distinctive electrophysiological characteristics. This makes it easy to locate them, and difficult to cause spurious retrograde labeling by spillage from one injection site to the other. Third, the projections originate from two completely different cell populations within layer VI (LeVay and Sherk 1981a); however there is no rigid spatial separation of the populations within the lamina (geniculate projecting cells are found throughout the thickness of the lamina, while claustrum projecting cells are found predominately in the middle of the layer, thus overlapping extensively with the geniculate projecting cells). Finally, on a physiological level, these two projection sites are very different. The cells in the visual claustrum have receptive field properties that appear very similar to those of cells in layer VI: they are orientation selective, and show the extreme summation for stimulus length and complete lack of end-inhibition characteristic of layer VI cells (Gilbert 1977, Harvey 1978, Henry et al. 1979). They differ from layer VI cells mainly by being strongly binocular (in contrast to the often strong bias to one eye in layer VI) and not particularly direction selective (whereas many layer VI cells are). In general, most of the response properties are explainable on the basis of the known physiology of layer VI.

In contrast, the physiological role of the cortico-geniculate pathway is rather obscure. Some evidence suggests that this pathway can change the level

of activity in the nucleus, either inhibiting or exciting certain classes of LGN neurons (Hull 1968, Kalil and Chase 1970, Tsumoto et al. 1978, Schmielau and Singer 1977). There have also been demonstrations of weak binocular influences in the LGN, presumably mediated by this feedback pathway (Schmielau and Singer 1977, Singer 1970). Nevertheless cells in the LGN clearly do not show the responses to long bars of light, or the orientation and direction selectivity characteristic of layer VI cells. Thus, whatever the role of the cortico-thalamic pathway may be, the claustrum and LGN projection systems apparently have fundamentally different influences in their respective target areas.

The overall result of this work has been to show that, in this system at least, the two efferent populations have dramatically different, non-overlapping patterns of distribution of intrinsic axonal and dendritic processes, and that, within each group, these patterns are remarkably homogeneous. It seems reasonable, therefore, that the large variety of different pyramidal cell types seen within the various laminae of visual cortex may be at least partly explained by the number of different efferent targets to which a lamina projects. These differences in cell form likewise imply that cells occupying virtually identical positions in cortex can be receiving information from different sources (as reflected in differences in dendritic field organization) and be sending information into non-overlapping local circuits (as shown by differences in intrinsic axonal arborizations).

MATERIALS AND METHODS

All experiments used adult cats of both sexes (over 6 months old, 2.5-4.5 kg), obtained from either a laboratory breeding colony or a commercial supplier.

In vivo injections

Cats, anesthetized with Nembutal (40 mg/kg, I.P.) and placed in a conventional stereotaxic frame, had their nictating membranes retracted with Neosynephrine (2.5%, Winthrop), pupils dilated with atropine (1%, Alcon), and corneas protected with zero power contact lenses. An electric heating blanket maintained body temperature.

The procedures for lateral geniculate nucleus (LGN) injections began with bilateral craniotomies from Horsley-Clark (H-C) coordinates 4-9 anterior-posterior, and 7 to 11 medial-laterally. Extracellular activity, recorded with glass-coated platinum-iridium or Elgiloy electrodes amplified and displayed with conventional techniques (including an audio monitor to detect visually driven responses), provided information on the location of the LGN. In early experiments a manual micromanipulator (Narishige) advanced the electrode, later experiments employed a stepping motor driven microdrive. At a depth of approximately 11 mm, the LGN was easily recognized by the sudden appearance of strong activity in response to visual stimulation of the eye contralateral to the electrode. The receptive fields of either single units or small groups of cells near or at the dorsal surface of the nucleus were approximately mapped with a small spot of light (about 1^{o} diameter) from a hand held ophthalmoscope projected onto a tangent screen 57 cm from the eyes. The positions of receptive fields were estimated by projecting the optic disks using a reversible ophthalmoscope. The areae centrali were taken to lie 16^{o} nasal and 6.5^{o} down from the centers of the optic disks (Bishop et al. 1962). Animals were not paralyzed, however the position of the optic disk, plotted before and after crude determination of the receptive field position, did not move significantly. The receptive field from the first penetration was used to deduce the approximate

position of the electrode in the LGN, according to the map of Sanderson (1971). Subsequent penetrations, made at various other positions (usually at least 6), generally mapped the extent of the LGN. All penetrations showed characteristic shifts from contralateral to ipsilateral and back to contralateral-eye driven responses; this provided an estimate of the thickness of the LGN at each site.

The recording electrode was then replaced with a 1 µl glass-tipped Hamilton syringe filled with the retrograde tracer, a suspension of fluorescent red latex microspheres ("beads") (see below for details of tracer preparation and characteristics). One-microliter bead injections (spaced 1 mm apart in the antero-posterior direction, and at least 1.5 mm apart medial-laterally), were made over a period of 3-5 minutes, distributed throughout the thickness of the LGN, at each of 6 sites previously characterized electrophysiologically. Pipettes remained in place for five minutes after each injection. These large injections maximized the number and extent of retrogradely labeled cells in A17.

Tracer injections into the claustrum followed the basic procedure described by LeVay and Sherk (1981a), except that animals in this case were not paralyzed during the mapping of geniculate receptive field positions. Briefly, a point on the antero-lateral portion of the LGN located using the procedure described above provided equivalent H-C coordinates from the map of Sanderson (1971). From this, the electrode was moved to a position equivalent to H-C coordinates 12.3 mm lateral and 11 mm anterior (the apparent center of the visual portion of the claustrum). No conclusive visually driven activity was seen at this site, however electrode penetrations consistently recorded cellular activity at the depths appropriate for the claustrum, and subsequent reconstruction of electrode tracks revealed that the electrodes passed through the claustrum. Injections of beads (2-3, 1 µl injections, spaced approximately 500 µm apart in anterior-posterior and medial-lateral directions) at this location and at the appropriate

depths produced excellent labeling in the visual cortex, identical in distribution and extent to that seen by LeVay and Sherk (1981a). Only injections which subsequent histological investigation showed to be in the claustrum produced labeling in A17; even very extensive injections of surrounding fiber tracts failed to produce any label whatsoever in A17 (see Results below).

Animals were given a prophylactic dose of 0.5 cc of penicillin post-operatively and allowed to recover from anesthesia. Cats survived from 2 days to 1 week post-injection until slices were prepared.

Slice preparation

Cats previously injected with beads in either the LGN or claustrum (as described above), were anesthetized with Nembutal (40 mg/kg, I.P.) and placed in a standard stereotaxic apparatus. Surgery began with a large craniotomy which exposed the posterior third of the brain followed by retraction of the dura overlying one hemisphere (operations described below were completed on one hemisphere, and repeated on the other side). A large section of the posterior portion of the brain (including the shaded area shown in Fig. 1) was removed by making deep medial-lateral and antero-posterior scalpel cuts, undercutting the white matter, and sliding the brain section out on a teflon spatula. This large chunk was immediately placed in a beaker of cool (15^{o}) artificial cerebro-spinal fluid (ACSF). The ACSF had the following composition (in mM): NaCl 124 mM, KCl 5mM, KH_2PO_4 1.25 mM, $MgSO_4$ 2 mM, $CaCl_2$ 3 mM, $NaHCO_3$ 26 mM, d-glucose 10 mM, pH 7.4. The brain chunk, trimmed with razor blades to the boundaries shown in the shaded area of Fig. 1 (e.g. medial-laterally from the fundus of the splenial sulcus to the fundi of the lateral and post-lateral sulci, and antero-posterior extent from H-C +2 to -15) had the pia gently peeled off with #5 Dumont forceps. The prepared brain was then placed on a 5 mm thick agar

Figure 1. Dorsal (above) and medial (below) views of the cat brain; shading indicates the area used for making cortical slices. The lateral borders correspond to the fundi of the lateral and post-lateral sulci, the medial border to the fundus of the splenial sulcus. Abbreviations: 0, Horsley-Clark 0; Cb, cerebellum.

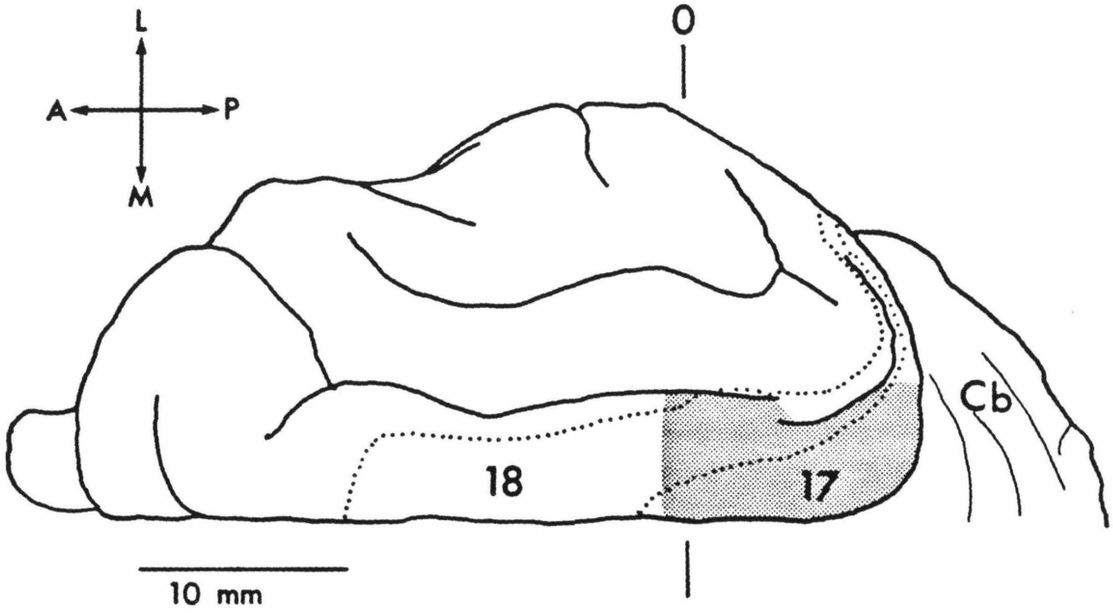
L
A
P
M
O
Cb
18
17
10 mm

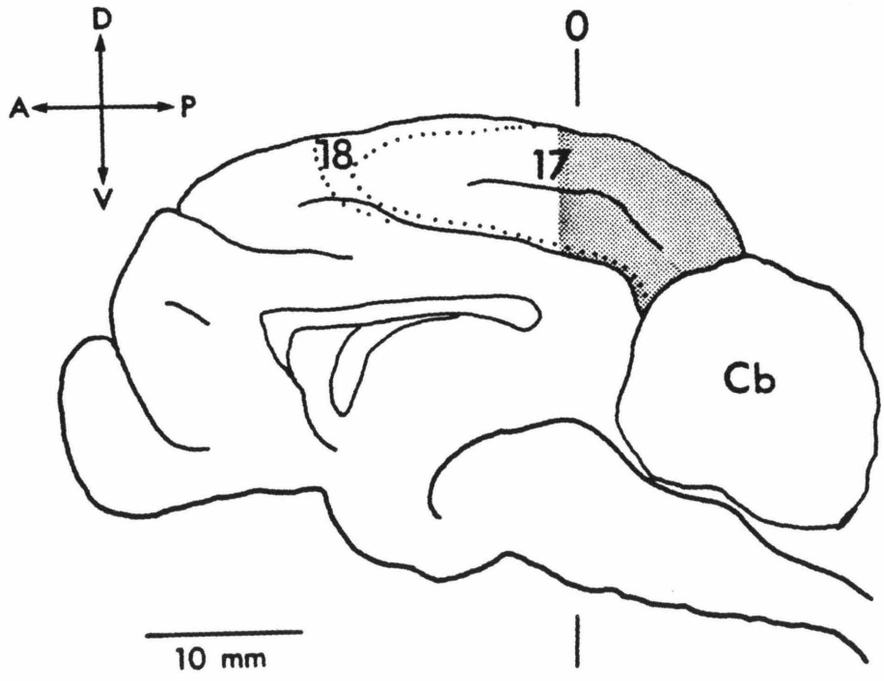
D
A
P
V
O
18
17
Cb
10 mm

slab (2% Difco Bactero-Agar in ACSF) on the stage of the slicing apparatus (see description below). Four hundred micrometer thick, coronal slices were used in all experiments.

After slicing, the chunk was transferred to a 10 cm diameter petri dish filled with cool (15^{o}) oxygenated ACSF. After gently separating each group of 6-8 slices with fine paintbrushes (Artec, series 610, #000) (Fig. 2a), one was removed, placed under a fluorescence microscope and checked for the presence of retrogradely labeled cell bodies. Individual slices were floated onto small rectangles (6mm by 8mm) of embedding bag paper (Spectrum), and placed (6 to a well) in a standard 4-well hippocampal slice chamber (Fig. 2b) (similar to the one described in Hatton et al. 1980). Polycarbonate filter membrane (12 µm pore size, Nucleopore Corp, Pleasanton, CA) whose smooth surface facilitated removing slices for transfer to the recording apparatus, replaced the standard nylon mesh slice supports. A temperature probe/feedback circuit kept the chamber at $33^{o}C$; a warmed, humidified mixture of 95% O_2, 5% CO_2 (approximate flow rate 175 ml/min) provided oxygenation. Although not continuously perfused, portions of the bathing fluid in each well were occasionally replaced with fresh ACSF. Slices, maintained at the air/water interface, remained viable for up to 16 hours. The entire slicing operation (from brain removal to placement in the holding chamber) usually took less than 15 minutes per hemisphere.

After removal of both hemispheres, the cat was perfused intracardially with 0.1 M phosphate buffer followed by 10% formalin in 0.1 M phosphate buffer. For verification of injection sites, appropriate portions of the brain were blocked, sunk in 30% sucrose in 0.1 M phosphate buffer, and sectioned at 40 µm on a freezing microtome. Sections were mounted on Gatenby slides, air dried, cleared in xylene for 1-2 minutes, and coverslipped using Fluoromount (Gurr).

Figure 2. a) The upper portion of the photograph shows a chunk of visual cortex just sliced by the tissue slicer (Fig. 3); the fine gold wires of the slicer are visible. In the lower portion of the field, slices have been separated from the chunk and are sitting in a ACSF-filled petri dish, awaiting transfer to the holding chamber. Scale bar: 1 cm. b) Cortical slices in one well of the holding chamber; the slices sit on small squares of embedding bag paper, which in turn rest on a membrane filter support. Scale bar: 1 cm. c) A single slice in the miniature chamber on the compound microscope stage. The chamber, constructed on a 3"x2" glass microscope slide, consists of: 1) Hollow plexiglas oxygen dispersion ring; outlets for oxygen are distributed around the circumference; some of these are indicated by arrows. 2) Silastic oxygen inlet tube. 3) Perfusion solution inlet tube--a 21 gauge hypodermic needle. 4) Chlorided ground wire. 5) Kimwipe wick, which fits under a narrow groove milled in the dispersion ring; this effectively isolates the slice from the suction line, which could otherwise draw lab air into the chamber. 6) Vacuum line. 7) Brain slice. 8) Slot for electrode access. Scale bar: 1 cm. d) Chamber ready for recording, and stage mounted slice-support systems. 1) 16X objective. 2) Heating element. 3) Sliding cover; the underside is lined with moistened filter paper. 4) Chamber clamps. 5) Recording electrode. 6) Oxygen humidifying tower (containing moistened Kimwipe tissue). 7) Power resistors to warm entire stage. 8) Glass radiator which warms inflowing oxygen. 9) Glass radiator which warms inflowing ACSF. 10) Vacuum line. 11) Ground wire. Scale bar: 1 cm.

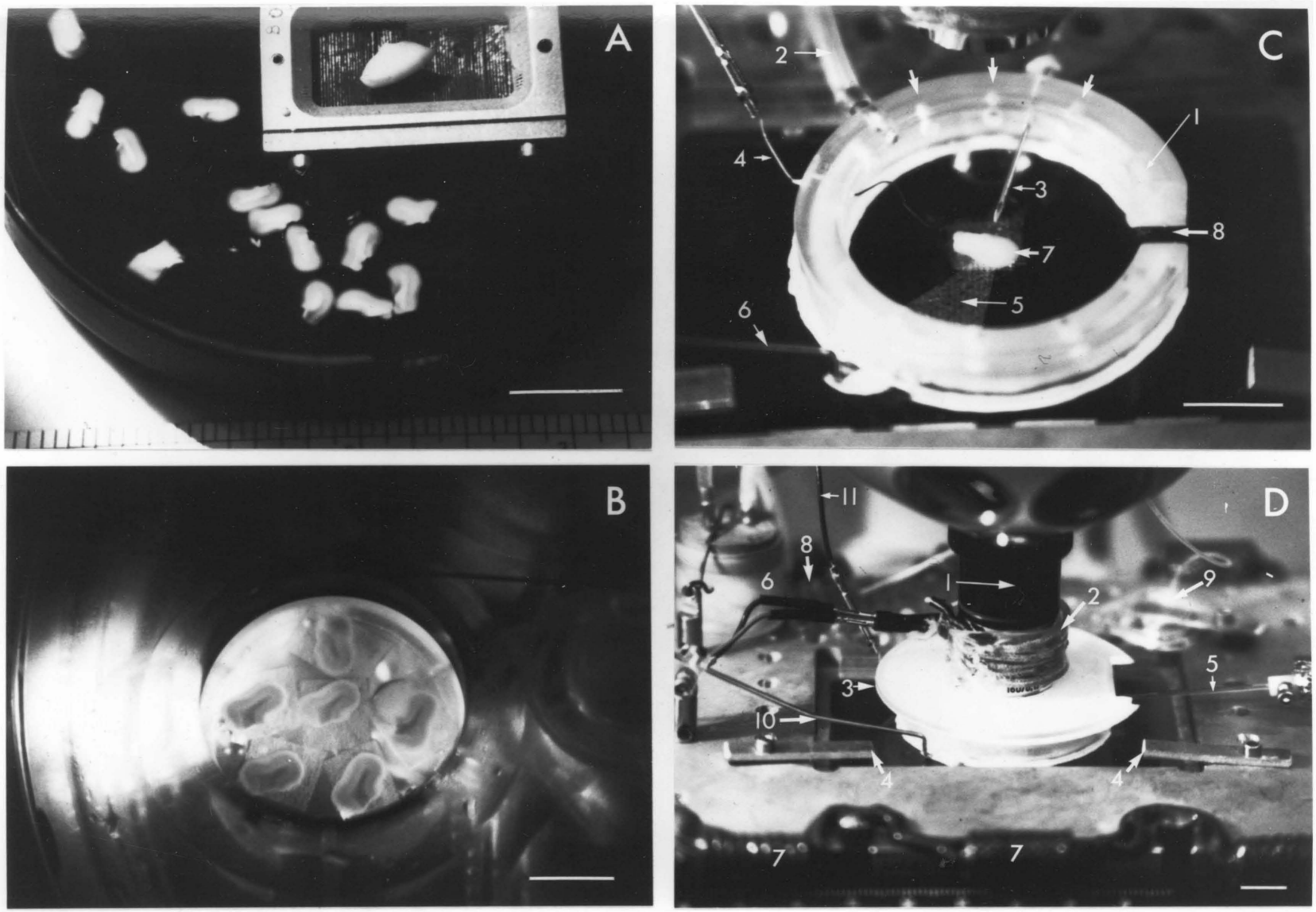
A
B
C
D
1
2
3
4
5
6
7
8
9
10
11

Description of the tissue slicer

The slicing process included extensive areas of cortex for two main reasons: first, the experiments demanded many slices, and second, it was not possible to know (because of the placement of tracer injections), before making slices, precisely where, either in the antero-posterior or medial-lateral directions, the greatest number of retrogradely labeled cell bodies would lie.

Conventional techniques for preparing slices--tissue choppers, the Vibratome, or by hand--are either too slow or cannot accommodate pieces of tissue larger than about 3 mm (reviewed and compared in Dingledine et al. 1980). A new type of brain slicer, designed to overcome some of the limitations of both speed and size, is shown in Fig. 3a.

The basic principle of operation is similar to a kitchen egg slicer. A spring-loaded arm holds a stainless steel grid which has a rectangular opening, 25 mm by 13 mm, across which are tightly stretched a series of 60 parallel,gold plated tungsten wires, 20 μm in diameter, 400 μm apart (Fig. 3b). Figure 3c shows the device ready to slice the portion of the brain described above. Release of the trigger causes the thin wires to pass through the brain and the agar pad, at high velocity, producing precise, 400 μm thick coronal slices, without visible compression or deformation of the brain (Fig. 3d). After slicing, the grid and the brain are removed from the slicer and placed in ACSF in a petri dish, and slices are separated as described above. The slicer allows preparation of up to sixty slices in one operation, can handle even quite large pieces of tissue, and produces slices with excellent viability (see below).

The slicing process usually resulted in slight stretching of the slicing wires. A specially designed winder rewound the grids with fresh wire before each experiment.

Figure 3. The brain slicer. a) Slicer in loaded position. 1) Spring loaded arm. 2) Removable base plate. 3) Cutting grid. 4) Grid releasing knob. b) Slicer set to slice the portion of cortex (shown in Fig. 1), which is sitting on an agar pad. c) The same piece of brain, immediately after slicing; the extremely fine wire cuts are not visible, and the brain is not deformed. The ruler in a, b and c indicates mm and cm.

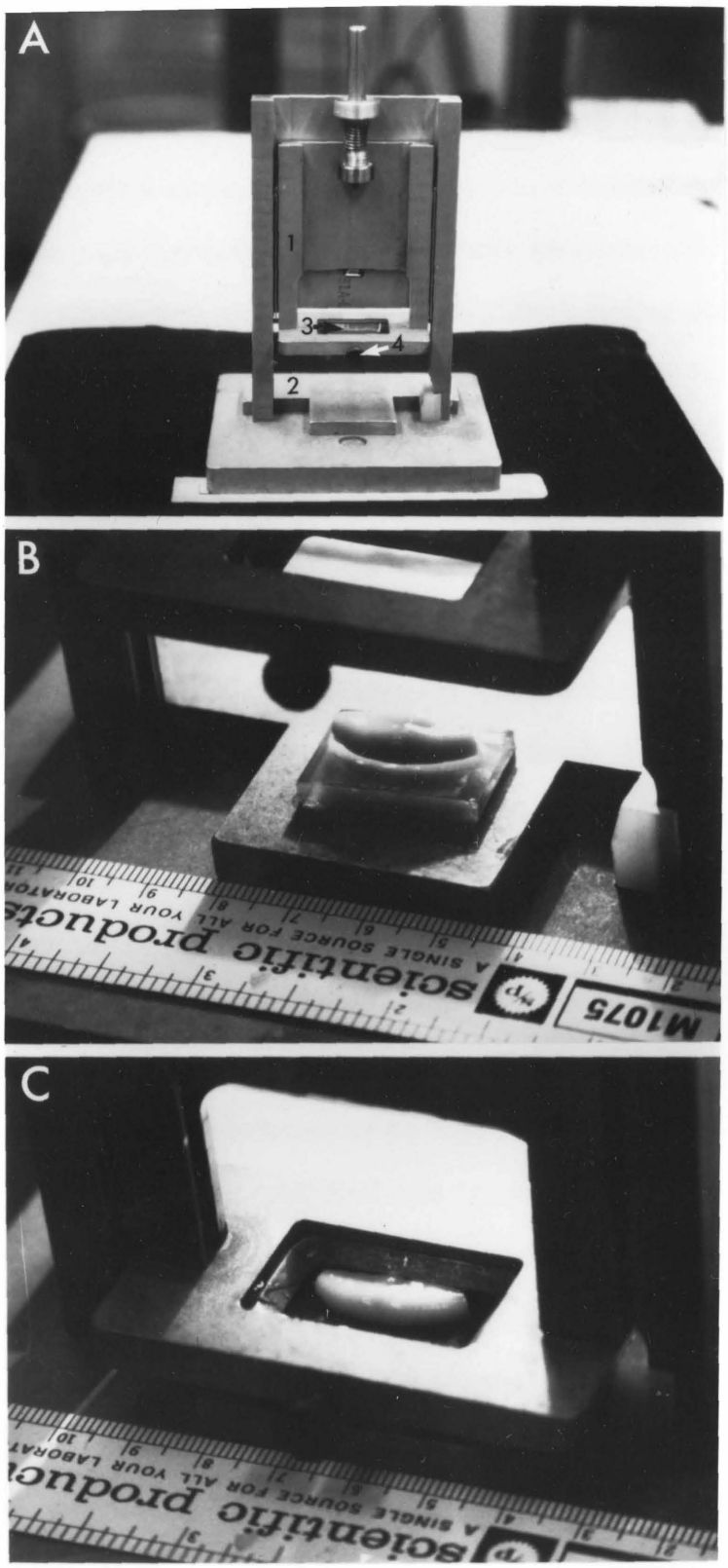
A
1
2
3
4
B
C

Intracellular recording and labeling

After a recovery time of at least 1.5 hours, individual slices were transferred from the holding chamber to a miniature chamber on the stage of a modified epifluorescence equipped Zeiss WL compound microscope (Fig. 2). The figure legend describes the details of the chamber construction. A heated 16X objective (N.A. 0.35) fit through a hole in the chamber's sliding cover (Fig. 2d).

In early experiments, conventional glass microelectrodes (pulled on a Brown-Flaming micropipette puller (Sutter Instruments) from 1.2 mm O.D. Omega dot tubing (Frederick Haer Co.), and filled with 20% lucifer yellow (Aldrich) in 0.1 M LiCl (Stewart 1978)), were advanced through the slice at a shallow (less than 20^{o}) angle with a hydraulic microdrive, in regions of retrogradely labeled cell bodies. Cells were intracellularly filled at random, producing a number of "double labeled" cells (e.g. those containing retrogradely transported beads and intracellularly injected lucifer yellow [Fig. 4c]) directly proportional to the number of retrogradely labeled cell bodies in the area (about 50% for the LGN projection, about 5% for the claustrum projection). In later experiments, the tips of micropipettes were bent to an angle of about 90^{o}, (Hudspeth and Corey 1978) permitting penetrations normal to the surface of the slice (and thus allowing an electrode to be "aimed" at a particular retrogradely labeled cell body). Both the modified and unmodified electrodes had initial resistances of approximately 350 megaohms; the tips were usually manually broken to a final resistance of 100-200 megaohms. The tips of the bent electrodes were aligned with retrogradely labeled cell bodies (by means of an eyepiece graticule), and advanced through the slice in 1-3 μm steps with the fine vertical control on a Leitz micromanipulator. Standard DC amplifiers and oscilloscopes amplified and displayed intracellular electrical activity, and an FM

tape recorder recorded potentials for later analysis. Cells were penetrated by applying large (90 mV) positive voltage pulses (200 msec duration) to the stimulus input port of the amplifier. Stable cells of interest (generally with action potentials of 40 mV or greater in amplitude and less than 1 msec duration at half height) were injected with lucifer yellow (trapezoidal current pulses, 10 msec rise/fall time, 200 msec duration, 4 Hz, 2.5 nA, electrode negative) for 1-10 minutes, usually until anode break action potentials and resting potential disappeared. After filling 4-6 cells (over the course of one hour), the slice was removed from the chamber and fixed in 10% formalin in 0.1 M phosphate buffer. Twelve to sixteen slices were used in this manner. Experiments lasted about 16 hours after slice preparation; after this time slices contained few healthy cells. After fixation (at least overnight, but for up to 6 months) individual slices were sunk in 30% sucrose in 0.1 M phosphate buffer and sectioned coronally (i.e. parallel to the slicing plane) at 60 μm on a freezing microtome. Sections were mounted on Gatenby coated slides, air dried, briefly dried on a slide warmer, cleared directly in xylene for 1-2 minutes, mounted in Fluoromount (Gurr), and examined and photographed on a Zeiss Standard WL epifluorescence microscope with rhodamine and fluorescein filters. Drawings of selected lucifer yellow stained cells were made with a 100X oil immersion objective and a camera lucida (final magnification, 1250X) on black paper with white pencils. All photography was done with Ektachrome film (ASA 200, Kodak).

Measurements of distances between labeled neurons in vitro (at 160X) and after processing showed virtually no shrinkage within the limits of measurements, thus shrinkage in the plane of the section was under 5%. Shrinkage orthogonal to the plane of slicing was not assessed, since all reconstructions were two-dimensional. No corrections, therefore, were made for tissue shrinkage in any of the data presented below.

Laminar and areal boundaries were delineated according to the criteria of Otsuka and Hassler (1962). Nomarski-differential-interference contrast optics provided a fairly reliable indication of laminar boundaries in uncounterstained sections, but for precise determination of boundaries, sections were subsequently counterstained with cresyl violet. This procedure destroyed the bead's fluorescence, but the lucifer yellow fluorescence persisted quite well.

Measurements of axon and soma sizes

Camera lucida drawings of retrogradely labeled cell somas (at 1250X) were entered (via a digitizing tablet) into a computer (Hewlett-Packard 2647 graphics terminal) which calculated somal area. Since axons were usually too thin to measure directly using an eyeiece graticule, estimates of axon diameters were obtained by photographing portions of the axon with a 100X objective (N.A. 1.25) and measuring the diameter of the photographic image using a compound microscope with a 10X objective and eyepiece graticule. This systems resolution was limited to approximately 0.25 μm.

Fluorescent latex microspheres

Characteristics and preparation. The accompanying manuscript (Chapter II) describes most of the salient features regarding the performance of "beads" as a retrograde tracer. Only a few points directly relevant to these experiments will be discussed.

Beads have several characteristics that make them extremely useful for this sort of experiment. Most important, they show absolutely no tendency to leak or diffuse out of cells, even after very long survival times, after the manipulations involved in preparing slices, or following prolonged storage of slices after an experiment. Thus one can be assured that a cell labeled with

beads did in fact project to the appropriate site. Second, illumination of beads does not seem obviously toxic to cells, which contrasts with the marked phototoxicity of many fluorescent dyes (e.g. lucifer yellow [Miller and Selverston 1979]) and probably relates to the fact that beads show very little bleaching under illumination (Gupta et al. 1981). The fluorescent intensity of bead labeled cells is a third important considertion: well labeled neurons are easily visualized at the relatively low magnification used in these experiments, and in uncleared, thick slices of tissue (Fig. 4a). This facilitates "aiming" for specific cells.

A large batch of beads, prepared by ultracentrifugation and used in all experiments, minimized the possibility that differences in tracer preparation might influence the number or extent of labeled cells.

RESULTS

A total of four cats received bilateral injections of beads into the LGN. Eight cats received injections directed at the claustrum; five of these showed retrograde labeling in A17 (the other cats functioned as controls for injections of the surrounding fiber tracts, see below).

Injections of beads into the LGN produced an identical pattern of labeling in all cases, with retrogradely labeled neurons confined to, and distributed throughout the entire thickness of, layer VI (Fig. 5a). In A17, approximately 50% of neurons in the lamina contained beads; labeling in areas 18 and 19 , also confined to VI, was somewhat sparser. The cell bodies containing label were mostly medium sized pyramidal, fusiform or ovoid cells characteristic of this layer (Fig. 5b) Most cells showed very dense, granular labeling in the soma, extending partway into the proximal portion of the apical dendrite (Fig. 5c). The observed pattern of labeling agrees precisely with that described by Gilbert and

Figure 4. a) Neuronal cell bodies in a living brain slice, retrogradely labeled with beads, following injection of the visual claustrum. In this 400 μm thick section, fewer than 5% of the cell bodies are labeled. Arrows indicate the out of focus cell bodies double labeled with lucifer yellow, shown in (b). b) Same field as (a) seen under lucifer yellow illumination wavelengths, showing two claustrum projecting cells intracellularly injected. The somas, dendrites, and even dendritic spines are visible. Scale bars: 100 μm. c) A claustrum projecting neuron double labeled by retrogradely transported beads and intracellularly injected lucifer yellow. The exposure on the right was made under rhodamine illumination, the section was then shifted slightly, and the exposure on the right was made, under lucifer yellow illumination. The background haze in the bead exposure results from weak fluorescence of lucifer yellow, even at rhodamine wavelengths. Scale bar: 20 μm.

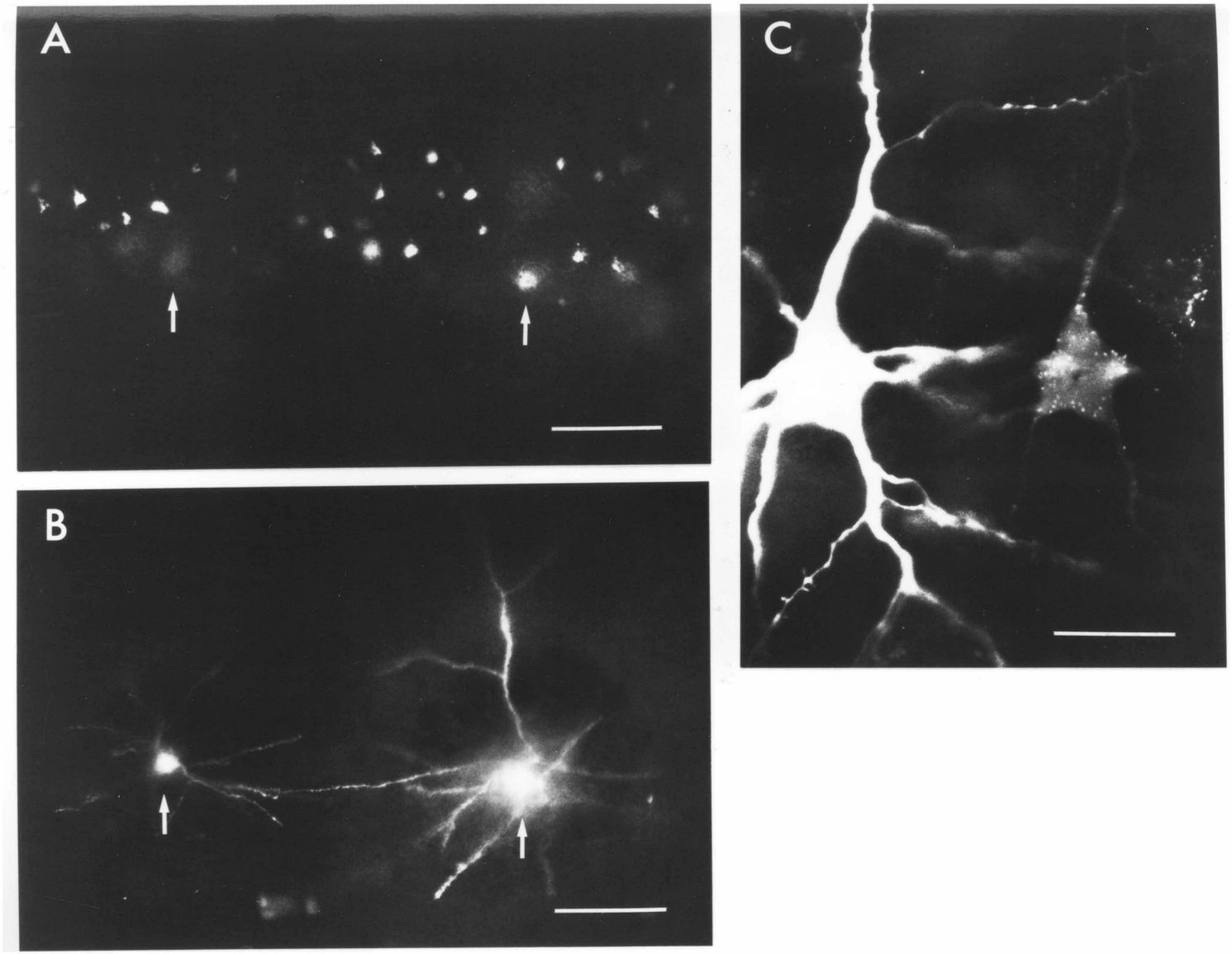
A
B
C

Figure 5. Retrograde labeling of the LGN projecting neurons in area 17. a) Bead labeling at the apex of the lateral gyrus following LGN injections. The occasional bright spots in the white matter and outside layer VI are artifact. Scale bar: 100 μm. b) Higher power view of retrogradely labeled neurons, mostly medium sized pyramidal cells, located throughout the thickness of layer VI. Scale bar: 50 μm. c) A single retrogradely labeled pyramidal cell, with a soma and apical dendrite densely packed with granular appearing beads. Scale bar: 10 μm.

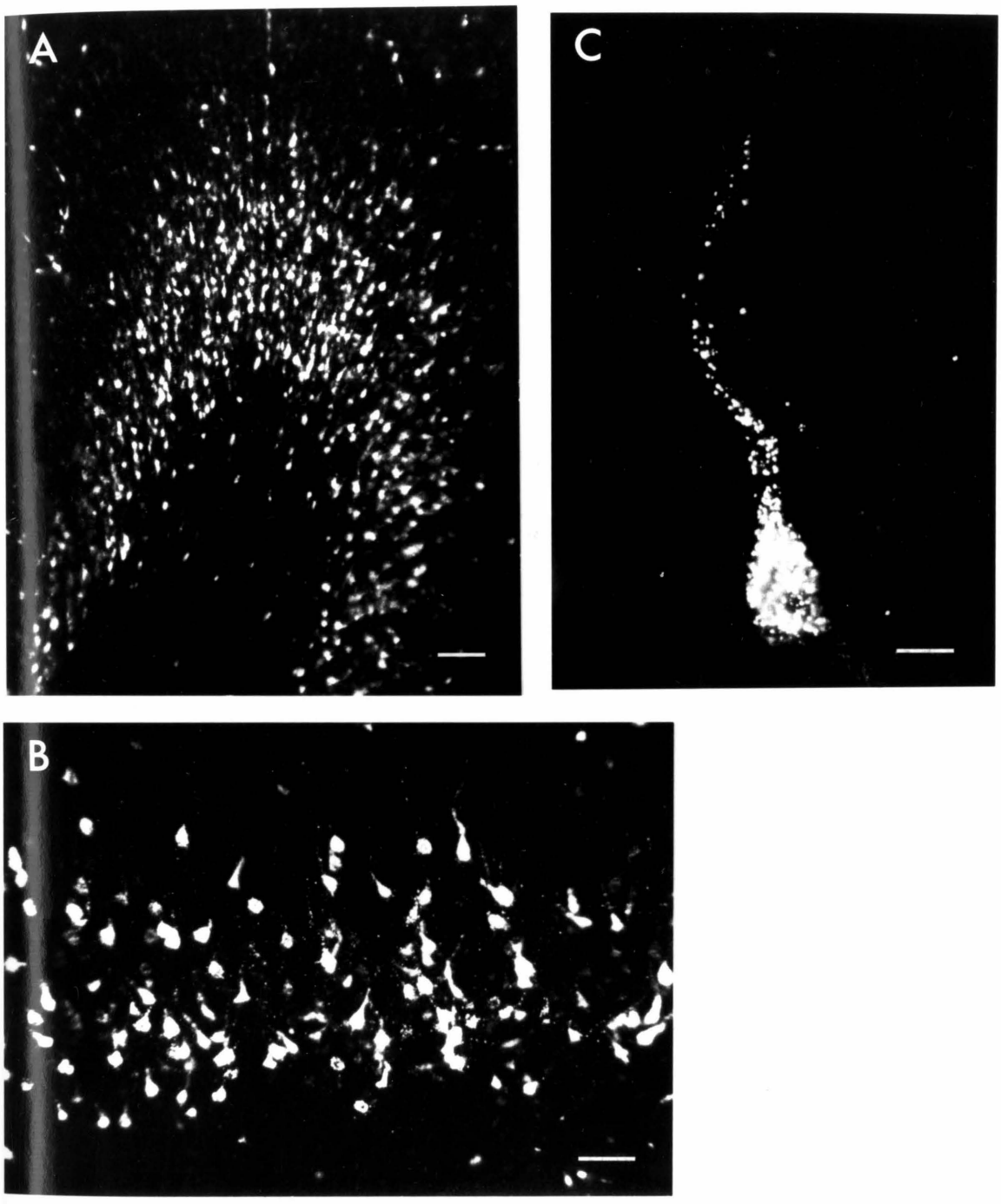
A
C
B

Kelly (1975) using HRP, and Baughman and Gilbert (1981) and LeVay and Sherk (1981a), using tritiated aspartate.

LeVay and Sherk (1981a) described the projection from the A17 to the claustrum as originating from cells in the middle of lamina VI, and comprising less than 5% of the cells in the layer. They also noted that more cells were labeled in the portion of A17 subserving the peripheral portions of the visual field than in the areas subserving central vision. In these characteristics, retrograde labeling by beads was identical. Figure 6 shows a portion of layer VI labeled after an injection of beads into the claustrum. In addition to the prominent label in a band of cells, 2-3 cell bodies thick, in the central portion of layer VI, very occasional cells were labeled in the more superficial layers, which was also noted by LeVay and Sherk. Such labeling was never seen if only the fiber tracts surrounding the claustrum were labeled. In the cases of succesful claustrum injections, the lateral geniculate nucleus was sectioned and examined as described in **Methods.** Since the geniculo-cortical and cortico-geniculate pathways follow the same course (Guillery 1967), if the apparent claustrum labeling in cortex resulted from spurious labeling by cortico-geniculate fibers, one would expect to see labeling in the geniculate as well from damage to the geniculo-cortical fibers. In no case was any labeling ever seen in the lateral geniculate, even after extensive claustrum injections.

The health of slices prepared using the slicer descibed in **Methods** was in general excellent, as determined by the number of cells intracellularly penetrated, the size and duration of their action potentials, and the length of time that penetrations remained stable. An average of 45 cells were intracellularly stained in each experiment, and in only one case was there a complete failure, for unknown reasons, to intracellularly impale any neurons. In the best experiment, 85 cells were intracellularly labeled with lucifer yellow.

Figure 6. Retrograde labeling of claustrum projecting neurons in area 17. a) Labeled neurons in the middle of layer VI (laminar boundaries indicated by arrows) following bead injection into the visual claustrum. The section is from a more central part of area 17 than (b), below, and fewer cells are labeled. Scale bar: 50 μm. b) same as (a), except that this section, taken from a more peripheral part of area 17, contains greater numbers of labeled neurons. The bright cell in the center was also labeled with lucifer yellow. Scale bar: 50 μm.

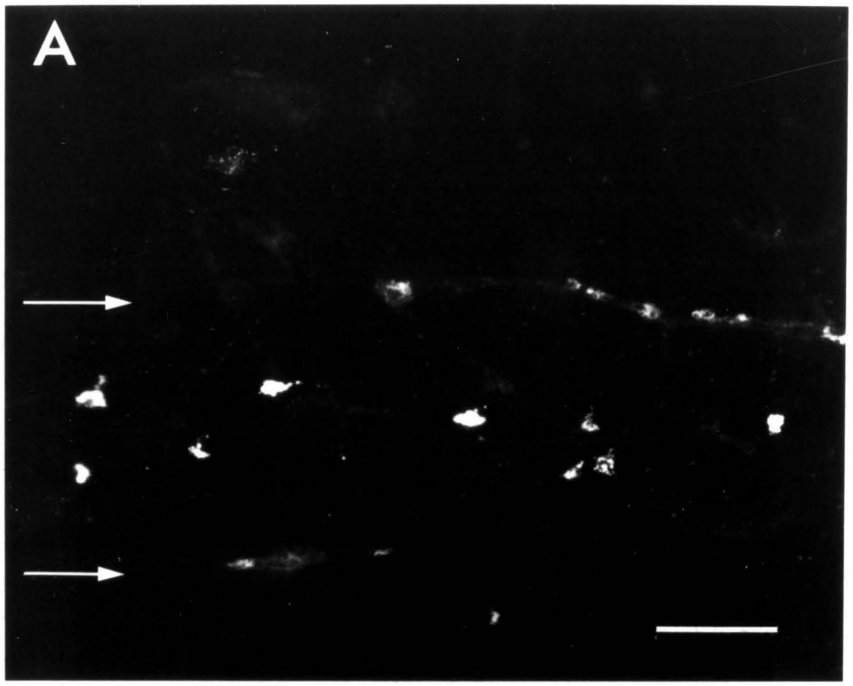
A

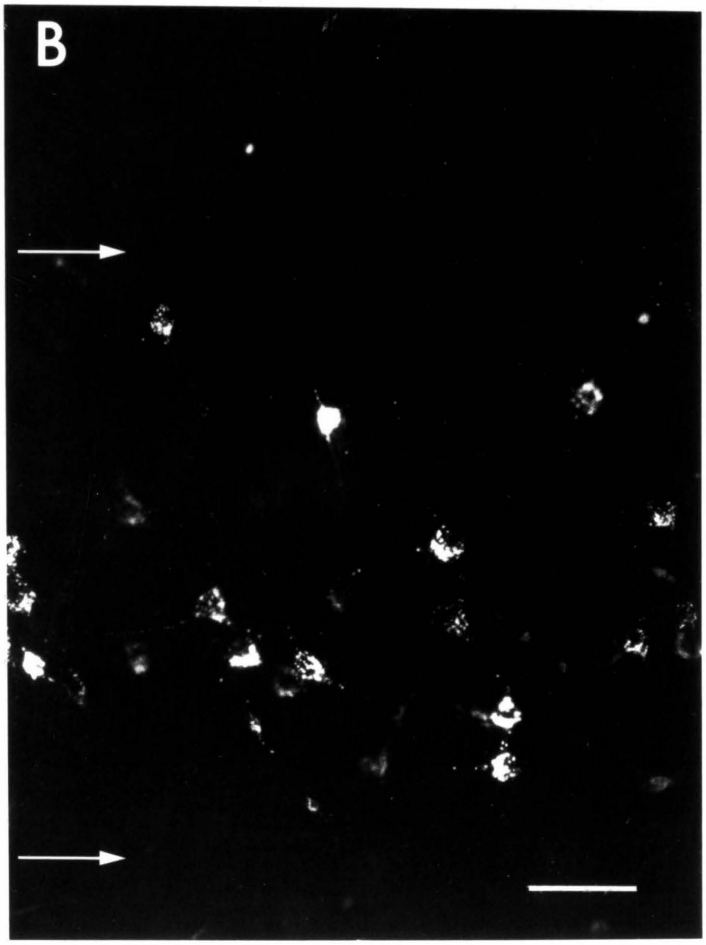
B

An example of the appearance of retrogradely and intracellularly labeled cells in vitro, during an actual experiment, is shown in Fig. 4. Although the aqueous environment degrades the image quality significantly, it is still relatively easy to focus on individual retrogradely labeled cell bodies, as well as visualize the somas and dendrites (and occasionally axons) of intracellularly filled neurons.

Figure 7 shows examples of the electrical activity recorded from cells later identified as projecting to either the claustrum or LGN. In both cases, action potentials were of normal shape and duration; the average amplitude was 45 mV, which was identical to the amplitude of cells not retrogradely labeled with beads. Observations showed no obvious differences in the length of time a retrogradely labeled cell could be held, or in the level or quality of its electrical activity, compared to an unlabelled cell. At this level of analysis, retrograde labeling by beads does not have any significant effects on the ability of neurons to maintain normal electrical activity. The amplitude of the action potentials in slices reported here (approximately 45 mV) is slightly lower than that reported for other slice preparations (Schwartzkroin 1975), probably due to the electrical properties of high resistance, lucifer yellow filled micropipettes, rather than the health of neurons in slices. Occasional recordings made with micropipettes filled with 3 M KCl, (resistance 50-70 megaohms), showed action potentials in the 60-70 mV range.

Not infrequently during experiments, action potentials of considerably smaller size--less than 30 mV--were recorded. Despite their small size, they had a normal duration (about 1 msec) and were quite stable. This contrasted with other small potentials which indicated cell injury--in such cases the small potentials were greatly prolonged and disappeared quickly. In all cases in which injections were attempted in cells which exhibited these small, fast potentials,

Figure 7. Intracellularly recorded action potentials from claustrum and LGN projecting neurons; no differences were seen in the size, shape, or duration of potentials either between the two projection classes, or compared to unlabeled neurons.

ACTION POTENTIALS

Claustrum projecting cells

LGN projecting cells

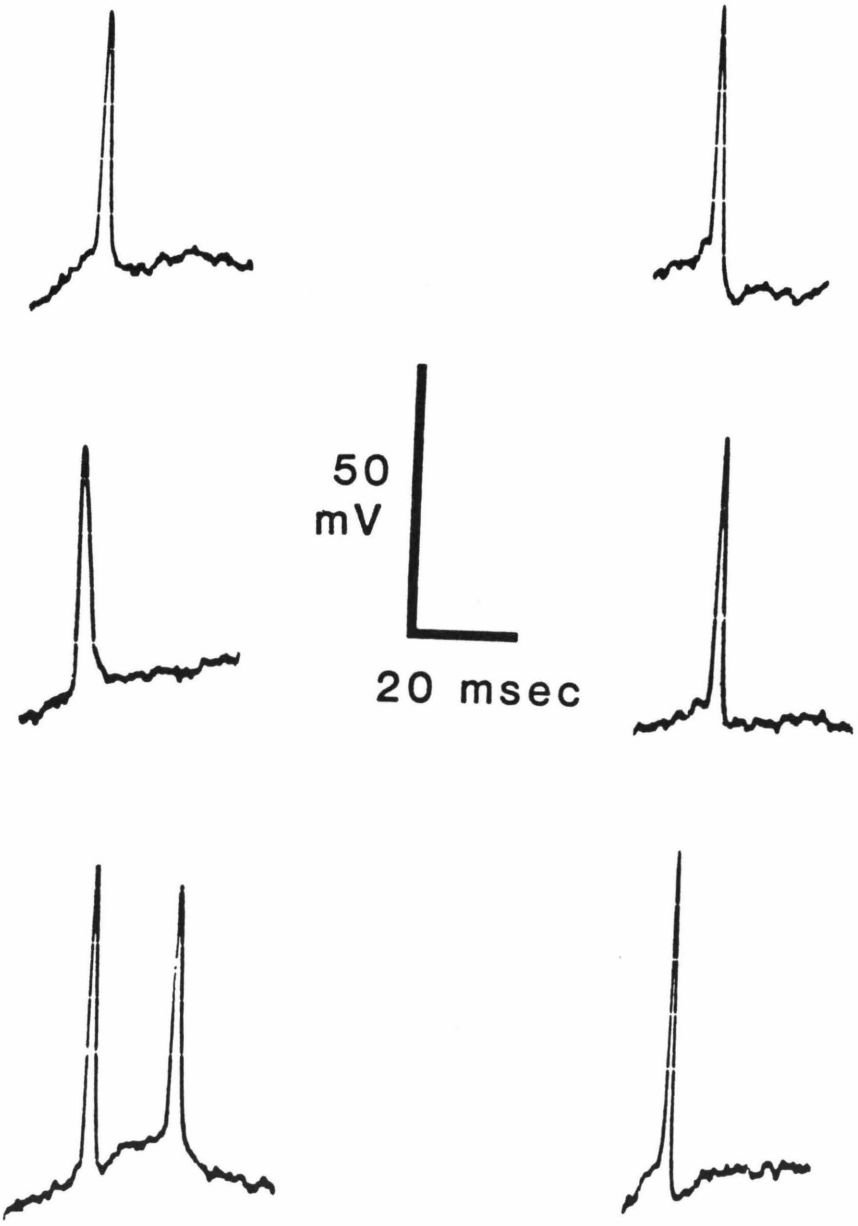

subsequent inspection (in vitro), with the electrode still in place, revealed cells which had been impaled in either the apical dendrite (in most cases), or, occasionally, in a basal dendrite. In some cases the recording electrode was over 150 μm from the cell body. Recordings from apical dendrites have been described previously in hippocampus (Wong et al. 1979, Masukawa and Prince 1984) and cerebellum (Llinas and Sugimori 1980, Llinas and Hess 1976), but not in neocortex. The size and shape of the potentials suggests that they originated from somal action potentials which invaded the dendrites.

Morphology of neurons projecting to the visual claustrum and lateral geniculate nucleus

Both qualitative and quantitative observations were made on these two cell types. The data base for qualitative observations consisted of 50 cells double labeled after injections of the LGN, and 30 cells double labeled after claustrum injections. An example of a neuron double labeled by lucifer yellow and beads is shown in Fig. 4c. After the initial identification of the distinguishing features of these two cell classes, some additional cells were examined which contained only intracellular lucifer yellow, but showed obvious features of one class or the other (none of these cells were used for quantitative analysis, however). Cells selected for observations were well filled, with no obvious distortion of the dendrites or axons, and not obviously truncated (cells located in the top 40 μm of the slice often had severely truncated dendritic and axonal processes). In general, cells that continued to show anode break action potentials for at least 4 minutes gave the best quality fills. Cells filled for 1-3 minutes often had well filled dendrites, but only fair filling of axon collaterals. Fills of less than 1 minute usually labeled the soma, basal dendrites, and part of the apical dendritic tree; the axon collaterals were either not visible or traceable for only short distances. Under

the conditions used in this study, even very fine (circa 0.2 μm diameter) collaterals could be visualized for distances of up to 1 mm. No processes significantly longer than this were seen, but it is not clear whether this is a limitation of the slicing procedure (i.e. truncation artifact), a limitation of the sensitivity of lucifer yellow, or a combination of both.

For quantitative observations on basal and apical dendritic arbors, using Sholl analysis (Sholl 1955), samples of seven cells from each of the two classes were selected for analysis on the basis of the most complete axons and dendrites. Cells selected for this analysis covered the range of morphological variability observed qualitatively. Because of these selection procedures, the sample is not random, but representative. The analysis consisted of counting the number of intersections of basal or apical dendritic processes with a series of concentric circles spaced at 20 μm intervals. For the basal dendrites, the center of the circles was placed in the center of the cell's soma; for apical dendrites it was placed at the base of the main apical dendritic arbor.

Claustrum-projecting cells: general morphological characteristics

Figure 8 shows several examples of double labeled claustrum projecting neurons. As a group, the claustrum projecting neurons exhibited a remarkable degree of similarity in their patterns of dendrites and axons. All were medium sized pyramidal cells, with a sparse basal dendritic field, and an apical dendrite that usually reached the lower boundary of layer I. The basal dendritic processes, although few in number, often had extensive horizontal spread within layer VI. The sparsely branched apical dendrite possessed a few short branches restricted to layers VI and V, with none ever observed in layer IV. Dendritic spines densely covered both the apical and basal dendrites. All these cells had an identical pattern of distribution of axon collaterals: three or four thin processes

Figure 8. Several intracellularly filled claustrum projecting neurons in layer VI. All three cells show many of the distinctive features of claustrum projecting cells: the thick, asymmetric basal dendritic process (indicated by open arrows in [a] and [c]), densely spined apical dendrite with short side branches (most clearly seen in [a] and [b]), and axons with thin, horizontally directed intrinsic collaterals (indicated by solid arrows in [a] and [b]). Figure 9 shows a camera lucida drawing of the cell in (a). Scale bars: 50 μm.

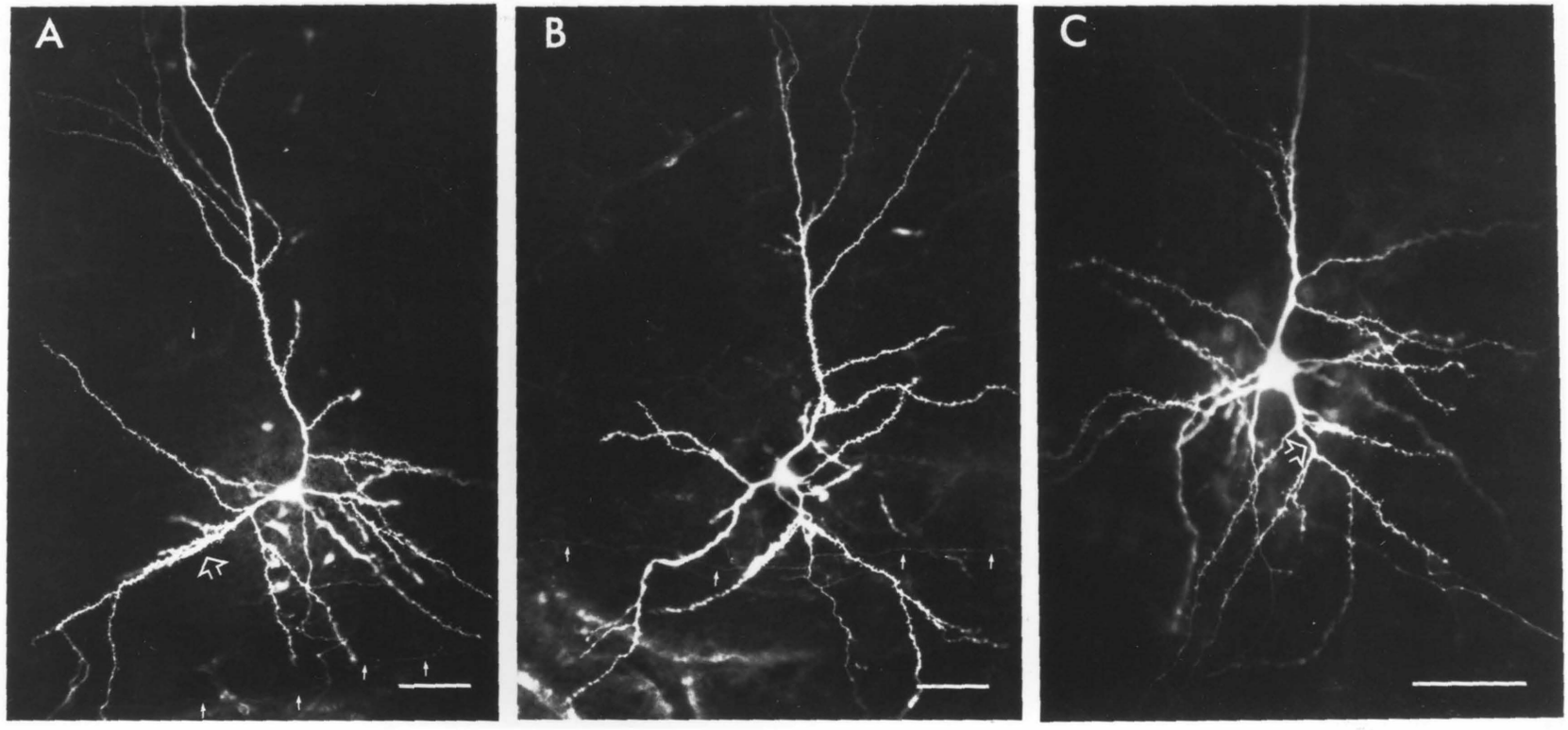
A
B
C

eminated from the main efferent axon and coursed horizontally within layer VI for up to 1 mm. Occasionally these gave rise to a small vertical branch that never reached beyond the lower portion of layer V. These characteristics, which can be seen in a camera lucida drawing of one claustrum-projecting cell in Fig. 9, will be considered in greater detail below.

Soma and basal dendrites

The soma shapes of claustrum projecting cells varied from pyramidal to oval and in some causes had almost a bipolar appearance (due to the presence of a thick basal dendrite, see below). The size of retrogradely labeled somas was normally distributed around a mean of 155 μm^2 (±34.7 S.E.M., n=100). The sample of double labeled cells had an average somal area of 149 μm^2 (±39.4 S.E.M., n= 24) (some of the sample of 30 such cells were not included because the soma was distributed between two sections, or was somewhat swollen or otherwise mildly distorted by the filling process). The difference between these two populations is not statistically significant (student's T-test, $p < .01$) (Fig. 10). No consistent trends in cell body size reliably distinguished these cells from those projecting to the LGN (see below).

Claustrum projecting cells had a very distinctive basal dendritic field structure, formed by 3-5 dendritic arms emanating from the soma (X=4.5 ± 1.0 S.E.M., n=24). Invariably one or two of these arms was significantly thicker (and often much longer) than the rest; this thick proximal portion gave the soma a somewhat fusiform or bipolar appearance (see Figs. 9, 11 and 12). The other dendritic branches were significantly thinner and usually less than 150 μm long. The thick processes, in contrast, extended for up to 1 mm horizontally in layer VI (e.g. Fig. 12) and branched extensively along this length, often resulting in highly asymmetric shapes of the basal dendritic field. Figure 13 shows an extreme

Figure 9. Camera lucida drawing of the cell shown in (a) of Fig. 8. In addition to the features described in that figure legend, this drawing shows the thin apical dendrite reaching layer I, the short dendritic branches originating from layer V, and the short, thin ascending vertical axonal subcollaterals described in the text. No dendritic side branches originate from, or pass into, layer IV. The marked difference in the horizontal extent of apical dendritic and basal dendritic branches is quite apparent in this cell.

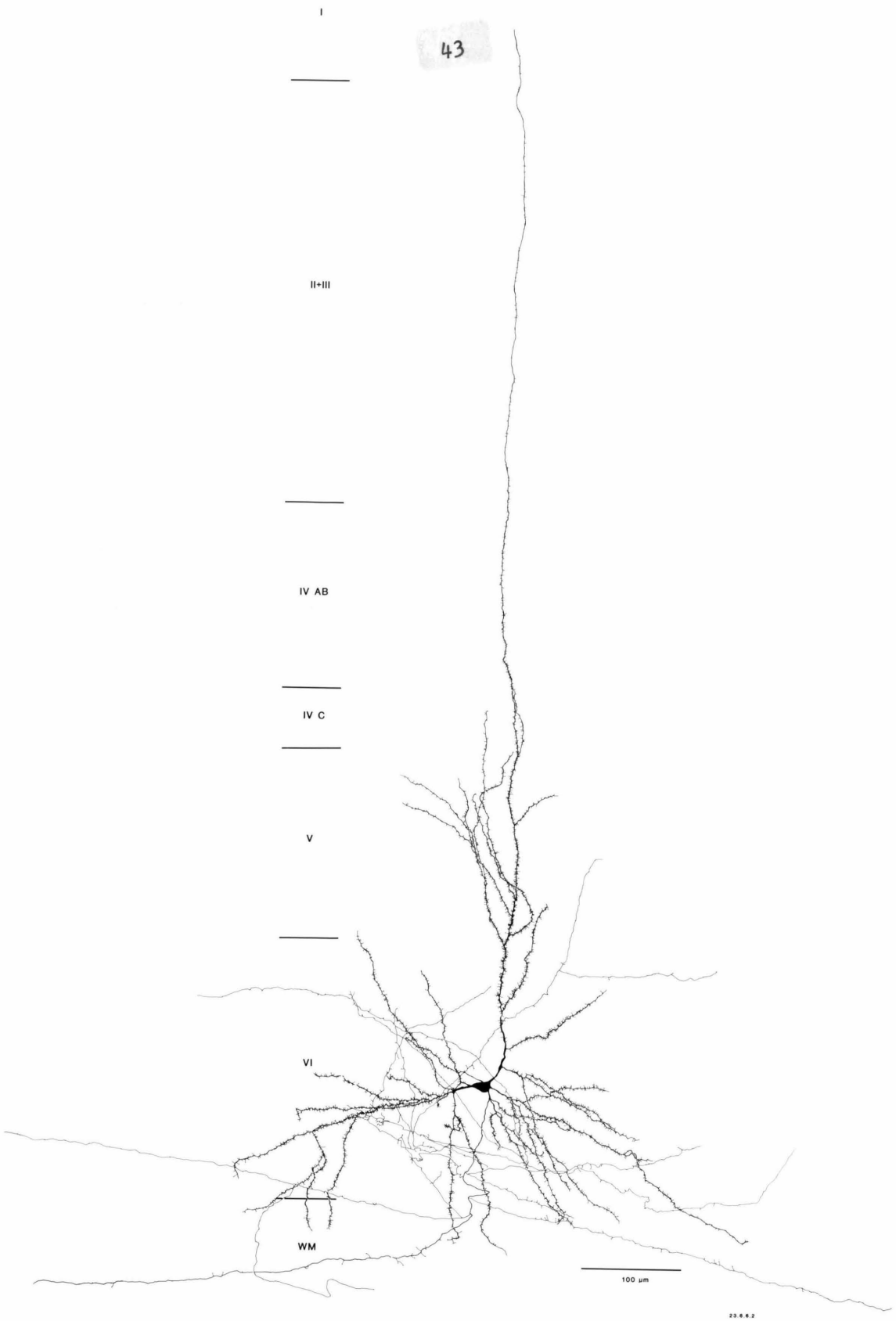
43
I
II+III
IV AB
IV C
V
VI
WM
100 µm
23.6.6.2

Figure 10. Size distributions of retrogradely labeled (open bars) and double labeled (solid bars) neurons after LGN (top) and claustrum (bottom) injections. Mean somal area of LGN-projecting cells was 143 μm^2 ± 41.5 S.E.M., n=100. Mean somal area of claustrum projecting cells was 155 μm^2 ± 34.7 S.E.M., n 100.

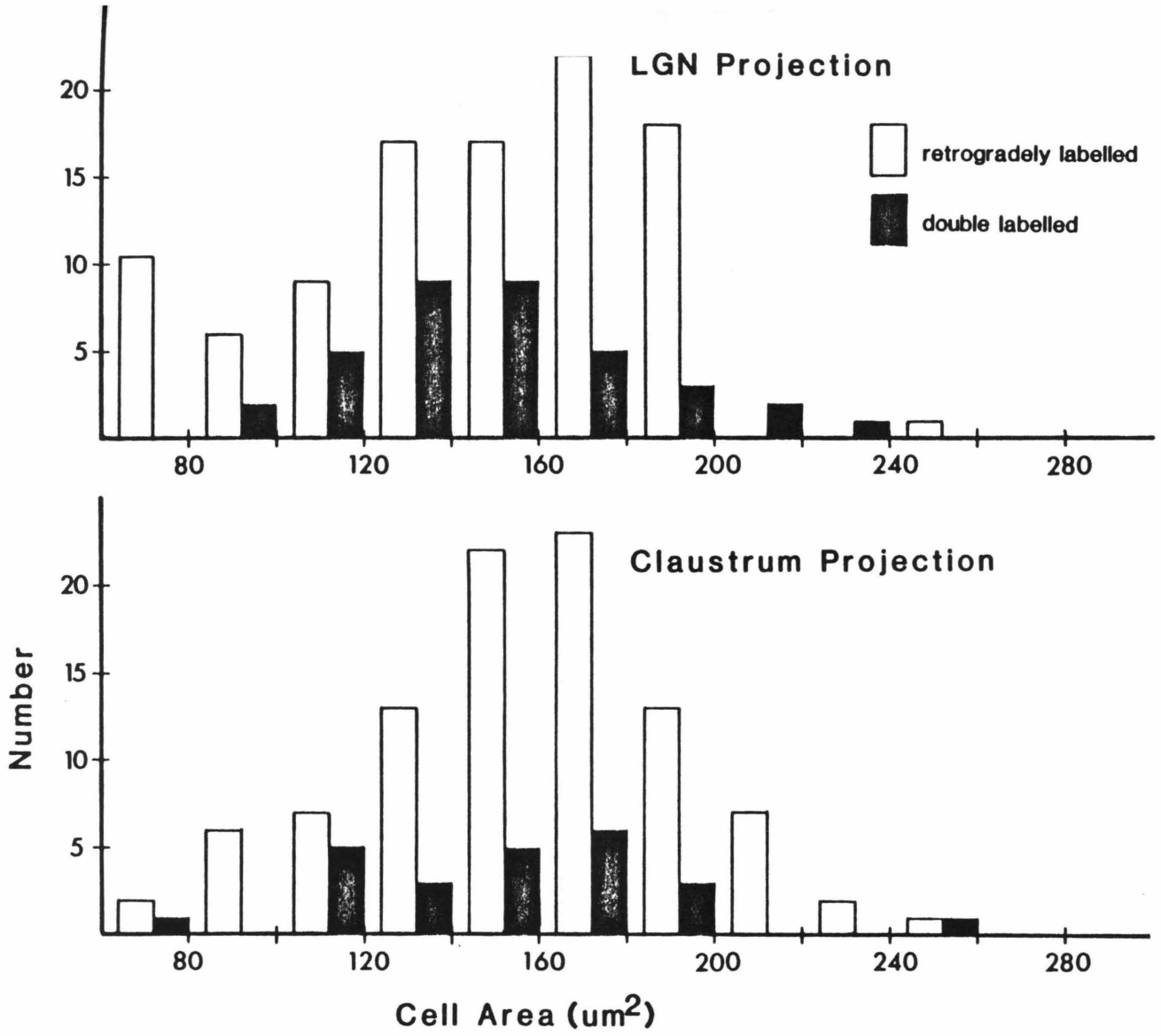
LGN Projection
retrogradely labelled
double labelled
20
15
10
5
80
120
160
200
240
280
Claustrum Projection
Number
Cell Area (um2)

example of this: two asymmetric basal dendritic processes each run horizontally, forming a dendritic field with a diameter of almost 1 mm. The overall branching pattern of these cells was reminiscent of an umbrella (with the "handle" pointing towards the white matter). The dendrites arched over an extensive area, but within that enclosed space, the processes tended to be short. This tendency is shown graphically by sector analysis of Sholl plots, which gave a rough indication of the length of dendrites in each sector (Fig. 14). These plots were obtained from Scholl analysis (as described above) in which the concentric cirles were divided into eight 45^{o} sectors, with a line running through the center of the cells soma, parallel to the apical dendrite, defining the 0^{o} axis. Although all cells had the thick dendritic process, in some cases (e.g. Figs. 15, 16) the absence of a long process resulted in a dendritic arbor considerably smaller (approximately 200 μm in diameter) and more symmetric than those described above. Since claustrum projecting cell bodies are generally located in the middle of layer VI, most of the observed asymmetries did not result simply from constraints on dendritic branching imposed by close proximity to the white matter.

These unusually extensive basal dendrites have not been described in Golgi preparations of cat cortex. However Lund and Boothe (1975) briefly mentioned a similar sort of cell in layer VI of monkey visual cortex, with an unknown efferent target. The structure of these dendrites has several implications for the types of input these cells can recieve. Clearly dendrites with the extent described here could integrate inputs from at least one ocular dominance column, or span a considerable portion of two. These cells may represent a population of layer VI cells that are binocular, in contrast to the majority, which are strongly monocular (and have, as the section on geniculate cells below describes,

Figure 11. A claustrum projecting cell with a bipolar soma, caused by the presence of a very thick basal dendritic process. This cell has a wide basal dendritic arbor, with processes extending into the white matter. The apical dendrite reaches only to the middle of layer IVab, with few side branches. The horizontal axonal collaterals are very extensive and well developed, and show numerous vertically oriented subcollaterals, seemingly in clusters spaced at about 300 μm intervals.

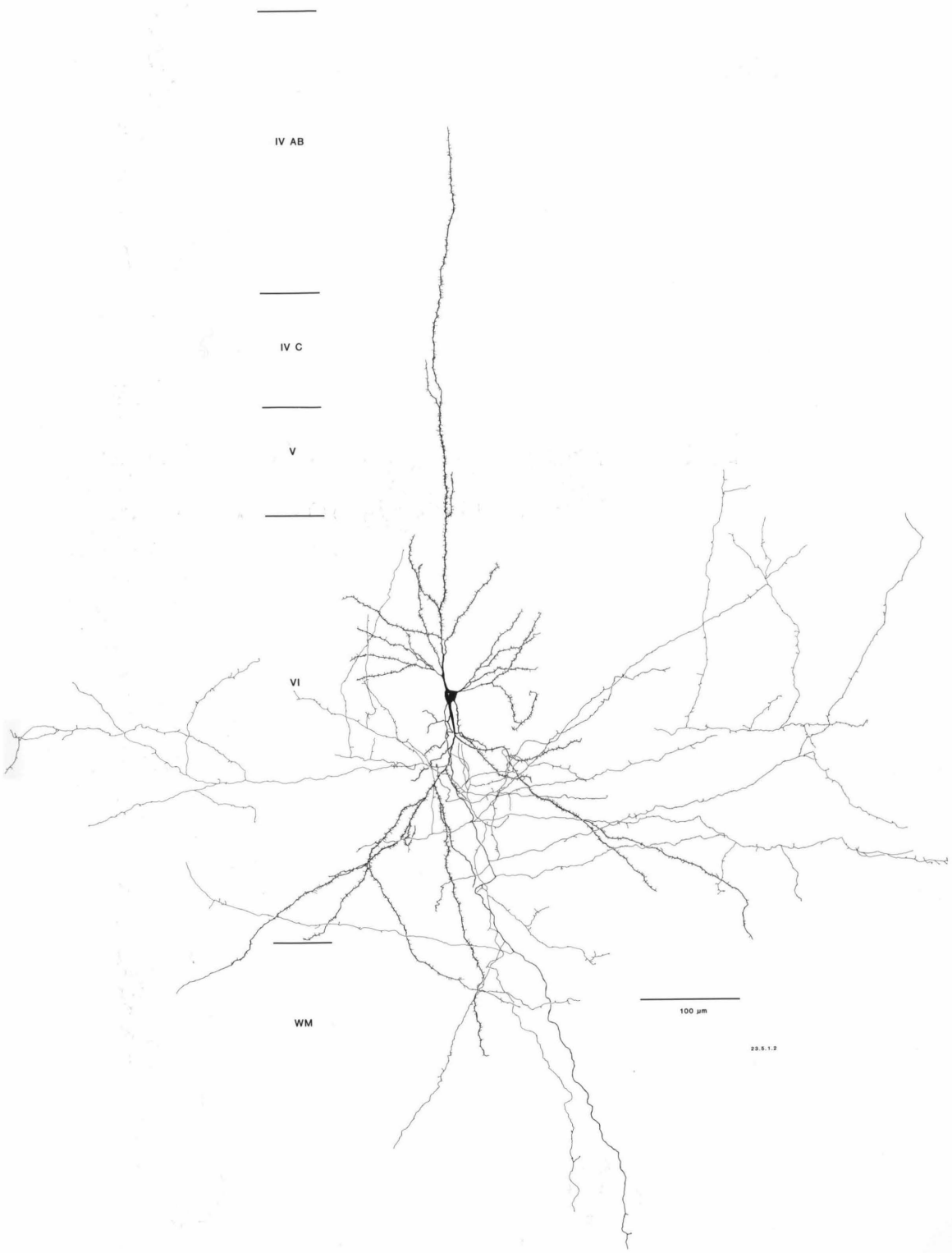
IV AB
IV C
V
VI
WM
100 µm
23.5.1.2

Figure 12. A claustrum projecting cell with a highly elongated basal dendritic process. Additionally, one of this cell's apical dendritic side branches appears to skip over an intervening segment of cortex, and arborize about 200 μm from the main cluster of apical dendritic branches (see also Fig. 15).

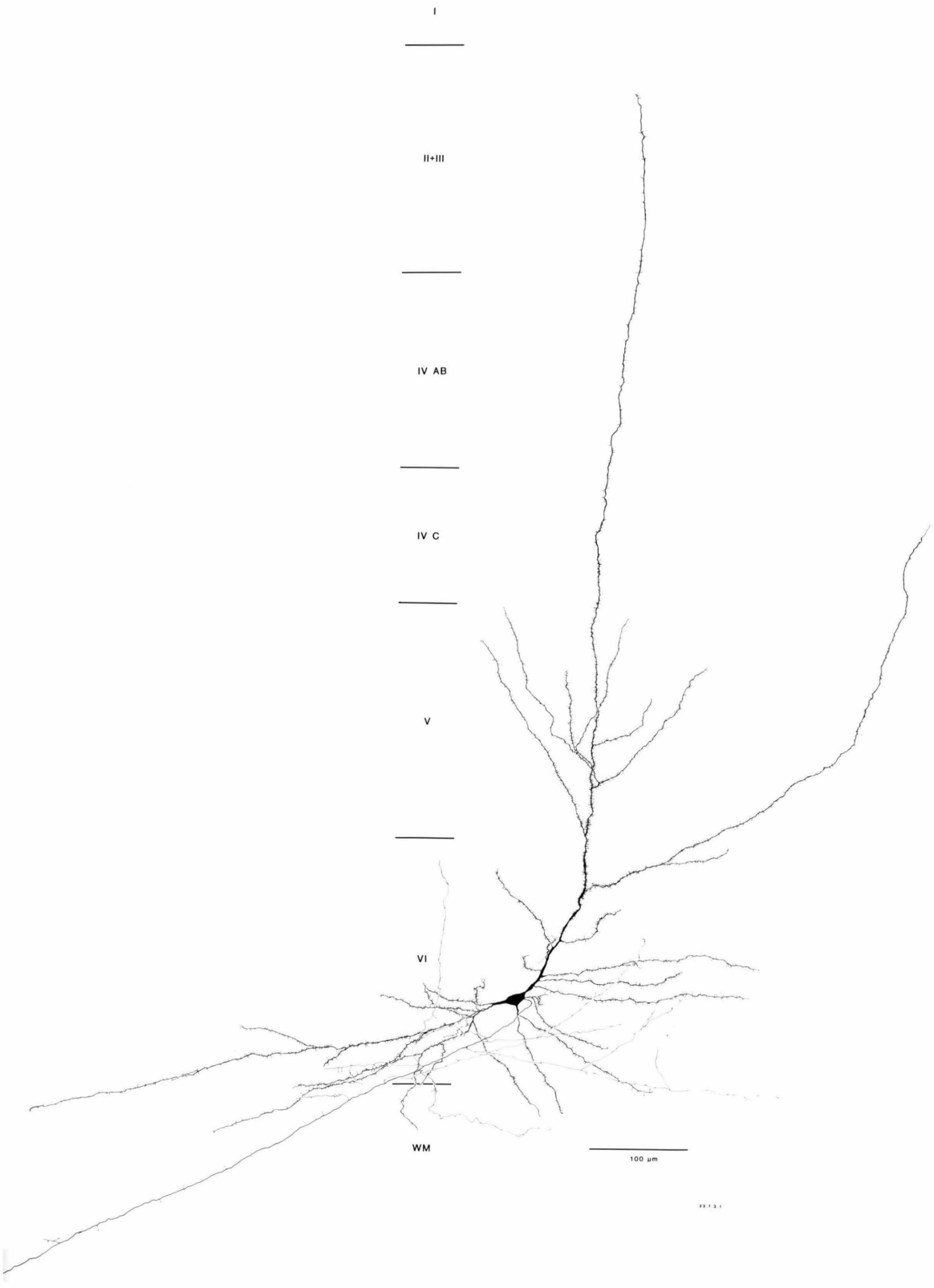
I
II+III
IV AB
IV C
V
VI
WM
100 µm

Figure 13. A claustrum projecting cell with an extreme example of the basal dendritic asymmetry, and the difference in horizontal extent of basal and apical dendrites. In this case, two asymmetric basal dendritic processes originate from the soma and run in opposite directions, forming an arbor almost 1 mm in diameter. In contrast, the spread of the apical dendritic side branches is about 200 μm.

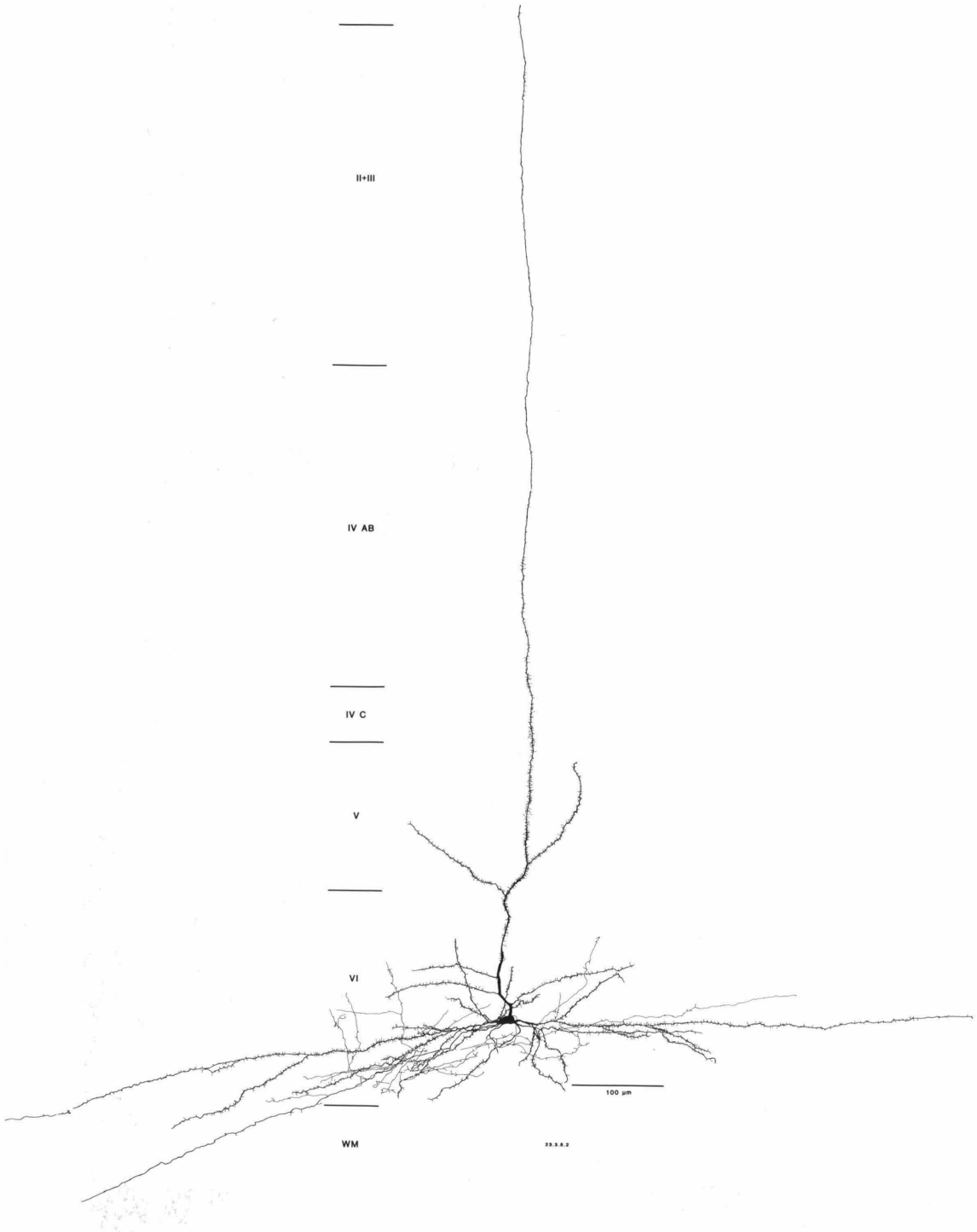
II+III
IV AB
IV C
V
VI
WM
100 µm
29.5.5.2

Figure 14. Sector Sholl analysis of the basal dendritic arbors of LGN and claustrum projecting cells, as described in the text. The characteristic asymmetric, umbrella shape of claustrum projecting cells' basal dendrites shows clearly, and contrasts with the considerably more regularly shaped basal dendrites of LGN projecting cells. In this figure, 0 refers to the direction of the apical dendrite, the concentric circles represent iso-length contours for the total length of dendrite in each of the sectors.

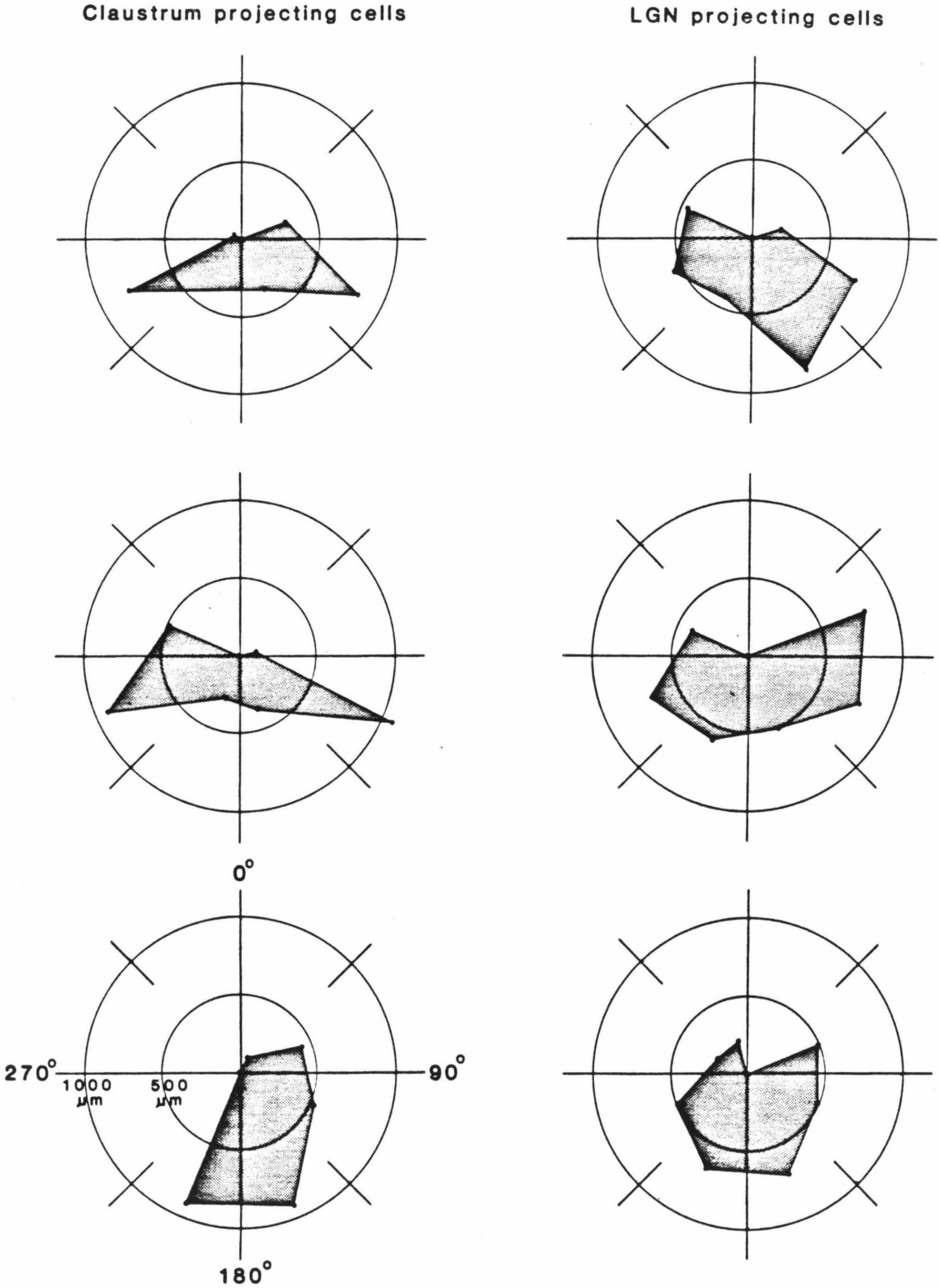
Claustrum projecting cells
LGN projecting cells
0°
270°
90°
180°
1000 µm
500 µm

considerably more restricted basal dendritic fields), which would fit well with the observed response properties of cells within the claustrum, which are strongly binocular (Sherk and LeVay 1981).

One other noteworthy feature of the basal dendritic field was that dendrites, in may cases, did not repect the grey/white matter border: portions of the basal dendrites often extended for up to 100 μm into the white matter (see, e.g., Figs. 9, 16, 17). As described in more detail below, these cells, as well as geniculate projecting cells, often have portions of their intrinsic axonal collaterals in this zone of white matter subadjacent to layer VI. Thus this region may be similar to layer I, in that it contains distal portions of dendrites as well as axon terminals, but contains very few cell bodies.

Apical dendrites

Most claustrum projecting cells possessed a long, thin apical dendrite that reached the bottom of layer I (Figs. 9, 15) In a few cells the apical dendrites only reached to layer IV (Figs. 11, 17). In both cases, the apical dendrite had occasional branches along its length, restricted to layers VI and V. In no case did branches either originate in or pass into layer IV. These apical side branches were usually short, less than 200 μm in length, and restricted in their horizontal extent. Branches that originated in layer V coursed upwards rather steeply and terminated at the V/IV border. After leaving the apical dendrite they either did not branch or branched once before terminating. The cells in Figs. 9, 13 and 18 illustrate these features well. As a rule, the horizontal spread of the apical dendritic arborization was considerably narrower than that of the basal dendrites. Although the function of apical dendrites is obscure, they are likely to play some sort of modulatory role on the responses of cells. In this regard it is interesting that the apical dendrites of these cells are "listening" to a much

narrower zone of a column than are the basal dendrites. It may be that in these cells the apical dendrite's effect, whatever specific form it takes, is rather reduced in comparison to the basal dendrite.

Occasionally cells had one process in layer V considerably longer and more horizontally extended than the others, as shown in Figs. 12 and 15. Interestingly, such processes always had roughly twice the horizontal extent of the main apical dendritic arbor. There were no intermediate forms, and thus these horizontal processes gave the impression of skipping over an area of cortex about 200 μm wide in order to arborize in some specific, more distant area.

Dendritic spines

A third distinguishing feature of these cells was the presence, on both apical and basal dendrites, of very large numbers of dendritic spines. Spines had a uniform size and morphology: usually a classic simple spine with a narrow (approximately 0.25 μm diameter) stalk, 3-5 um long, topped by a sphere approximately 0.5 μm in diameter (Fig. 19).

A brief investigation of the distribution of spines was conducted in order to investigate for any possible relationship between synapse density and innervation from the claustrum. Along the apical dendrite, spines reached their highest density in the upper portion of layer VI and the lower portion of layer V (Fig. 20). Spine density, high throughout layer V, dropped off dramatically in the upper layers.

The basal dendrites' spine density, although also heavy, did not reach the density of the spiniest portion of the apical dendrite. As in most pyramidal cells, the middle section of dendrites had the greatest spine density (Jones 1975, Cajal 1911). In particular the long, thick process usually had the highest spine density, and the portions of the dendrites in the white matter were sparsely spined.

The relationship between spine density and patterns of claustrum afferents is detailed in **Discussion.**

Axonal collaterals

The structure of the intrinsic axonal arbor provided the most obvious, consistent feature of claustrum projecting cells. Observations on the laminar distribution pattern of collaterals showed virtually identical patterns in every cell, and these differed completely from the pattern observed for LGN projecting cells, as discussed below. Claustrum projecting cells had a main efferent axon, approximately 0.7 um in diameter, which emanated from the lower part of the cell body or from the initial portion of a basal dendrite. Before entering the white matter, it emitted 3-5 fine (0.2 μm diameter), horizontally directed collaterals (Fig. 21). These collaterals continued in layer VI for at least 500 μm and frequently longer, up to 1 mm (Figs. 9, 15). Along this course they periodically showed various specializations, such as swellings (about 0.5 μm diameter) and spine like appendages, which probably represent sites of en passant synapses (LeVay 1973). At periodic intervals, these horizontal processes emitted shorter vertically directed subcollaterals of the same or finer diameter, which rose no higher than the lower half of layer V, where they terminated (Figs. 11, 15). These subcollaterals exhibited many of the spine like appendages seen on the horizontal processes. In several cases the vertical processes seemed to form clusters of terminals, as previously described for other cortical neurons by Gilbert and Wiesel (1983). Subjectively, the course of the vertical collaterals seemed to run as if associated with the apical dendrites of some unidentified postsynaptic cells.

The cells whose apical dendrite terminated in layer IV (Figs. 11, 17) had the most extensive horizontal collaterals, as well as the best examples of clustered

Figure 15. A claustrum projecting cell with a thick, basal dendritic process, but having an overall symmetric basal dendritic arbor. This cell has well developed horizontal collaterals, with a cluster of vertically ascending processes in the vicinity of the apical dendrite. Additionally, one apical dendritic side branch has an arbor about 200 μm distant from the apical dendrite, giving the appearance of having skipped over the intervening portion of cortex.

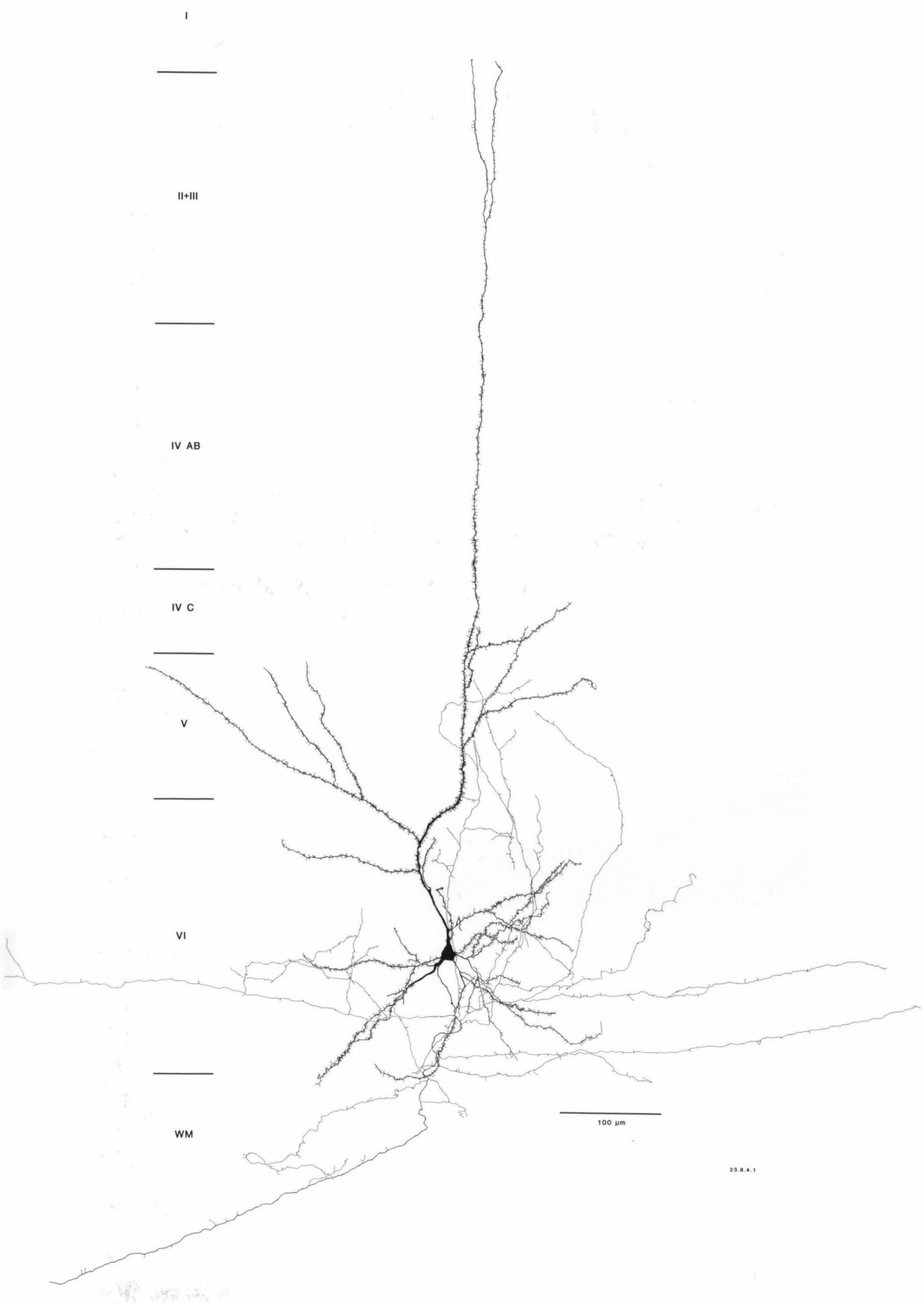
I
II+III
IV AB
IV C
V
VI
WM
100 µm
23.8.4.1

Figure 16. Another claustrum projecting cell, which, like the one in Fig. 15, has a thick basal dendritic process but an otherwise symmetric arbor. This cell has extensive portions of its dendritic arbor in the white matter immediately subadjacent to layer VI; numerous short axonal collaterals originate within that zone as well.

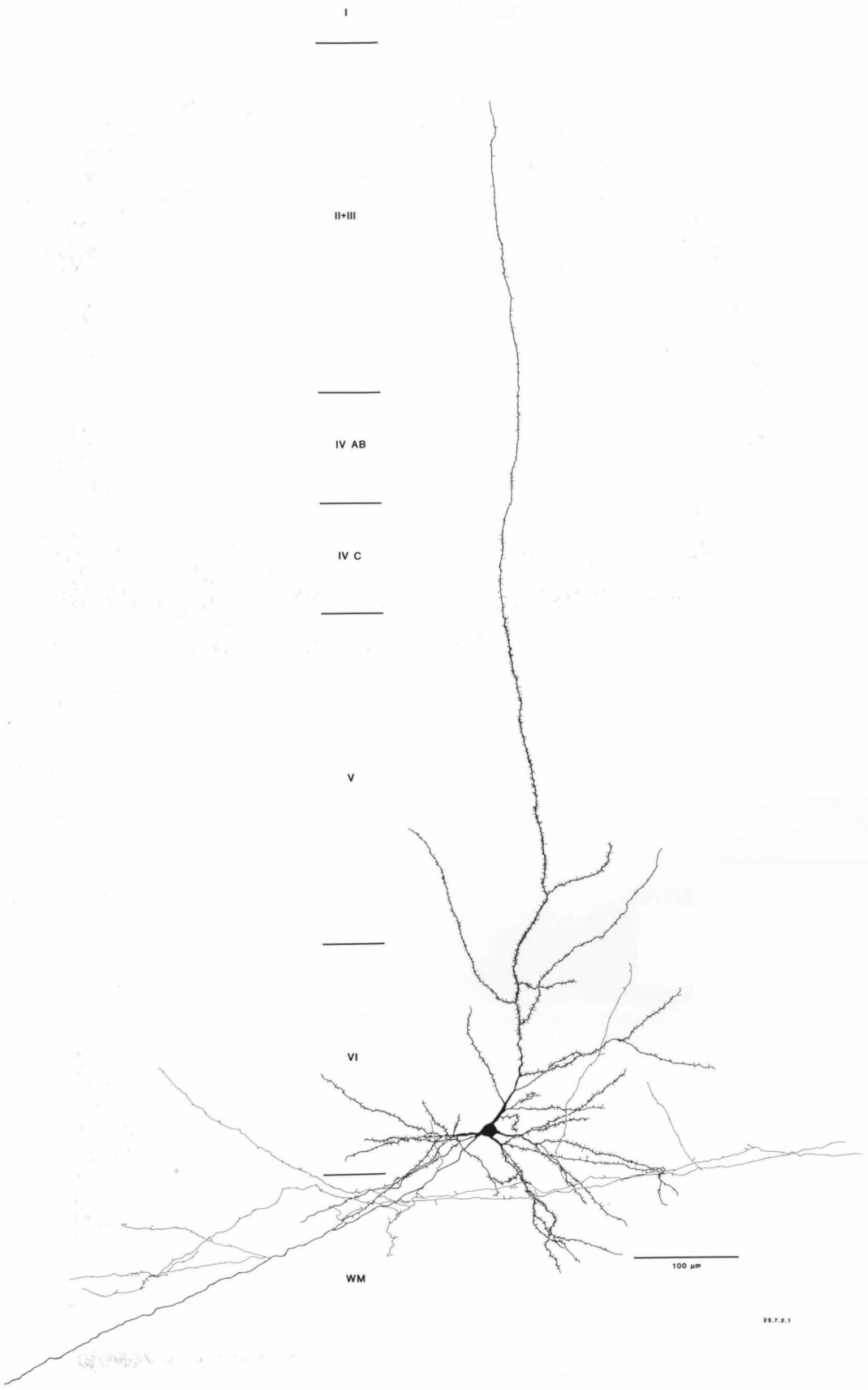
I
II+III
IV AB
IV C
V
VI
WM
100 µm
23.7.2.1

Figure 17. A claustrum projecting neuron similar to that shown in Fig. 11. The apical dendrite goes no higher than the middle of lamina IVab; the extensive horizontal collaterals give rise to a dense cluster of vertical subcollaterals immediately to the right of the apical dendrite, in layer VI. Considerable portions of the basal dendrite arborize within the white matter subadjacent to layer VI.

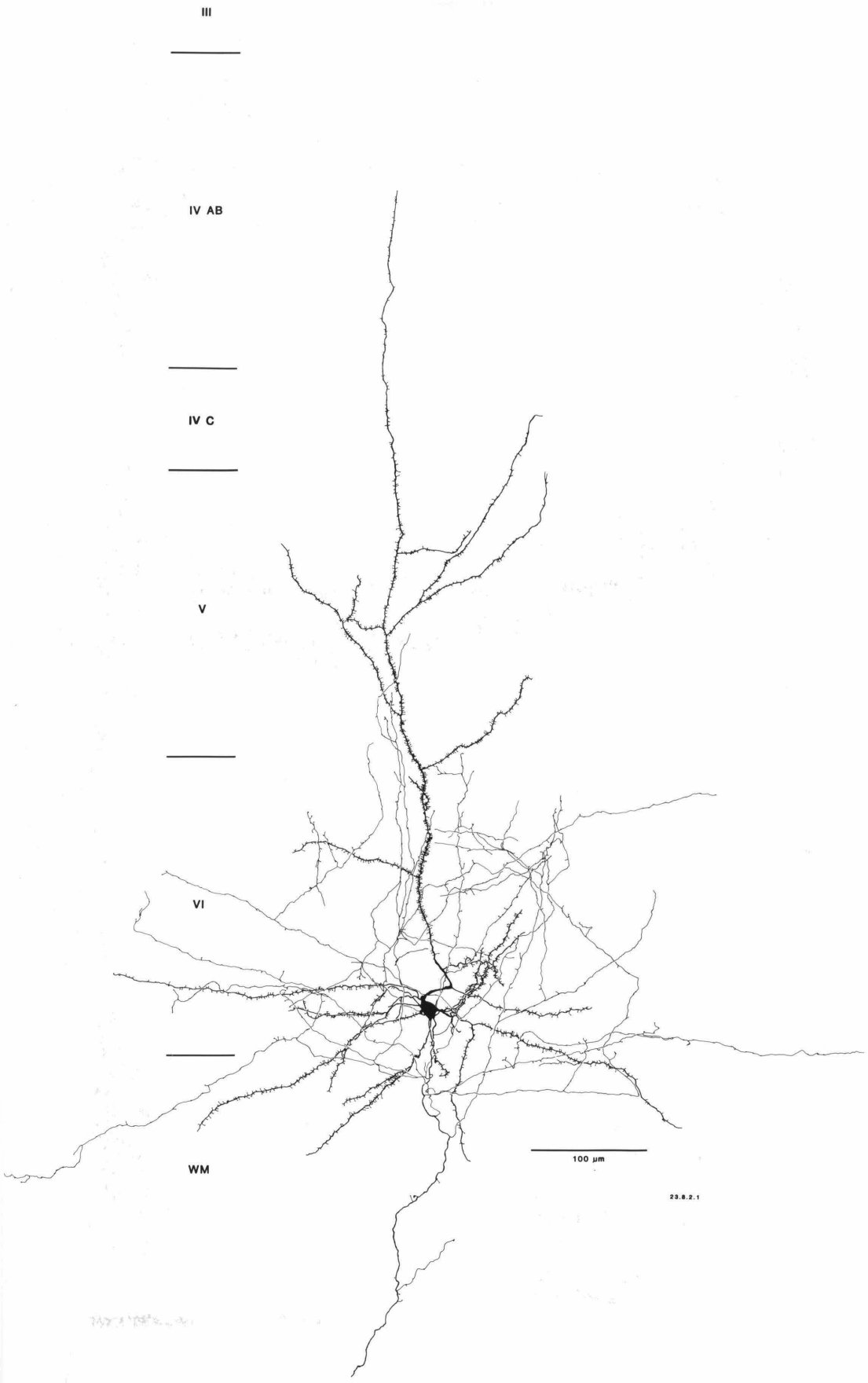
III
IV AB
IV C
V
VI
WM
100 µm
23.8.2.1

Figure 18. An unusual claustrum projecting neuron with two thin apical dendrites reaching to the top of layer II. In other respects the cell shows standard claustrum projecting cell features: an umbrella shaped (although symmetric) basal dendritic arbor, restricted horizontal extent of apical dendrite branches, and horizontal intrinsic axonal collaterals, with vertical subcollaterals reaching lower layer V.

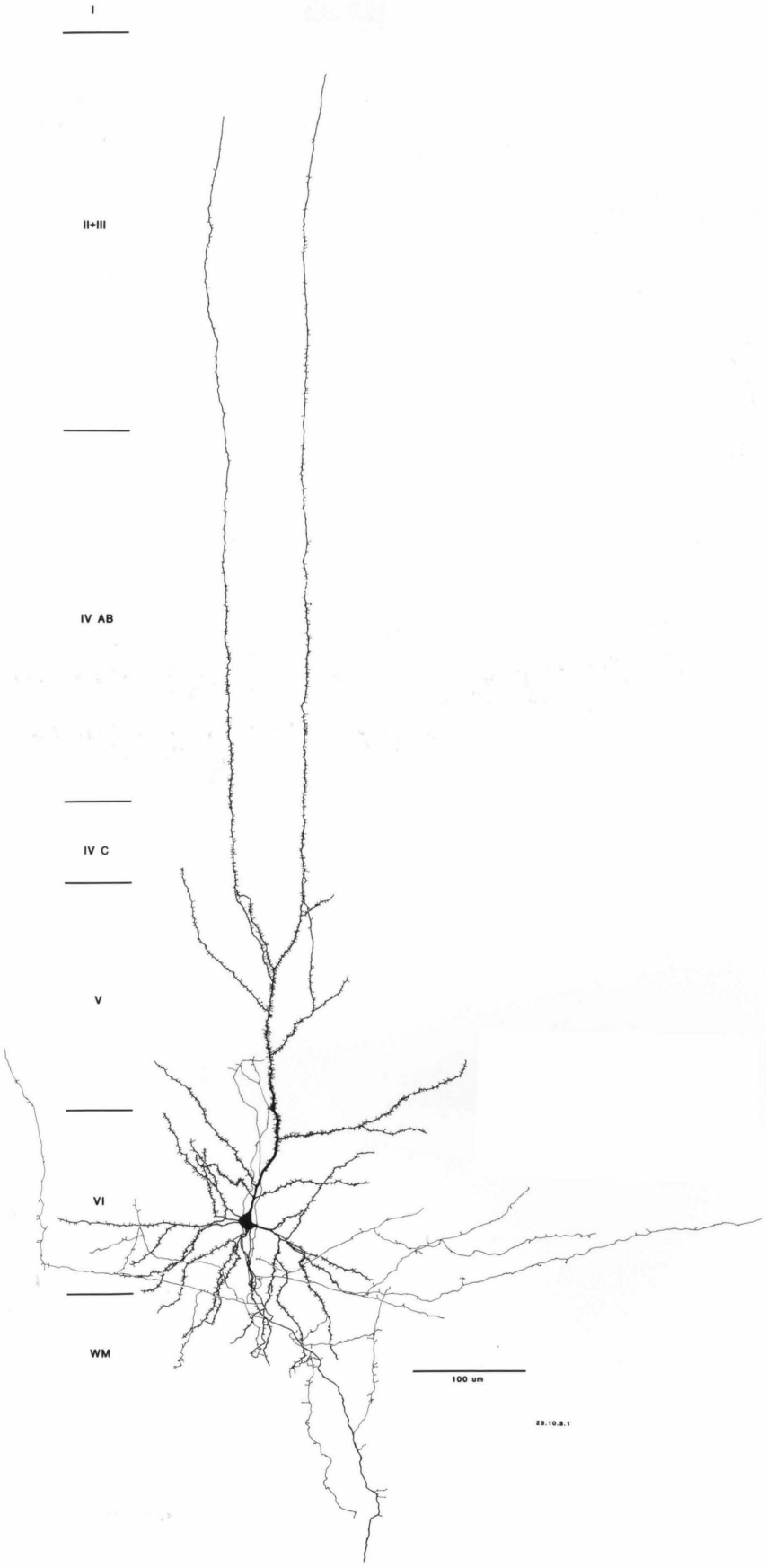
I
II+III
IV AB
IV C
V
VI
WM
100 um
29.10.9.1

Figure 19. A high-power view of a portion of a claustrum projecting cells' apical dendrite, at the border between laminae VI and V. The dendrite is densely covered with simple spines with narrow stalks topped by small spheres. The spines appear to be roughly uniform in size and shape. Scale bar: 20 μm.

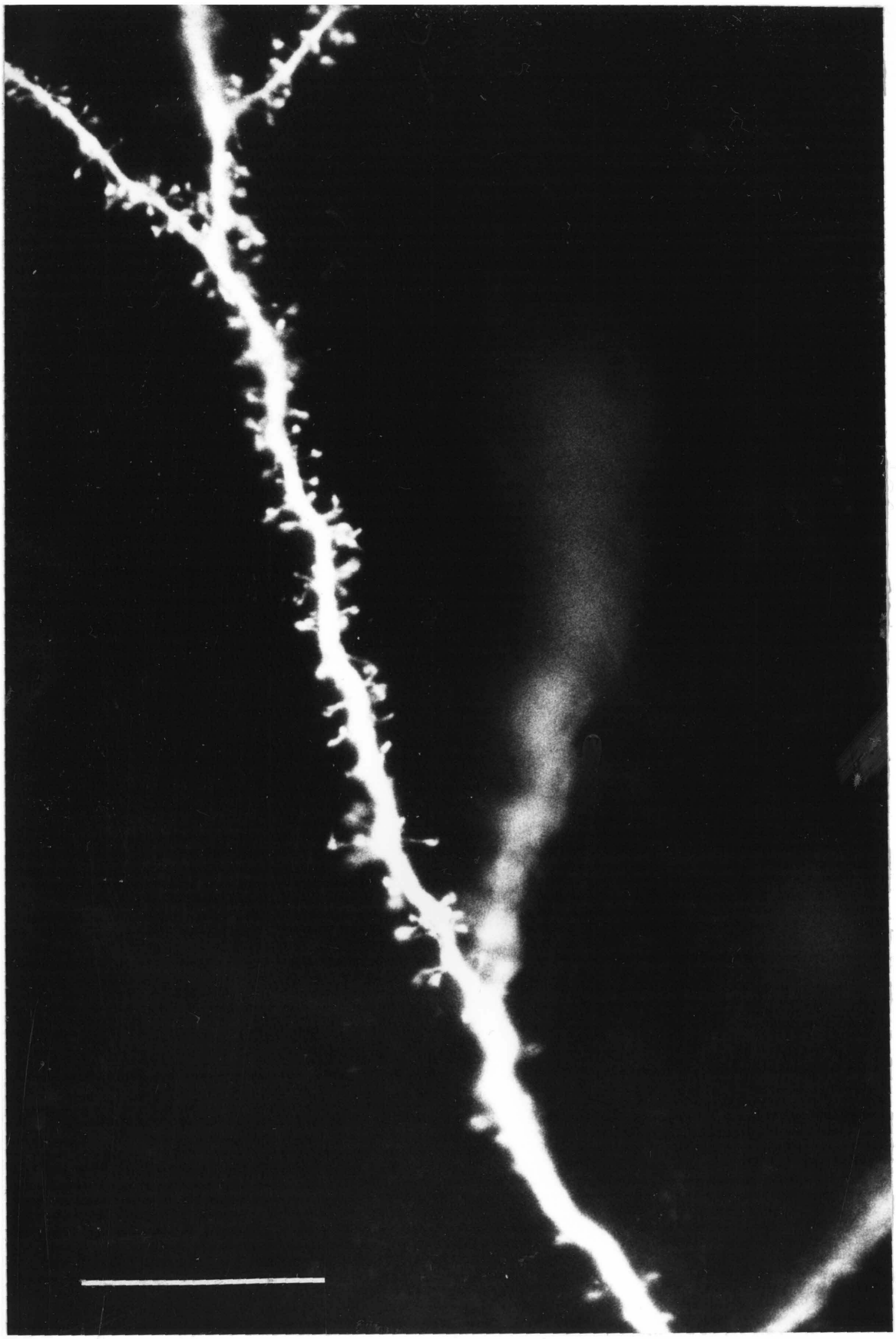

Figure 20. Numbers of spines along the apical dendrite of representative claustrum and LGN projecting neurons. Counts were made along 40 μm long segments; the Roman numerals on top of each histogram refer to boundaries of the cortical laminae. Both projection classes showed a prominent peak of spine density at the layer VI/V border, some claustrum projecting cells had a smaller secondary peak at the IVc/IVab border.

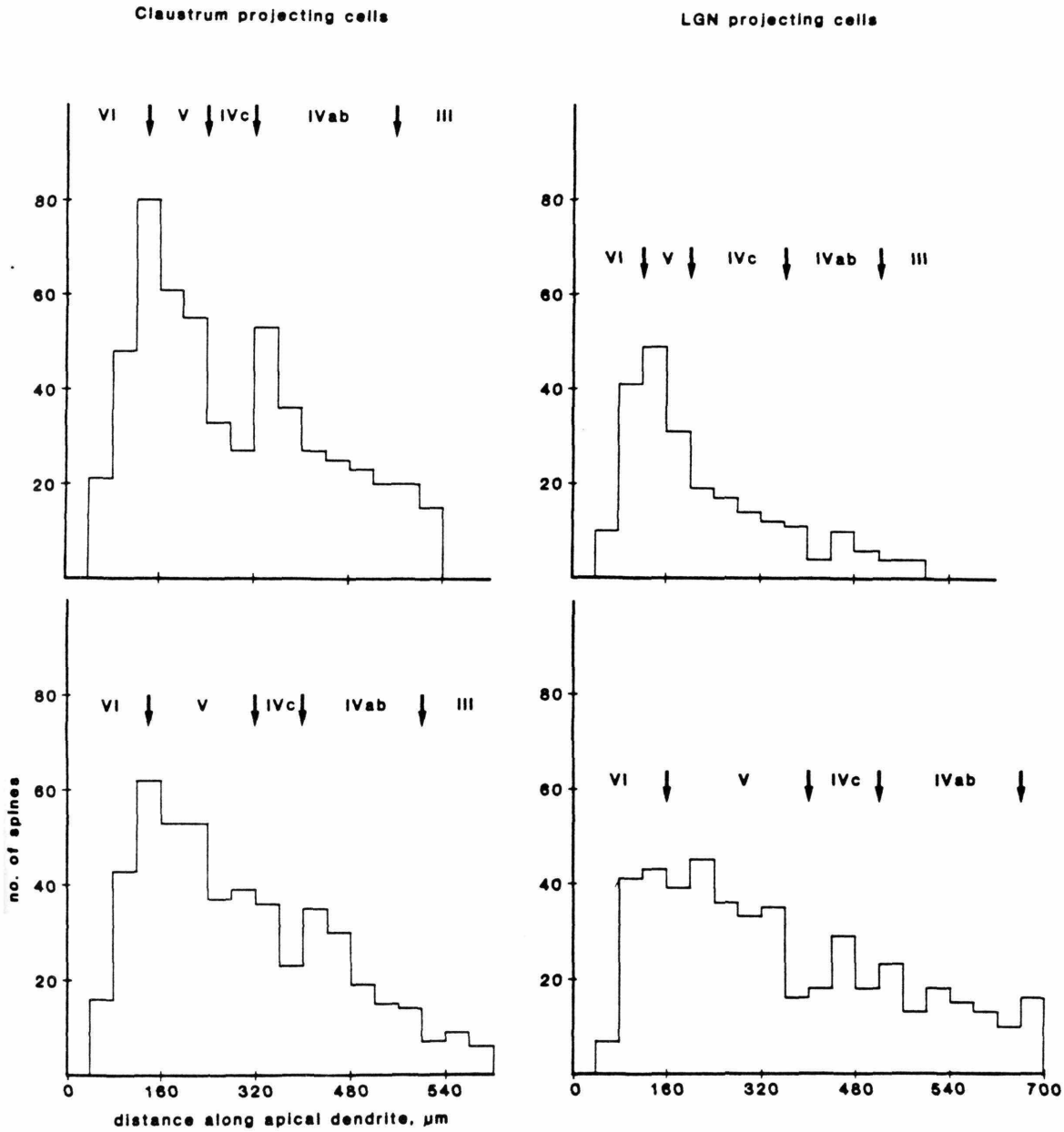
Claustrum projecting cells
LGN projecting cells
VI
V
IVc
IVab
III
80
60
40
20
no. of spines
0
160
320
480
540
700
distance along apical dendrite, µm

Figure 21. Close-up view of the efferent axon and horizontal collaterals of the cell shown in Fig. 8a. The thick arrows point to the very thin, horizontally directed subcollaterals, which are considerably thinner than the main efferent axon. The thin arrow shows a small subcollateral originating in the white matter. Scale bar: 20 μm.

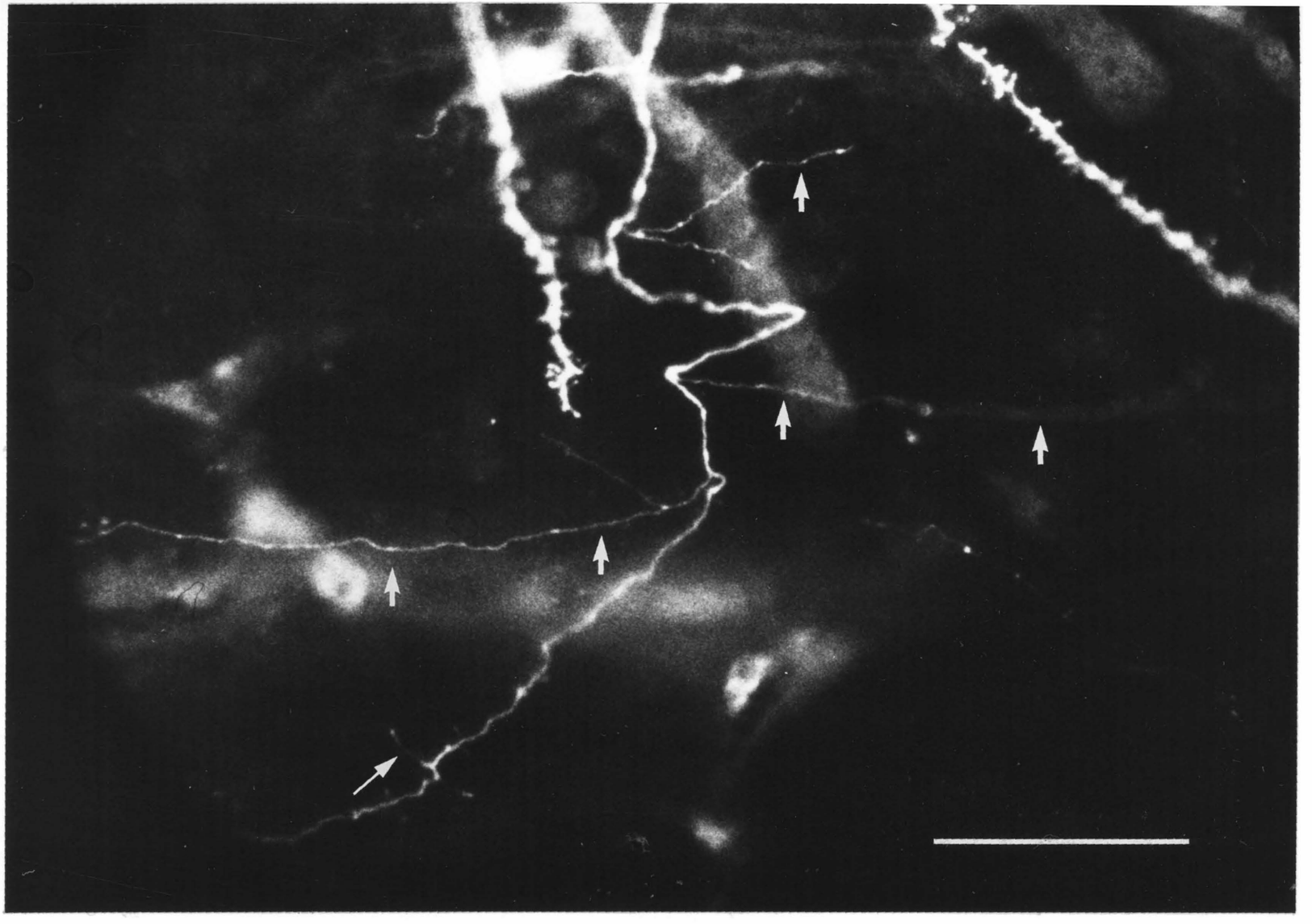

Figure 22. Detail of a claustrum projecting cell's axonal subcollateral (thin arrows) with several en passant boutons (arrowheads) originating from the main efferent axon (thick arrows) within the white matter. The thicker process at the top of the figure, a dendritic process from the same neuron, also arborizes in the white matter. Scale bar: 20 μm.

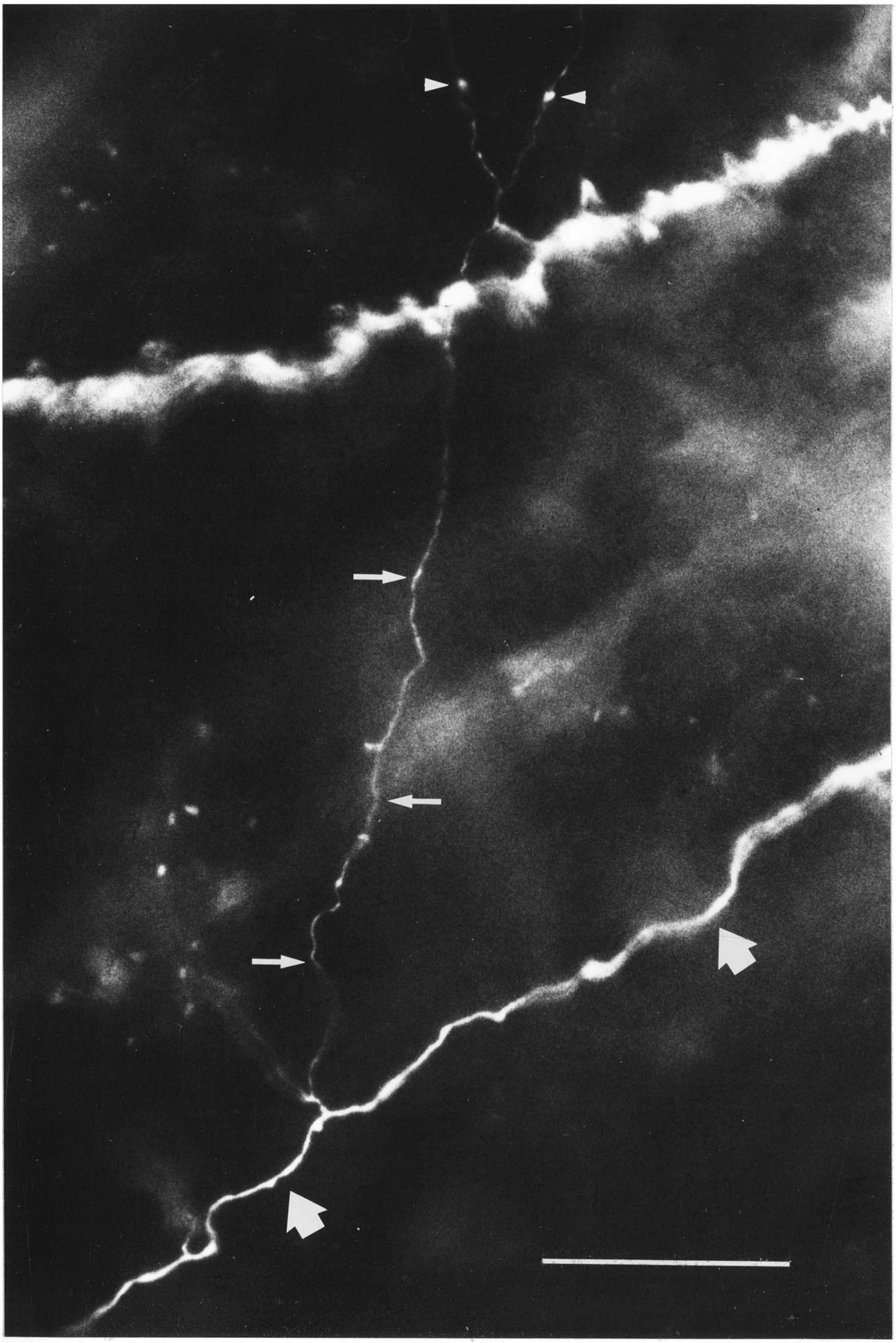

ascending collaterals. In these examples clusters of vertical collaterals seemed spaced at about 300 μm intervals.

Claustrum projecting cells often had a short collateral originating from the main axon after it had entered the white matter (Fig. 22). These collaterals did not show the marked horizontal orientation of the collateral originating in the grey matter; however their existence (along with the presence of dendritic processes from these cells) suggests, as within layer I, the presence of synaptic contacts in an acellular zone. The main axon itself frequently exhibited spine like appendages in this same zone (see, for example, Figs. 9, 17, 18)

Lateral geniculate nucleus projecting cells: general morphological characteristics

As a group, the geniculate projecting cells showed somewhat greater morphological variability. Most (>80%) were medium to large pyramidal cells with a dense, symmetric basal dendritic arbor, and a highly branched apical dendrite, reaching no higher than layer III, with branches in VI, V, and IV. These cells had few if any axon collaterals in layer VI, possessing instead strong recurrent collaterals to layer IV. Based on differences in the horizontal spread of their ascending dendritic and axonal arbors, these cells were termed class I and II cells. Another set of geniculate projecting cells (class III cells) had a smaller and less profuse (although generally symmetric) basal dendritic field, with apical dendrites that reached no higher than the bottom of layer IVc. The apical dendrite branched occasionally in layer VI, but no branches originated from higher levels. The intrinsic axons of these cells, thin and sparse, did not extend significantly within layer VI, and reached no higher than layer V. In the detailed descriptions given below, the properties of the class I and II cells are considered together since they form the bulk of the geniculate projecting cells;

the characteristics of the type III cells are considered separately.

The separation of these cells into three classes is not completely arbitrary. As discussed in more detail below, the differences between these three classes bear at least some resemblance to the differences between the functionally distinct X, Y and W systems of cortical afferents.

Soma and basal dendrites: class I and II cells

Figure 23 shows several examples of these cells. Most class I cells had a distinctive, small, oval soma, approximately 12 μm along the long axis, which ran parallel to the grey/white matter border. Somal area was less than 120 μm^2, thus placing these cells on the small side of the distribution of geniculate projecting cell sizes (as a group, retrogradely labeled geniculate projecting cells had an average size of 143 μm^2 ± 41.5 S.E.M., n=100) (Fig. 10). These cells had 6-8 basal dendritic arms (X = 6.6 ± 1.0 S.E.M., n=24 for combined class I and II cells), emanating from all points around the soma. These processes, all of similar thickness and length, branched profusely, close to the cell body. As a consequence, the basal dendritic arbor of these cells appeared very dense, compact and highly symmetric, with a radius of approximately 150 μm (Figs. 24, 25).

Class II cells generally possessed a standard pyramidal shaped cell body, somewhat larger than the class I cells. Like the class I cells, these cells had 6-8 dendritic arms, all of equal thickness, which originated from symmetric positions around the soma. However, these dendrites tended not to show nearly as extensive branching as the class I cells, consequently the basal dendritic arbor had a somewhat sparser appearance (Fig. 26). Despite this difference, class II cell dendrites are all of approximately equal length (similar to class I cells, 150 μm) and the basal dendrites show the same sort of symmetric pattern.

Figure 23. Intracellularly stained class I (a and b) and class II (c) lateral geniculate nucleus projecting cells. (A), (b), and (c) all show the dense, symmetric basal dendritic arbor typical of these cells. In (a), the widespread apical dendritic arbor is visible; in (b) some of the processes, particularly some of the extensive side branches, are located on adjacent sections, (see Fig. 24). Arrows indicate the characteristic thick, ascending vertical axonal collaterals. Scale bars: 50 μm.

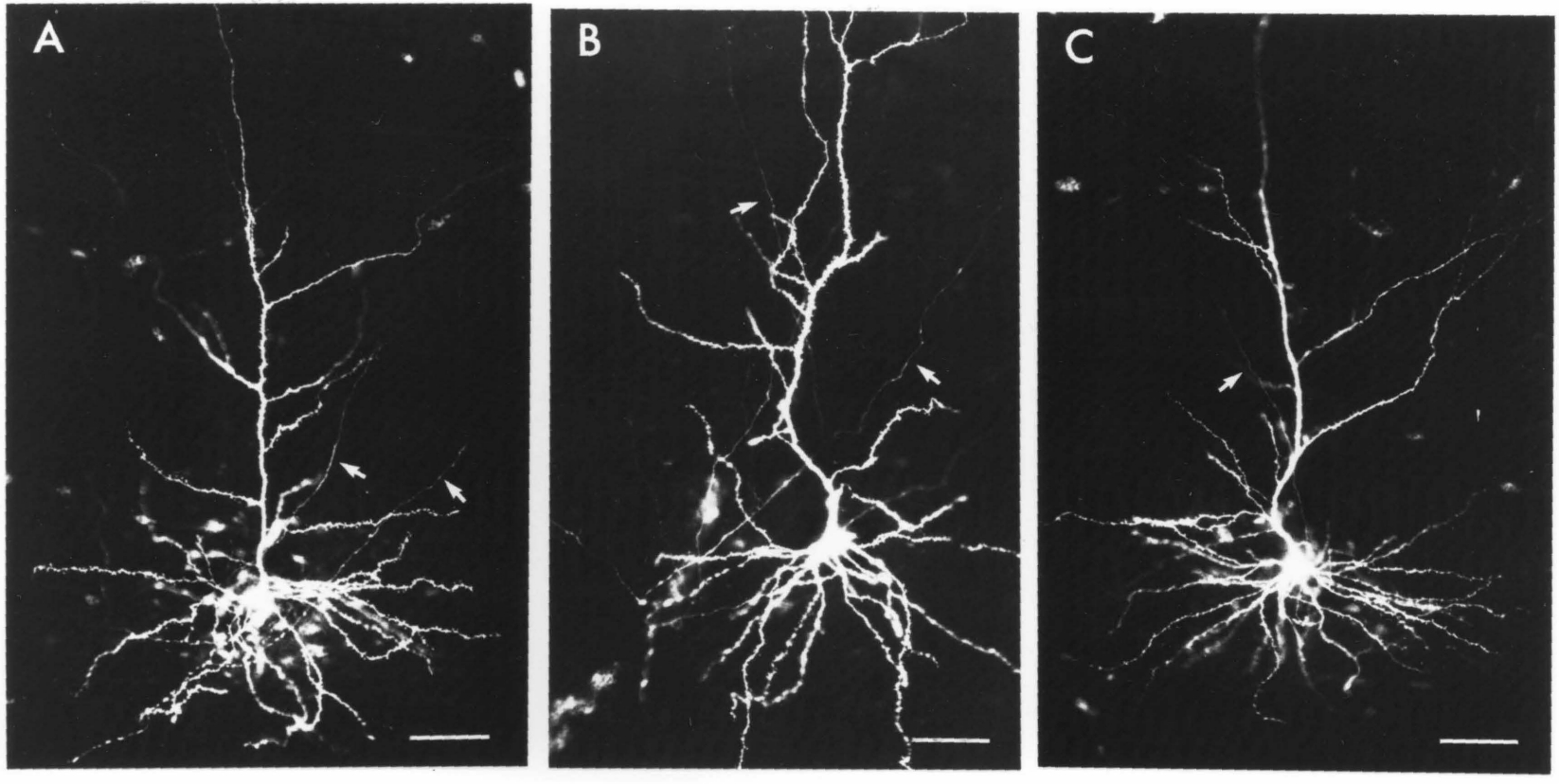
A
B
C

Figure 24. An example of a typical class I LGN projecting neuron. This cell has a small soma, with seven basal dendritic arms of equal length arranged radially around it. The apical dendrite reaches only to layer III, with long horizontal side branches in V and IV. Note the extensive collateral arborization in layer IV, the thick ascending collaterals, and the complete absence of horizontal collaterals within layer VI. A few unmyelinated collaterals originate from the axon in the white matter immediately subadjacent to layer VI.

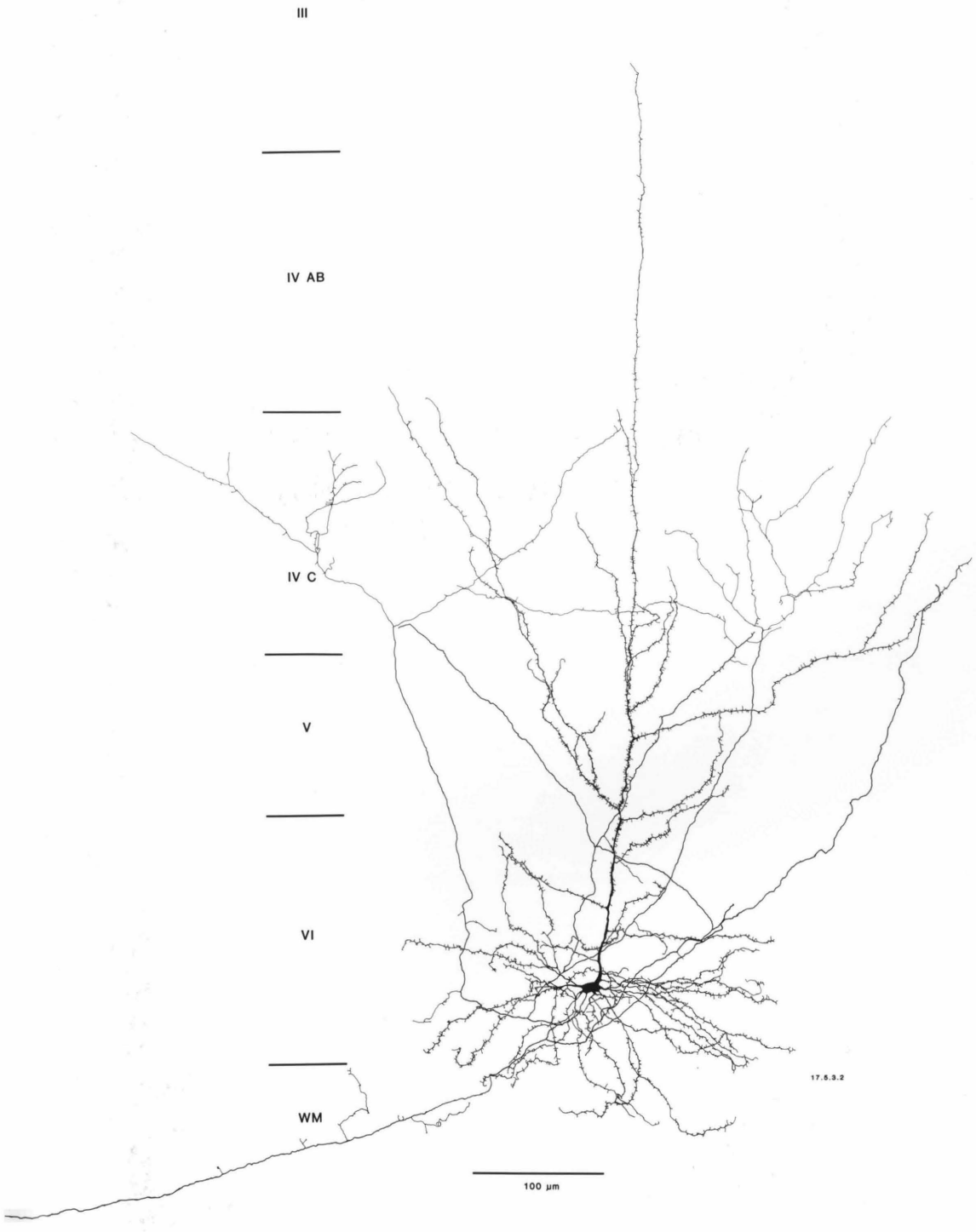
III
IV AB
IV C
V
VI
WM
17.5.3.2
100 µm

Figure 25. A second class I LGN projecting neuron, similar to Fig. 25. In this neuron the apical dendritic branches in layer V form an arbor over 500 μm in diameter, in contrast with the considerably smaller basal dendritic arbor, which is about 300 μm in diameter. The thick ascending collaterals, which have only a small subcollateral in layer VI, arborize over an extensive area in Layer IV.

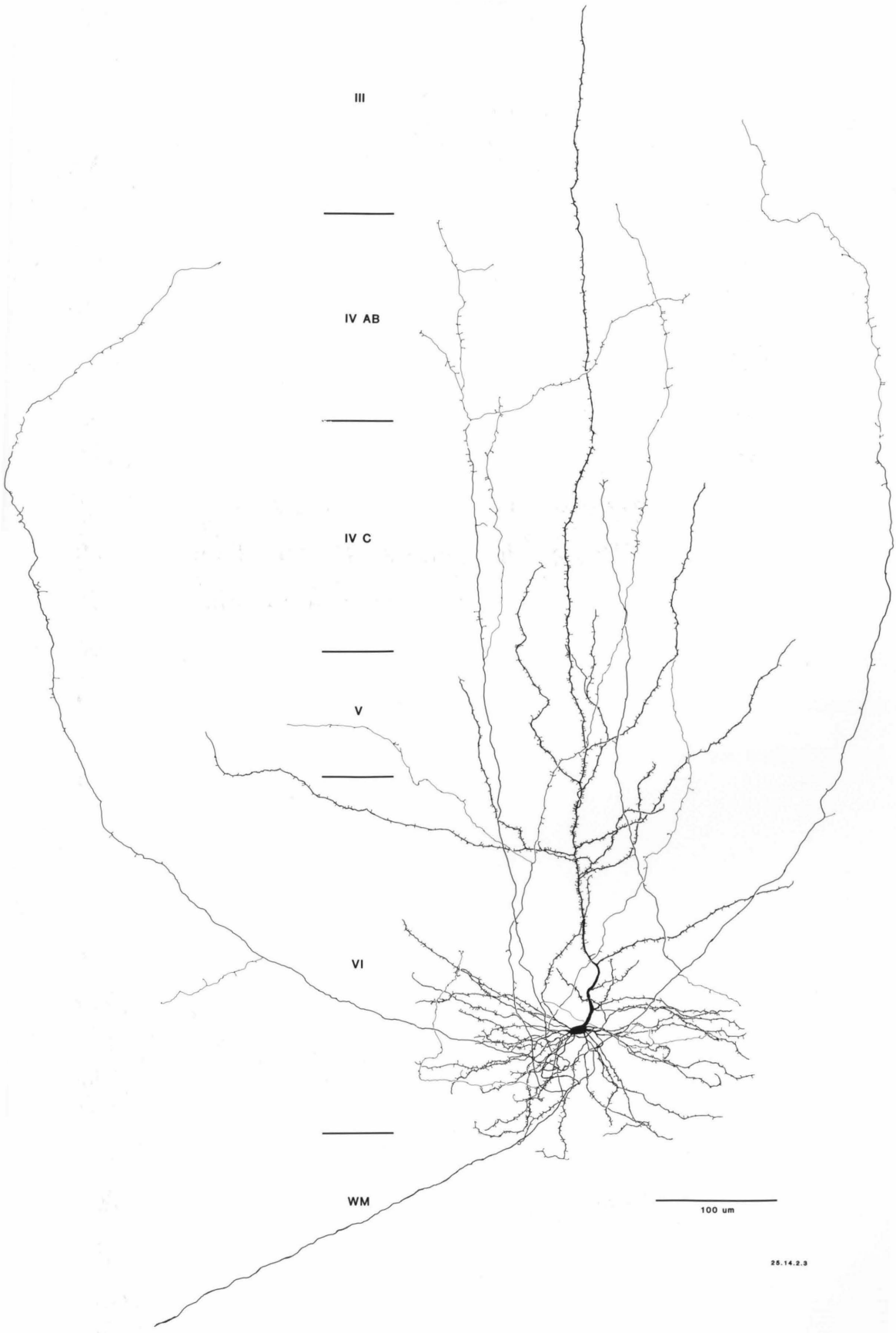
III
IV AB
IV C
V
VI
WM
100 um
25.14.2.3

Figure 26. An example of a class II LGN projecting neuron. The cell has a medium sized, pyramidal soma, with six radially arranged basal dendritic arms. The dendritic arbor is somewhat sparser than that of class I cells. The apical dendrite extends to layer III, with side branches more vertically directed than those of class I cells. The ascending axon collaterals, thinner and more vertically oriented than class I cell's axons, also have somewhat greater number of collaterals, thin and unmyelinated, within layer VI. The ascending axons terminate within layer IV.

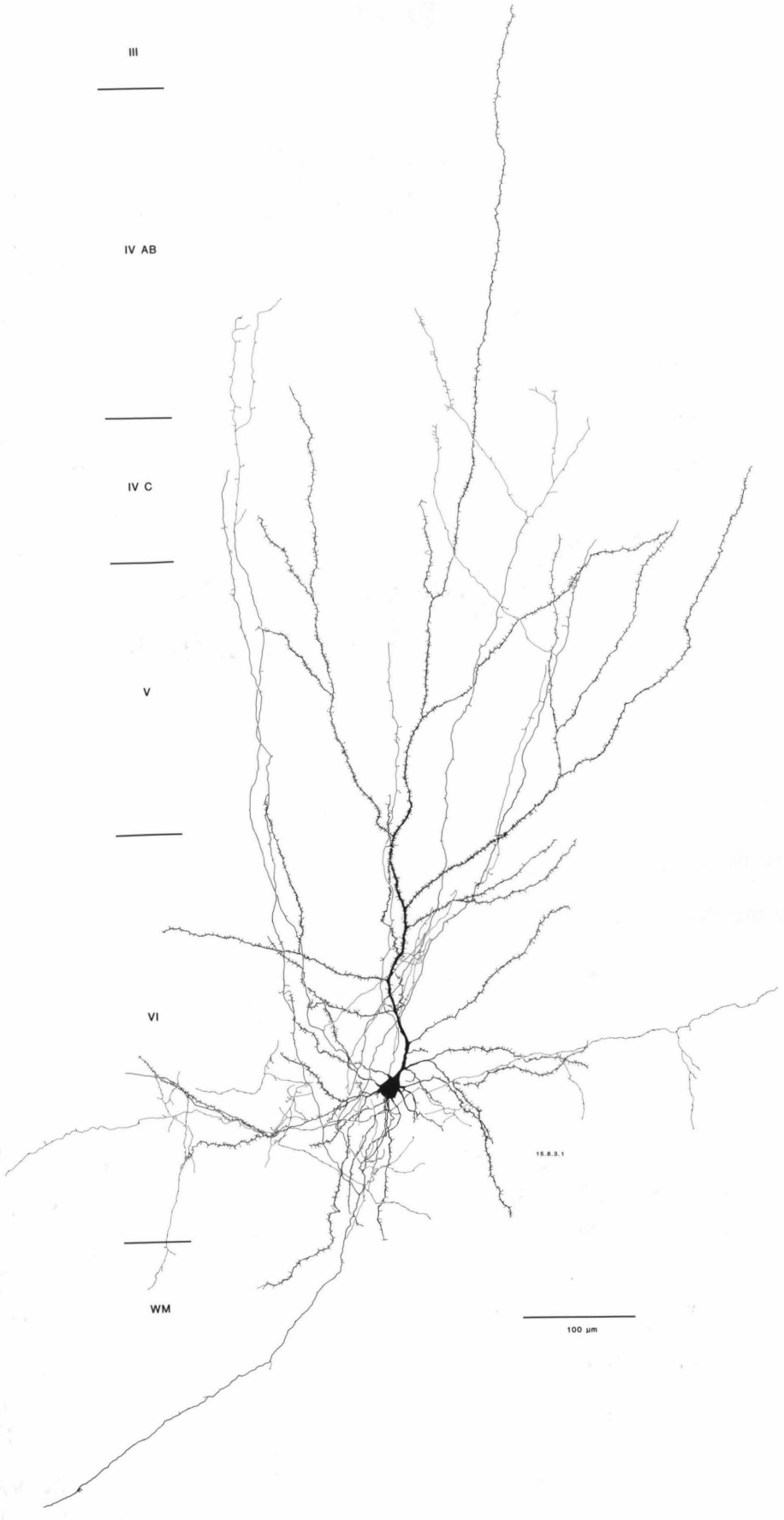
III
IV AB
IV C
V
VI
WM
15.8.3.1
100 µm

The shapes of the basal dendritic arbor were analyzed by the sector Sholl method as described for claustral projecting cells (Fig. 14). Although most cells show the symmetric pattern, some deviate markedly from it, usually as a consequence of the position of the cell body relative to the grey/white matter border. Unlike claustrum projecting cells, geniculate projecting cells basal dendrites generally avoid the white matter. Cells close to the border often orient their dendrites parallel to the border rather than penetrating it, thus producing bilaterally symmetric, but not radially symmetric patterns.

Apical dendrites: class I and II cells

Both class I and class II cells possessed apical dendrites never traced higher than layer III. Along their course, these dendrites emitted numerous branches in layers VI, V and IV. However, the horizontal extent and form of these side branches differed somewhat between the two classes. Class I cells typically had very long horizontal branches originating from layer V, which, at their point of exit from the apical dendrite, made an angle of almost 90^{o} with it. Such branches coursed horizontally within layers V and IVc for up to 400 µm on either side of the apical dendrite, thus endowing some of these cells with an apical dendritic arbor of over 700 µm in width (Fig. 25). Other branches, particularly those in layer IV, formed considerably steeper angles with the apical dendrite and did not show such considerable horizontal extent. Both types of dendritic collaterals of type I cells branched either once or not at all after leaving the apical dendrite.

The side branches of class II cells left the apical dendrite at considerably steeper angles than the horizontally directed dendrites of class I cells, thereby forming an apical dendritic field with about with about half the horizontal extent observed for the class I cells (Fig. 26). Also, these processes tended to branch

multiple times during their ascending course, increasing the total dendritic length significantly.

The horizontal extent of the apical dendritic field was always greater than that of the basal dendrites, a difference most pronounced for the class I cells, in which apical dendritic spread was often twice, and occasionally up to three times that of the basal dendrites. For the class II cells, the difference was not as dramatic, but still on the order of 1.5 times as extensive.

Dendritic spines: class I and II cells

Both classes of cells had light to moderate numbers of spines. Spine morphology and size varied considerably, ranging in shape from the classic simple spine with a narrow stalk topped by a sphere, to stalks without spheres, and occasional thorn-like projections (Fig. 27), and ranging in size from 5 μm long down to less than 1 μm. On the apical dendrites, the concentration of spines peaked at the top of layer VI and the lower portion of layer V (Fig. 20b). Spine density remained rather high through layer V but dropped off considerably in layer IV. The basal dendrites showed a lower spine density (Fig. 27), with an average of 1 spine per 5 linear microns of dendrite.

Axon collaterals: class I and II cells

As with the claustrum projecting cells, the appearance of the intrinsic axonal arbor formed the most consistent and obvious feature of the geniculate projecting cells. Class I and II cells showed similar distribution of processes. Both had a prominent efferent axon (0.5-1.0 μm diameter) which entered the white matter. Before this point, the axon emitted 3-5 thick, vertically directed axonal collaterals, which ascended with only occasional branching, and terminated in layer IV. These collaterals, only slightly less thick than the parent

Figure 27. Spines on the dendritic processes of LGN projecting cells. a) Spines on the apical dendrite as it passes through the VI/V border. Spines are of many shapes and sizes, and considerably less dense than those on claustrum projecting cells (Fig. 19). b) Spines on the middle portion of a basal dendrite (where spine density is highest); even at this point spines are quite sparse. Scale bars: 20 μm.

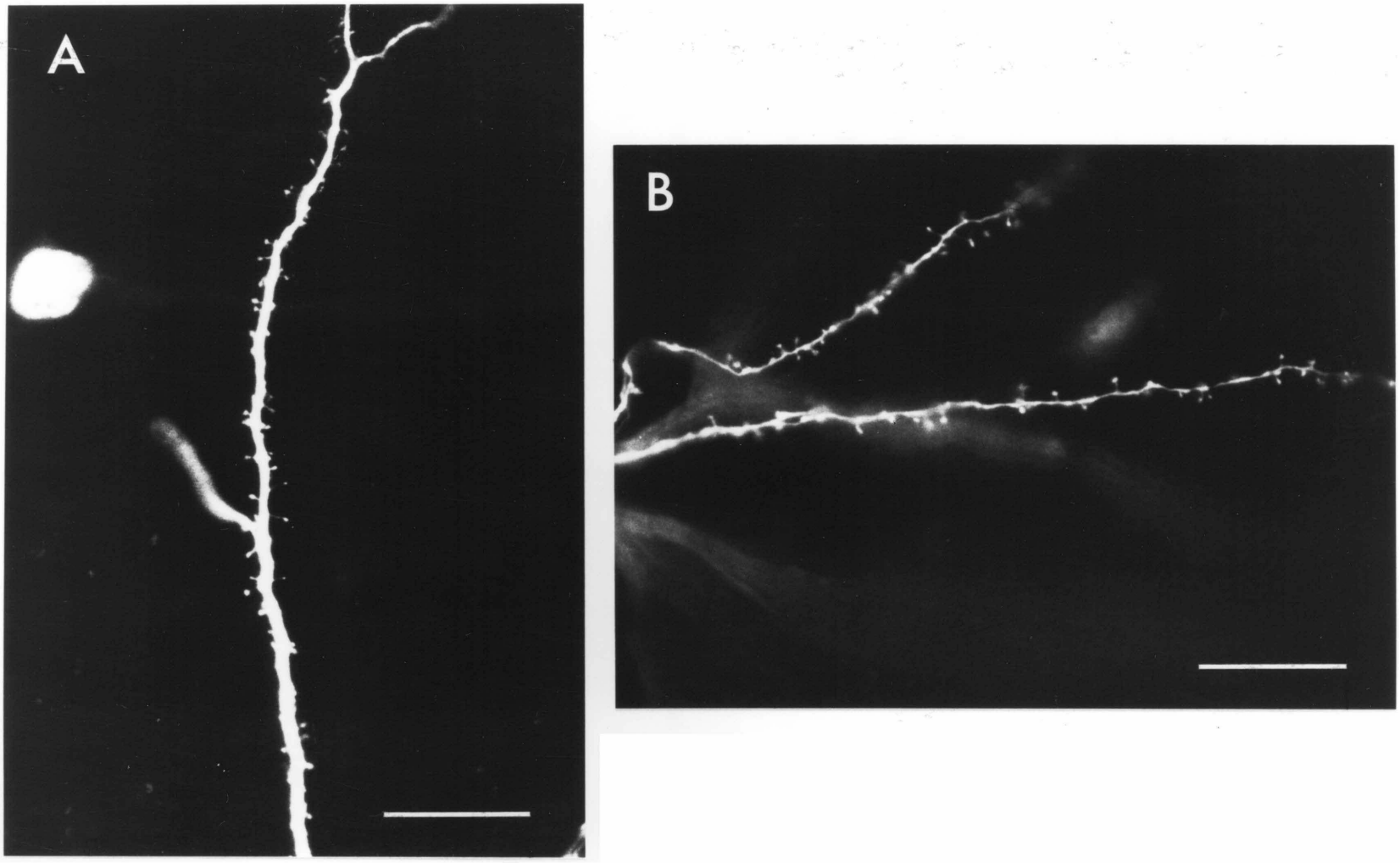
A
B

axon, and myelinated until they reached the lower boundary of layer IV, then lost their myelination and began branching extensively, with prominent spine like appendages at frequent intervals along their length in layer IV (Figs. 24-26). In contrast to this well developed ascending collateral system, these cells produced minimal numbers of axon collaterals within layer VI. Class I cells usually had no more than an occasional axonal twig, less than 50 μm long, in layer VI; class II cells occasionally had slightly greater collateralization within VI. Figure 26 shows the cell which had one of the most extensive layer VI collateral systems of any geniculate projecting cell encountered.

In terms of axonal arborization, class I and II cells differ principally in the thickness and horizontal spread of the ascending collaterals. Class I cells all had widespread, thick ascending collaterals 0.7-0.9 μm in diameter. As they coursed through layer V, the processes emitted few if any appendages or subcollaterals. The lateral spread of these collaterals could extend up to 1 mm (measured at the boundary of layers V and IVc). The fine terminal collaterals had an even greater lateral spread than the parent trunks.

The ascending collaterals of the class II cells were considerably thinner (0.3-0.5 μm diameter) and more restricted in horizontal extent than those of class I cells: in general the collaterals remained within the confines of the cells apical dendritic arbor. The terminal arbors of these cells did not fill with dye as well as those of class I cells (probably because of the thinner ascending collaterals). As they coursed through layer V, class II collaterals showed occasional spine-like appendages, or short, unmyelinated branches (Fig. 28a), only rarely seen in the type I cells (Fig. 28b).

The difference between the patterns of distribution of intrinsic axons of geniculate and claustrum projecting cells forms a striking dichotomy. The absence of horizontal collaterals in geniculate projecting cells does not result

Figure 28. Ascending axonal collaterals of LGN projecting cells. a) Collateral of a class I neuron, as it courses through layer V, showing the characteristically thick, smooth process with only an occasional appendage (arrow). b) Collateral of a class II cell in layer V, considerably thinner than the process in (a), and showing frequent spine-like appendages (arrows). Scale bars: 20 μm.

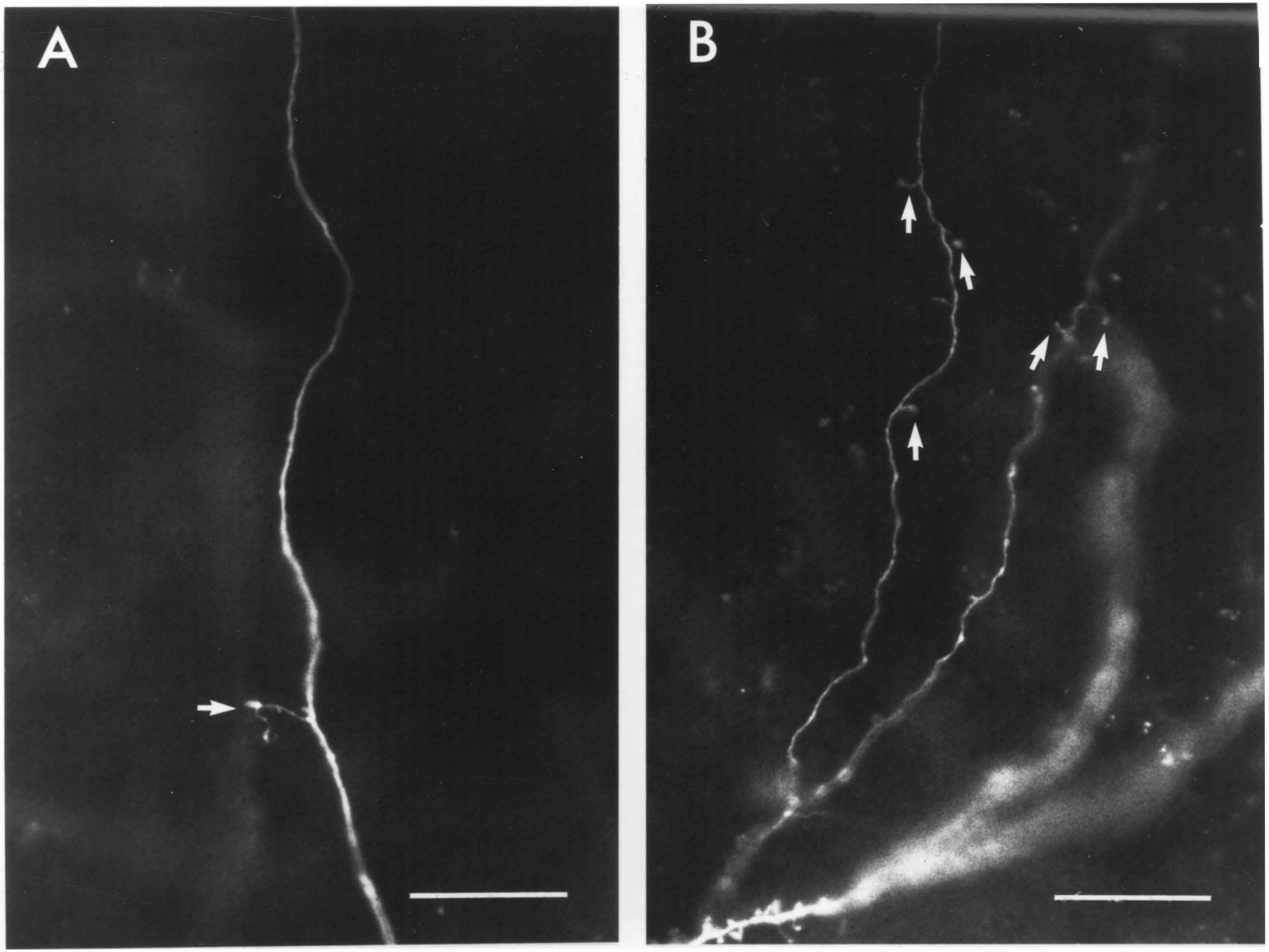
A
B

from a failure to fill such processes, or consistent truncation of them in the slicing process. Gilbert and Wiesel (1979, 1981, 1983) have published several examples of cells in layer VI filled in vivo with HRP. Even in their very complete fills, cells with ascending collaterals to layer IV have virtually no axonal arbor within layers VI and V. However, apparently the extent of filling of the terminal arborization of these cells is significantly more complete in vivo than in vitro, although the pattern of distribution of processes is identical. Thus one must be cautious in interpreting the absence of processes in slices; the possibilities of truncation and/or failure to fill fine terminals pose genuine problems.

Both classes of cells exhibited occasional short collaterals and spine-like appendages in the zone of white matter approximately 100 μm below the border of layer VI and white matter. The post-synaptic targets of such processes are unclear. Since most geniculate projecting cells dendrites do not cross the grey/white matter border, these short collaterals probably do not make extensive contacts with the basal dendrites of other geniculate projecting neurons.

Soma and basal dendrites: class III cells

These cells had a range of soma sizes and shapes indistinguishable from those of the class I and II cells. Occasionally a very small cell, such as the one shown in Fig. 29 was filled, but many were of the standard pyramidal shape and size (e.g. Fig. 30).

Similarly, class III cells had a dendritic field structure virtually identical to the class I and II cells, with 6-8 thin basal dendritic arms, of the same length, arranged radially around the soma (Fig. 30). When the soma was located near the white matter (Fig. 31), the dendrites adjacent to the white matter were somewhat shorter than the rest. The dendrites extended in a symmetric fashion,

Figure 29. A small class III LGN projecting neuron. This cell has a very small soma, with 7 basal dendritic arms. The apical dendrite is restricted to layer V, and the axon collaterals are thin and sparse. Dendrites are moderately spined.

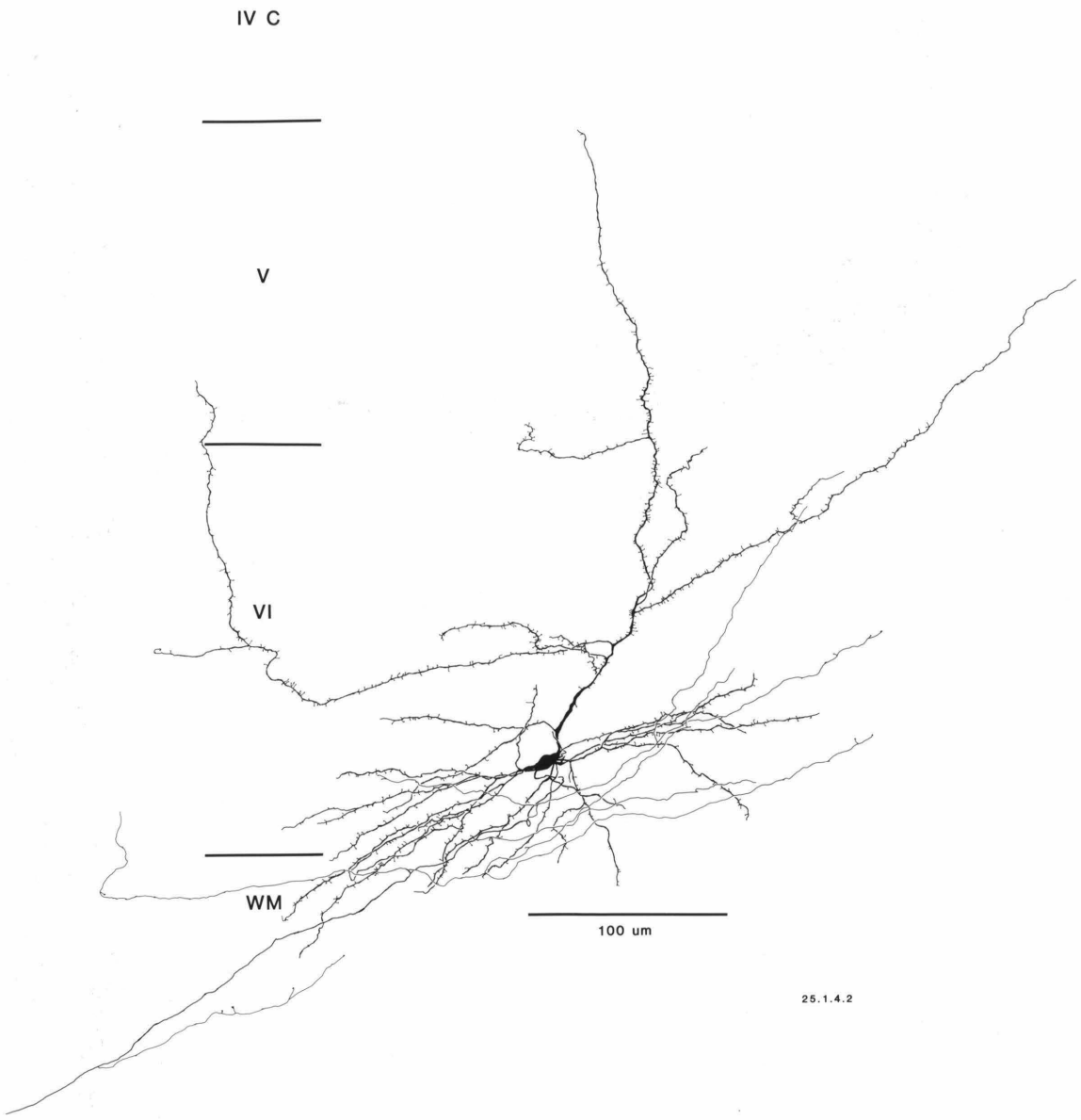
IV C
V
VI
WM
100 um
25.1.4.2

Figure 30. An example of a sparsely spined class III LGN projecting neuron. This cell has a medium sized pyramidal shaped soma, with eight dendritic branches. The apical dendrite is weakly developed and appears almost vestigial. The axon collaterals, thin and with little horizontal extent in layer VI, reach no higher than layer V.

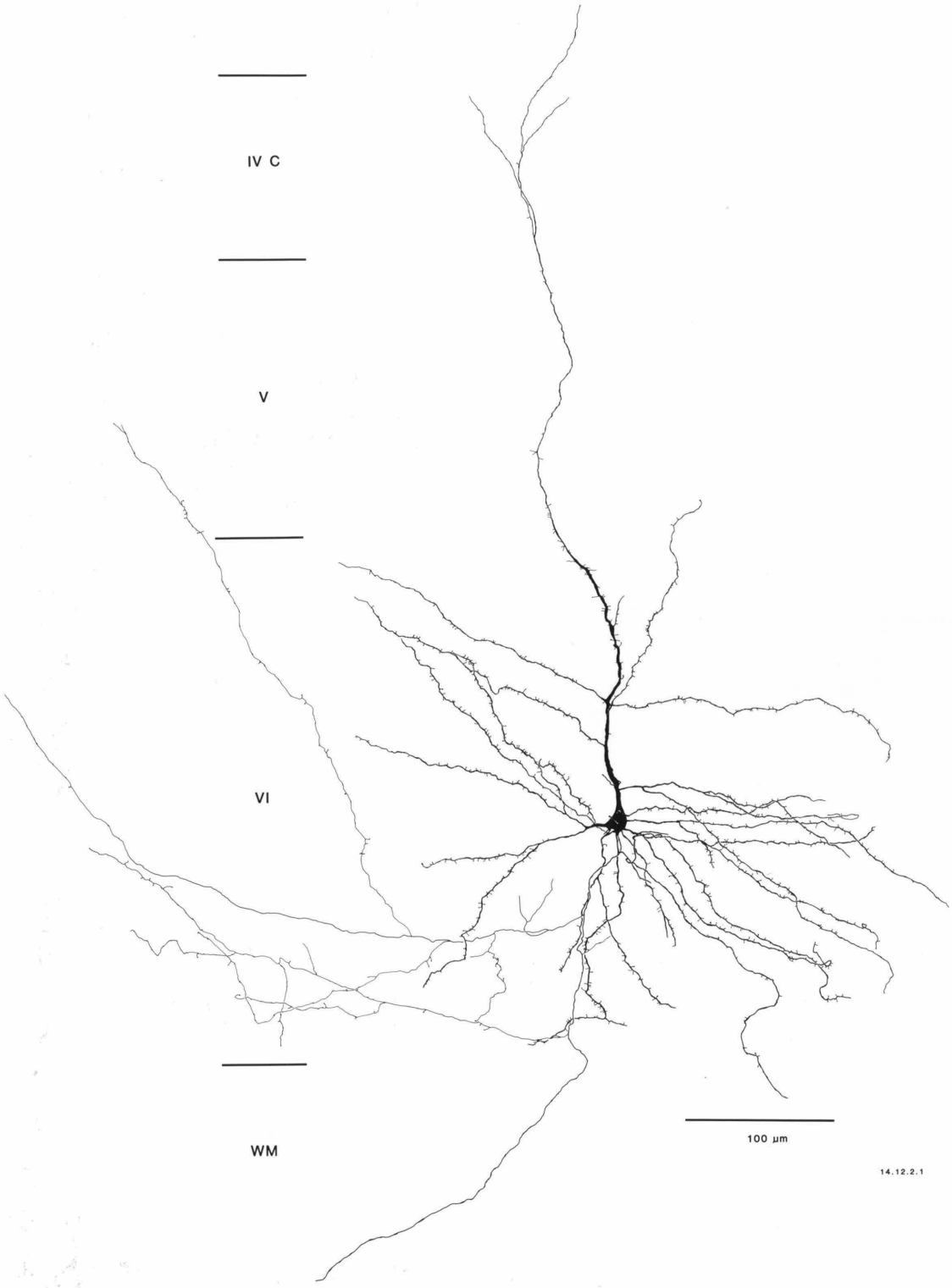
IV C
V
VI
WM
100 µm
14.12.2.1

Figure 31. A class III LGN projecting neuron with a soma located at the grey/white matter border. The close proximity to the border gives the dendritic arbor a bilaterally, rather than radially, symmetric appearance. The apical dendrite reaches no higher than lower lamina IV, and side branches originate in VI only. The intrinsic collaterals are sparse.

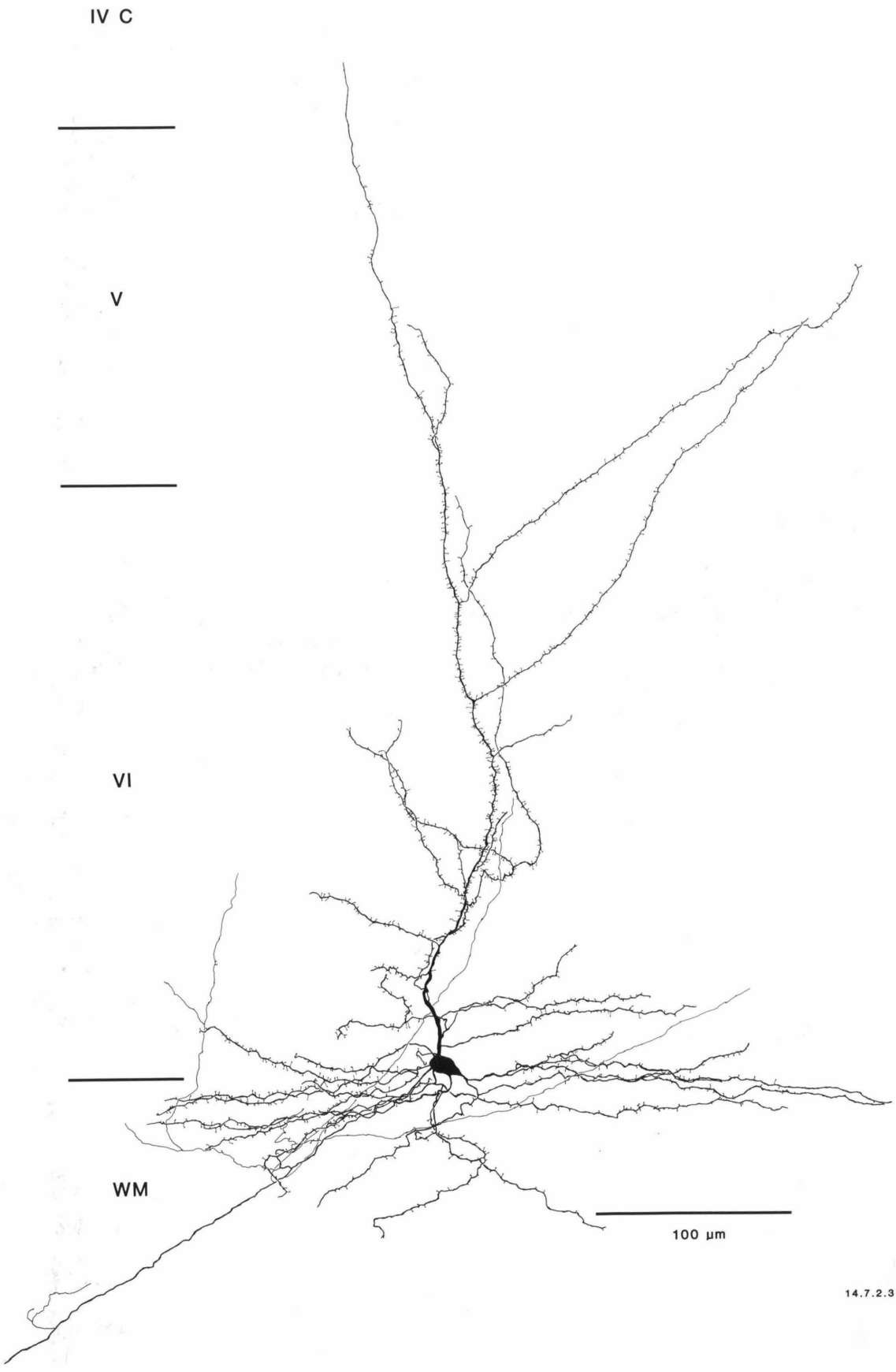
IV C
V
VI
WM
100 µm
14.7.2.3

forming an arbor about 150 μm in diameter.

Apical dendrites: class III cells

All class III cells had poorly developed apical dendrites which extended no higher than the lower part of layer IV, and usually no higher than the V/IV border. Within layer VI, the apical dendrite gave rise to several short side branches, with a horizontal extent less than that of the cell's basal dendrites (Figs. 29-31). These branches coursed primarily through layer VI, occasionally reaching and ending within layer V. No side branches originated from the apical dendrite above the VI/V border.

Dendritic spines: class III cells

Both the basal and apical dendrites of these cells exhibited dendritic spines of numerous shapes and sizes, similar to those described for the class I and II cells. Their density ranged from moderate (e.g. Fig. 31) to quite sparse (Fig. 30). Dendritic spine distribution on the apical dendrites of class III cells differed from that observed on the class I and II cells in that class III cells had their dendritic spines concentrated on those portions of the apical dendrite that lay within layer VI, with a marked diminution of spine density after the dendrite entered layer V (in contrast, the spine density of class I and II cells, initially low within layer VI, peaked at the V/VI border, and remained quite high within layer V).

Axon collaterals: class III cells

In comparison to the class I and II cells, class III cells had considerably restricted intrinsic axon collaterals. None of the very thin (0.2-0.3 μm diameter) ascending collaterals reached higher than layer V. Horizontally, within layer VI,

the collaterals were highly restricted as well, with no significant arborization seen much outside the boundaries of the basal dendrites. Figure 30 shows the cell with one of the most extensive collateral systems encountered.

Thus in general class III cells greatly resemble the class I and II cells in terms of basal dendritic structure, but show marked differences in the apical dendritic and intrinsic axonal arborizations.

Axon diameters of lateral geniculate nucleus projecting neurons

After looking at many geniculate projecting cells, it became clear that they, unlike the axons of claustrum projecting cells, exhibited considerable heterogeneity in the diameters of both the efferent and especially the intrinsic ascending axons. As Fig. 32 (top) shows, this variability did not result as a simple consequence of cell size; soma area alone could not predict the size of the cell's axons. In Fig. 33, the number of cells in each group of efferent and recurrent axon diameters is shown. Because of the limited resolving power of the light microscope (about 0.2 μm) and the small diameter of these axons to begin with, no distinctions can be made on a fine enough level to decide whether these groupings reflect distinct classes, or the distribution of a parameter along a continuum. Nevertheless, there is at least a three-fold difference between the smallest and largest diameter axons. It is also important to note that axon diameter is a shared property of the efferent and recurrent axon collaterals: the two diameters are very highly correlated ($r=0.88$, $p < 0.001$). One observation that suggests that this distribution may in fact represent distinct classes of neurons is that the larger size collaterals (those greater than 0.6 μm diameter) are almost always (11 of 13 class I cells) associated with the class I dendritic morphology described above, the smaller diameter axons belonged to either class II or III cells. In order to rigorously separate this continuum into classes

Figure 32. Comparison of soma area with efferent (top) and recurrent (bottom) axon diameters: the efferent axons show a weak correlation, the recurrent axons have none.

LGN PROJECTING CELLS

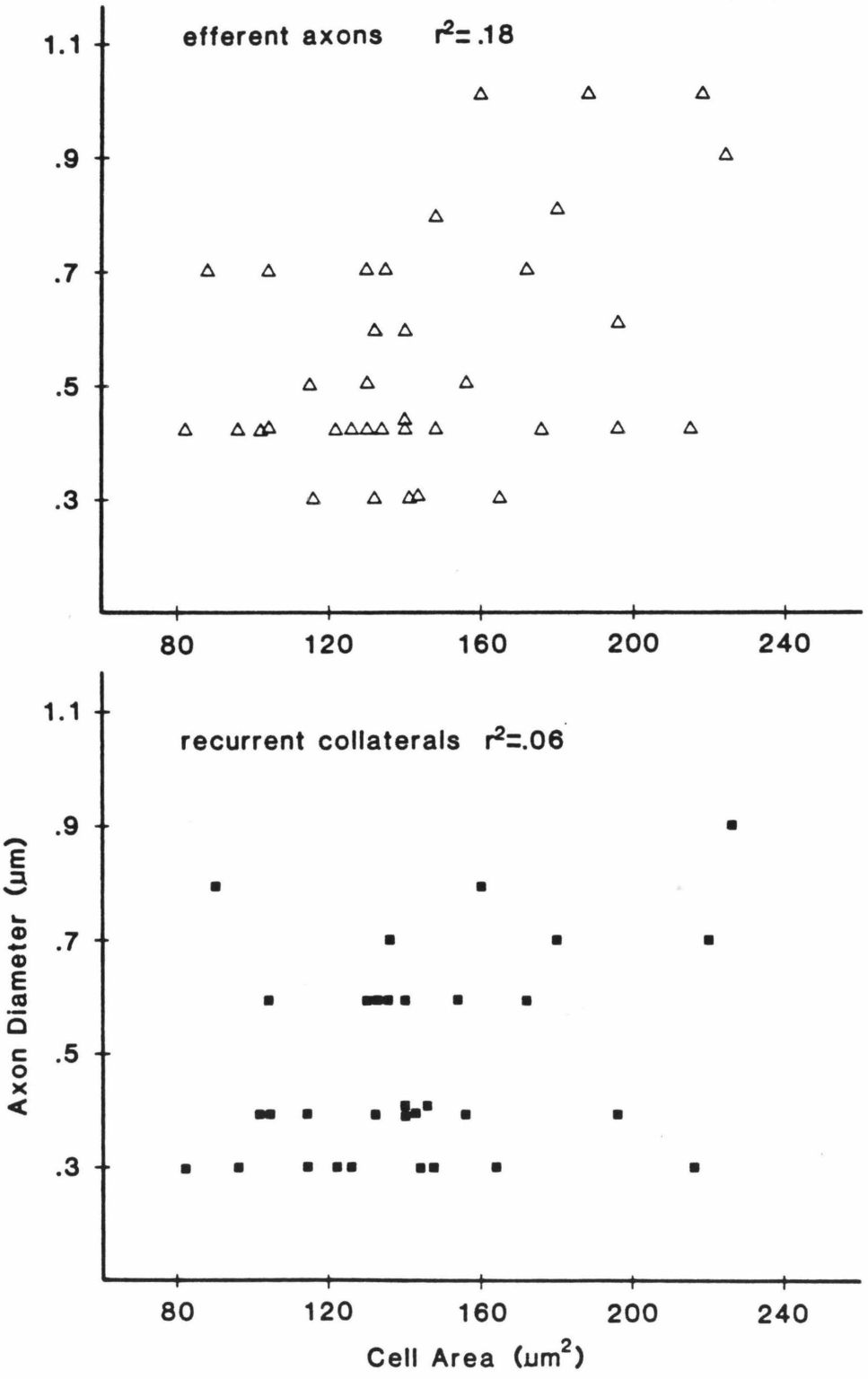

Figure 33. Histogram of the number of cells with efferent and recurrent axon collaterals in the smallest intervals resolvable by the light microscope. Although both types of axons are apparently distributed along a continuum, there is over a three-fold difference in the diameters of the largest and smallest axons. Recurrent axons are in general slightly thinner than efferent axons (about 75% of the diameter), but for any one cell the thickness of the efferent and recurrent processes is very highly correlated.

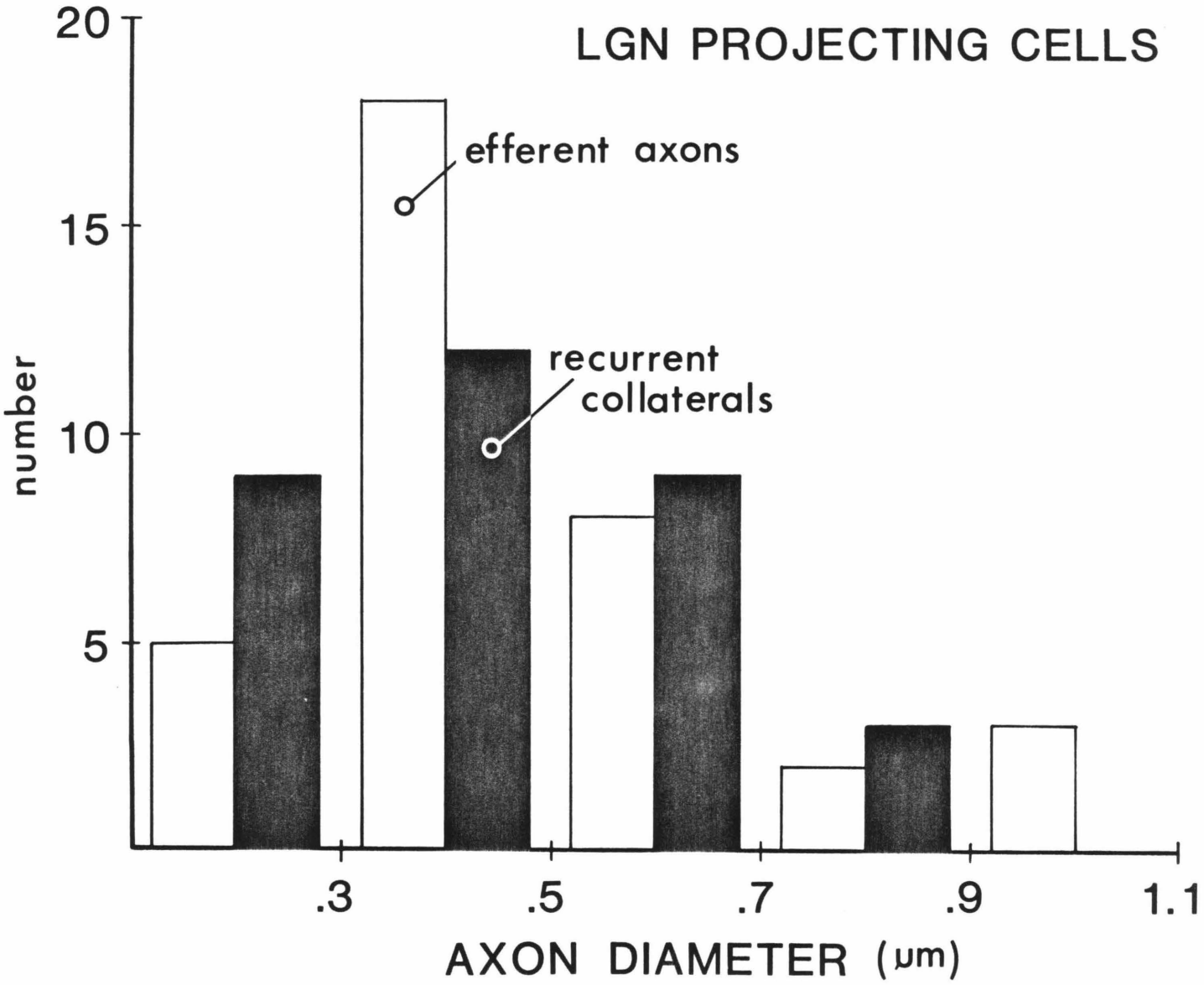
LGN PROJECTING CELLS
20
15
10
5
number
efferent axons
recurrent
collaterals
.3
.5
.7
.9
1.1
AXON DIAMETER (μm)

(indeed, if it can be so separated) additional, independent criteria, such as distinct patterns of inputs to these three putative classes, will be required.

It is well known that there are three independent, functionally distinct classes of afferent fibers to A17 arising from the lateral geniculate: the parallel Y, X and W systems (Hoffman and Stone 1971, reviewed by Lennie 1980). The morphology and terminal sites of these systems are also distinct--Y afferents are large, fast conducting, and show widespread terminals in layer IVab and upper layer VI, X afferents are medium sized, slower conducting, and terminate narrowly within layer IVc and upper layer VI, and W afferents are very thin, slowly conducting, and terminate within layers V and I (Ferster and LeVay 1978). The ratio between the thickness of Y:X:W axons is approximately 2:1:0.8, which is very similar to the apparent size differences in recurrent collaterals shown in Figs. 32 and 33. In this regard, the varying thickness of the intrinsic recurrent collaterals is intriguing, as it may represent separate feedback streams corresponding to the different afferent information channels.

If in fact these various layer VI cells were functionally related to the X or Y systems, one might expect that their axon terminals would show distinct patterns of sub-laminar termination within layer IV that corresponded to the channel with which they were involved. Gilbert and Wiesel (1979, 1983) have published drawings of some layer VI cells that have their terminal arborizations primarily restricted to layer IVab, and others whose terminals distribute throughout layer IV. Similar patterns were occasionally observed in the various LGN projecting cells described here. However, no conclusions regarding the relationship of axon diameter or dendritic morphology to mode of termination within layer IV have been drawn here, for the following reason. As mentioned previously, there are significant limitations on the completeness of filling of some of the more distal branches of long axons. Although in most cases, some

axon collaterals of LGN projecting cells could be traced to layer IV, in no case was the entire axonal arborization within layer IV visualized. Thus, apparent laminar restrictions might be artifactual. It is possible, however, that using HRP as an intracellular marker, which is probably more sensitive for visualizing such processes, might indeed reveal a relationship between axonal termination patterns and dendritic morphology.

Summary comparison of claustrum and geniculate projecting cells

Cells that project to the lateral geniculate or to the claustrum have completely different, and in some respects, non-overlapping patterns of distribution of basal and apical dendrites, dendritic spines, and intrinsic axonal arborizations.

Somas and basal dendrites

Statistical comparison of the distributions of cell body areas for claustrum and LGN projecting cells showed no significant difference (Fig. 10). The very smallest cells of the geniculate class (<80 μm^2) were, however, smaller than the smallest of the claustrum projecting cells.

Claustrum projecting cells have about one third fewer basal dendritic arms (3-5) than lateral geniculate projecting cells (6-8), a difference which is highly significant (students t-test, $p < 0.01$). The presence of one or two thick, long dendrites, a feature never observed in geniculate projecting cells, gives the claustral cells a markedly asymmetric basal dendritic field, compared to the characteristically symmetric field of geniculate projecting cells. However, the two projection classes show similar branching patterns for the initial 100 μm of dendritic length as assessed by Sholl analysis (Figs. 34 and 35). Claustrum projecting cells dendritic processes do not generally respect the grey/white

Figure 34. Sholl analysis (using 20 μm spacing between concentric circles) of the basal dendritic arbors of claustrum (top) and LGN (bottom) projecting neurons. Each curve represents an individual cell. Despite considerable variability, the claustrum projecting cells show a clear "tail" in this analysis, due to the presence of a long, asymmetric process. In both projection classes, neurons that have a large number of intersections close to the soma have a more restricted total radius; cells with reduced numbers have arbors extending over greater distances.

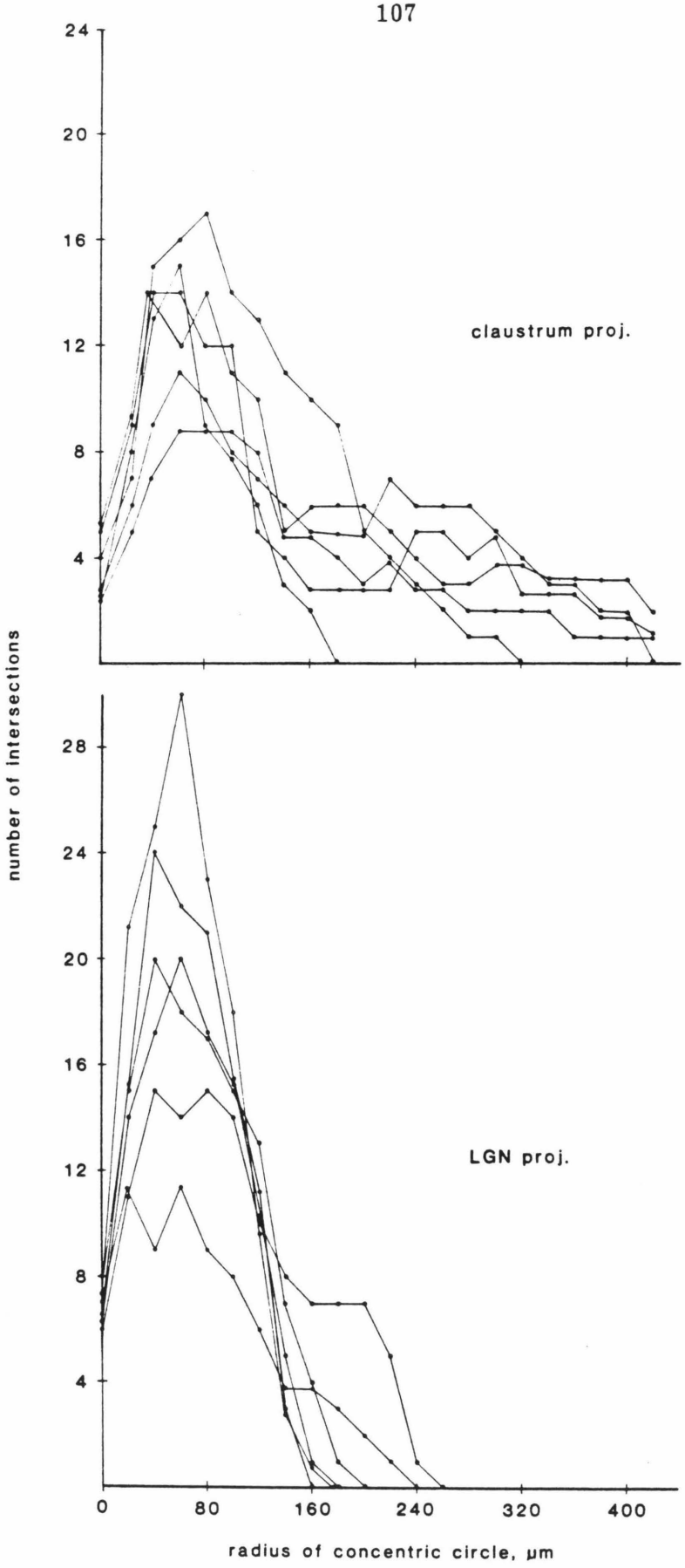
24
20
16
12
8
4
claustrum proj.
28
24
20
16
12
8
4
LGN proj.
number of intersections
0
80
160
240
320
400
radius of concentric circle, µm

Figure 35. Data from Fig. 34 averaged to show general trends. The points represent average values from 7 cells of each projection, the error bars are ± S.E.M. Although both LGN and claustrum projecting cells have peak numbers of intersections at about 80 μm from the soma, the LGN neurons arbor is significantly denser, due principally to the greater number of dendritic arms. The asymmetric process of claustrum projecting cells gives rise to a long "tail", absent from the geniculate projecting neurons.

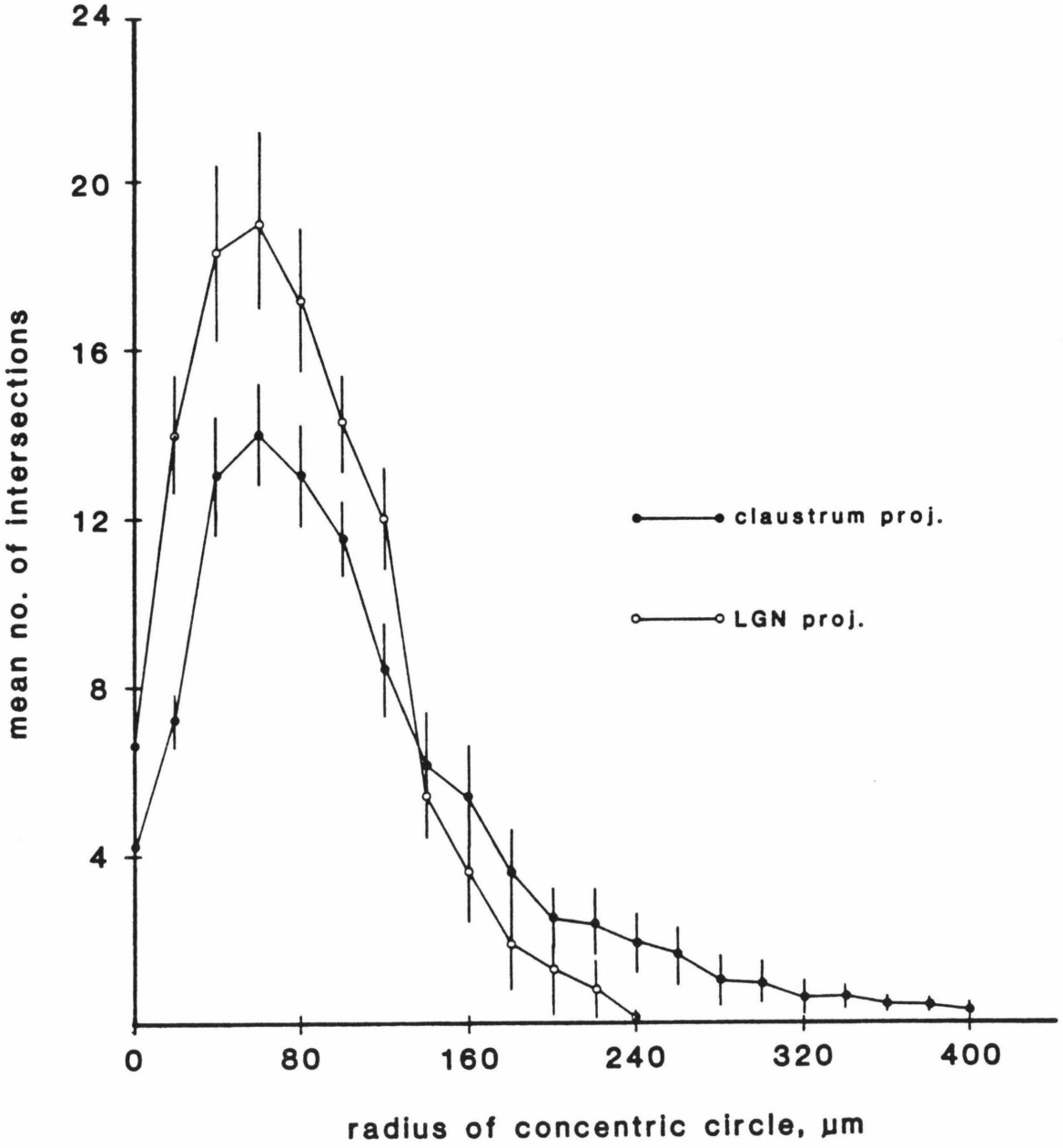
24
20
16
12
8
4
mean no. of intersections
0
80
160
240
320
400
radius of concentric circle, µm
claustrum proj.
LGN proj.

matter boundary, but those of geniculate projecting cells usually do.

Apical dendrites

The apical dendrite of claustrum projecting cells characteristically reaches layer I; geniculate projecting cells never reach above layer III. However, the geniculate projecting cells have a quite extensive apical dendritic arbor, with branches in layers VI, V and IV. Figure 36 shows a Sholl analysis of the apical dendritic branching patterns of geniculate and claustrum projecting cells, which demonstrates the more profuse branching of the geniculate projecting cells' apical dendrites. The horizontal extent of these branches is often considerably greater than that of the basal dendrites. In contrast, the apical dendrite of claustrum projecting cells has only short branches in layers VI and V, so that the horizontal extent of the apical dendritic arbor is typically considerably narrower than that of the basal dendrites. In terms of total length, geniculate projecting cells have an apical dendritic arbor about 50% larger than claustral projecting cells (Fig. 37).

Dendritic spines

Claustrum projecting cells have an overall spine density higher than that of geniculate projecting neurons, with spines more uniform in shape and size. In terms of peak density (at the layer VI/V border), claustrum projecting cells have roughly twice as many spine per length of dendrite as geniculate projecting cells. The two projections share one feature of spine distribution both have peaks of spine density at the VI/V border. Geniculate projecting cells tend to have a peak of spine density at the III/IV border as well, a feature not observed in claustrum projecting neurons.

Figure 36. Sholl analysis of the apical dendritic arbors of LGN and claustrum projecting cells (using 20 μm spacing between concentric circles), each point shows the average of 7 cells, ± S.E.M. Both the greater horizontal and vertical extent of the apical dendritic arbor of LGN projecting cells are apparent.

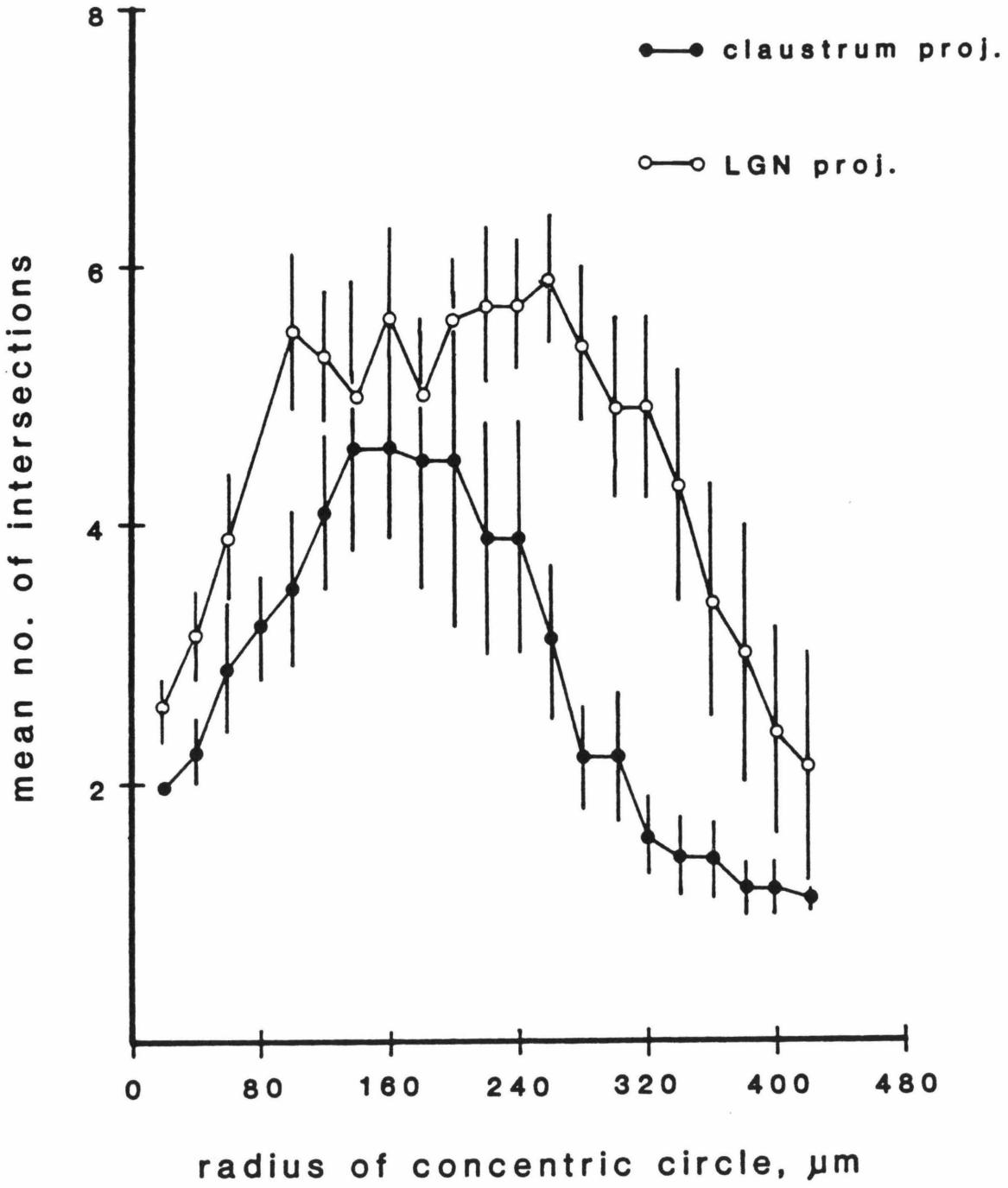
claustrum proj.
LGN proj.
mean no. of intersections
8
6
4
2
0
80
160
240
320
400
480
radius of concentric circle, µm

Figure 37. Cumulative dendritic length of claustrum and LGN projecting neurons, derived from the average values obtained in the analysis shown in Fig. 36. LGN projecting cells have substantially greater amounts of apical dendritic length; this, coupled with the data on distribution of such processes (see text) implies that these cells can collate information from significantly larger areas of the upper layers than can the claustrum projecting neurons.

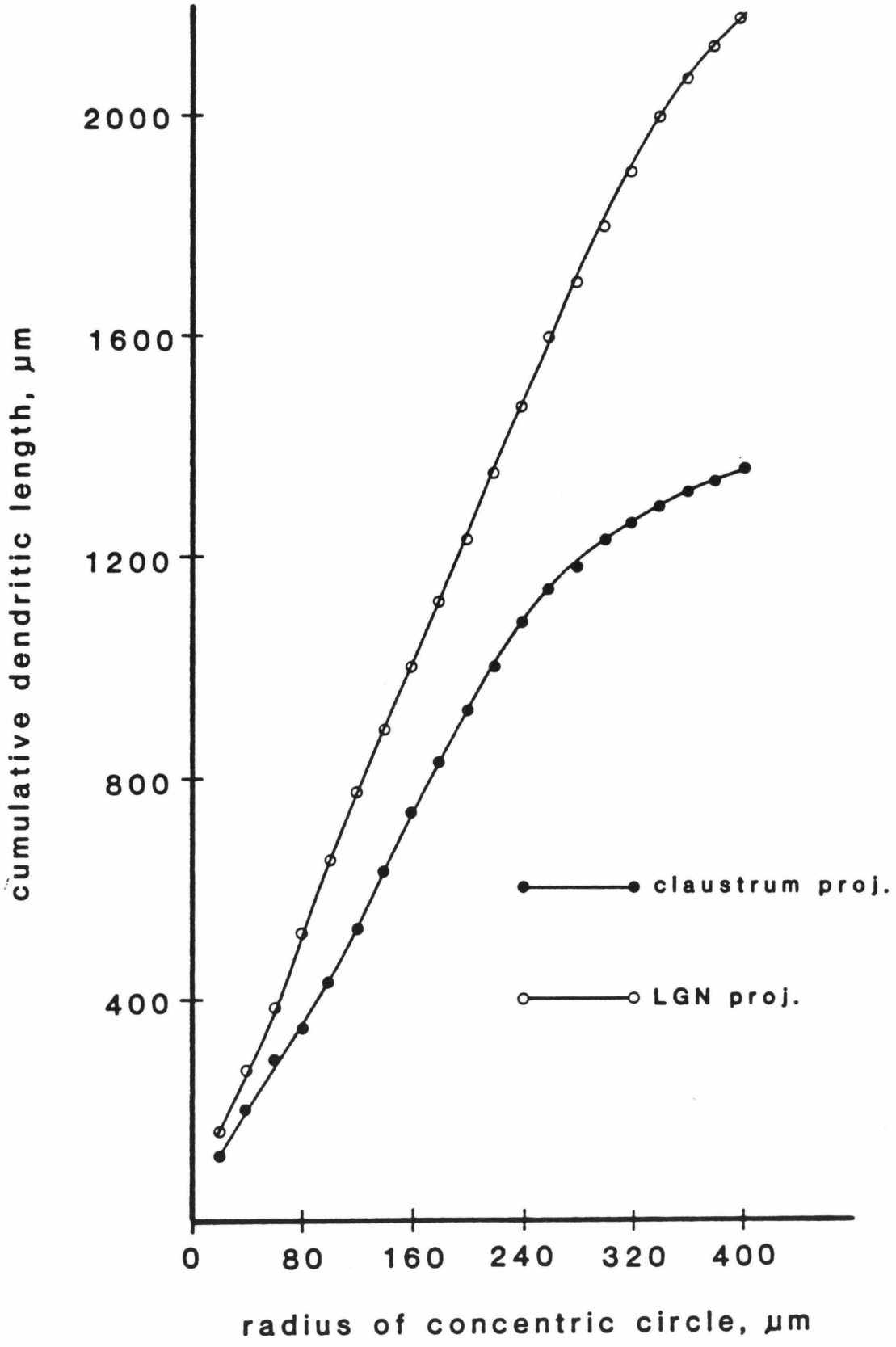
2000
1600
1200
800
400
cumulative dendritic length, µm
claustrum proj.
LGN proj.
0
80
160
240
320
400
radius of concentric circle, µm

Intrinsic axonal arborizations

All claustrum projecting cells had thin, horizontally directed axon collaterals which coursed extensively within layer VI and never rose above layer V. The geniculate projecting neurons, in marked contrast, had virtually no horizontal collaterals within layer VI, but possessed instead thick, ascending collaterals that arborized extensively within layer IV. The efferent axons of both cells had occasional collaterals or appendages within a 100 μm thick zone of white matter immediately subadjacent to layer VI.

Non-projecting pyramidal cells in layer VI

Studies on the neuronal constituents of layer VI have revealed a puzzling discrepancy. Large, extensive injections of various retrograde tracers into the lateral geniculate nucleus label at most 60% of the cells in layer VI (Gilbert and Kelly 1975, LeVay and Sherk 1981). According to LeVay and Sherk (1981), and the work presented here, fewer than 5% of layer VI cells project to the visual claustrum. Electron-microscopic (Lund 1981) and immunocytochemical (Ribak 1978) studies suggest that, outside layer IV, fewer than 10% of the neurons are spine-free or sparsely spined interneurons. Totaling these percentages leaves 25% of the cells unaccounted for. Several trivial explanations could potentially account for the discrepancy. For instance, certain populations of projection neurons may be very difficult to retrogradely label using current techniques, thus the actual percentages of projecting neurons might be higher than the numbers stated above. Another possibility, although somewhat less likely, is that certain glial cells have been consistently misidentified as neurons, thus artifactually raising the percentage of unlabeled cells.

However, at least some, and perhaps most, of these "lost" cells are

pyramidal cells that lack an efferent axon. In early experiments, random lucifer yellow fills of cells in layer VI suggested that approximately 20% of the cells filled lacked an efferent axon, despite excellent filling in all other respects. Figure 38a shows an example of one commonly encountered cell of this type. In such cells, a thick axonal process left the soma, proceeded towards the white matter for about 100 μm, and then abruptly turned pially, forming a distinct "U" turn. The axonal process of another such cell shows this in more detail in Fig. 38b. At the bottom of the "U", the thick axon occasionally possessed a short, very thin, unmyelinated collateral that either ended within layer VI or continued briefly within the white matter before terminating. Before the "U" turn, the thick axon also sent off several collaterals only slightly thinner than the parent axon. These processes followed the course of the parent axon, i.e., towards the pia. Occasionally along their length in layer VI they gave rise to thin, unmyelinated, vertically directed subcollaterals that arborized within layer V. Although in some cases both the parent and daughter collaterals could be traced for over 1 mm, the final terminal arborizations of these cells were not found. The overall pattern of the intrinsic axonal arbor strongly resembled either class I or II geniculate projecting cells: thick, vertically oriented axons with only very sparse collateralization within layer VI.

In most cases the dendritic arborizations as well resembled that of either class I or II geniculate projecting neurons. The basal dendritic field consisted of 6-8 dendritic arms, all of approximately equal thickness and length, forming a symmetric field. The apical dendrites did not rise higher than layer III, with frequent side branches in layers VI and V. Moderate numbers of spines covered both apical and basal dendritic processes (Fig. 39).

A second type of intrinsic pyramidal cell, encountered much less frequently, had features of basal and apical dendrites, as well as intrinsic axonal

Figure 38. a) intrinsic pyramidal cell with morphological characteristics resembling LGN projecting neurons. The arrow indicates the main axon, which makes an abrupt "U" turn. Figure 39 is a camera lucida drawing of this cell. Scale bar: 50 μm. b) A close up view of the "U" turn (arrows), in a cell similar to that described in (a). Scale bar: 20 μm.

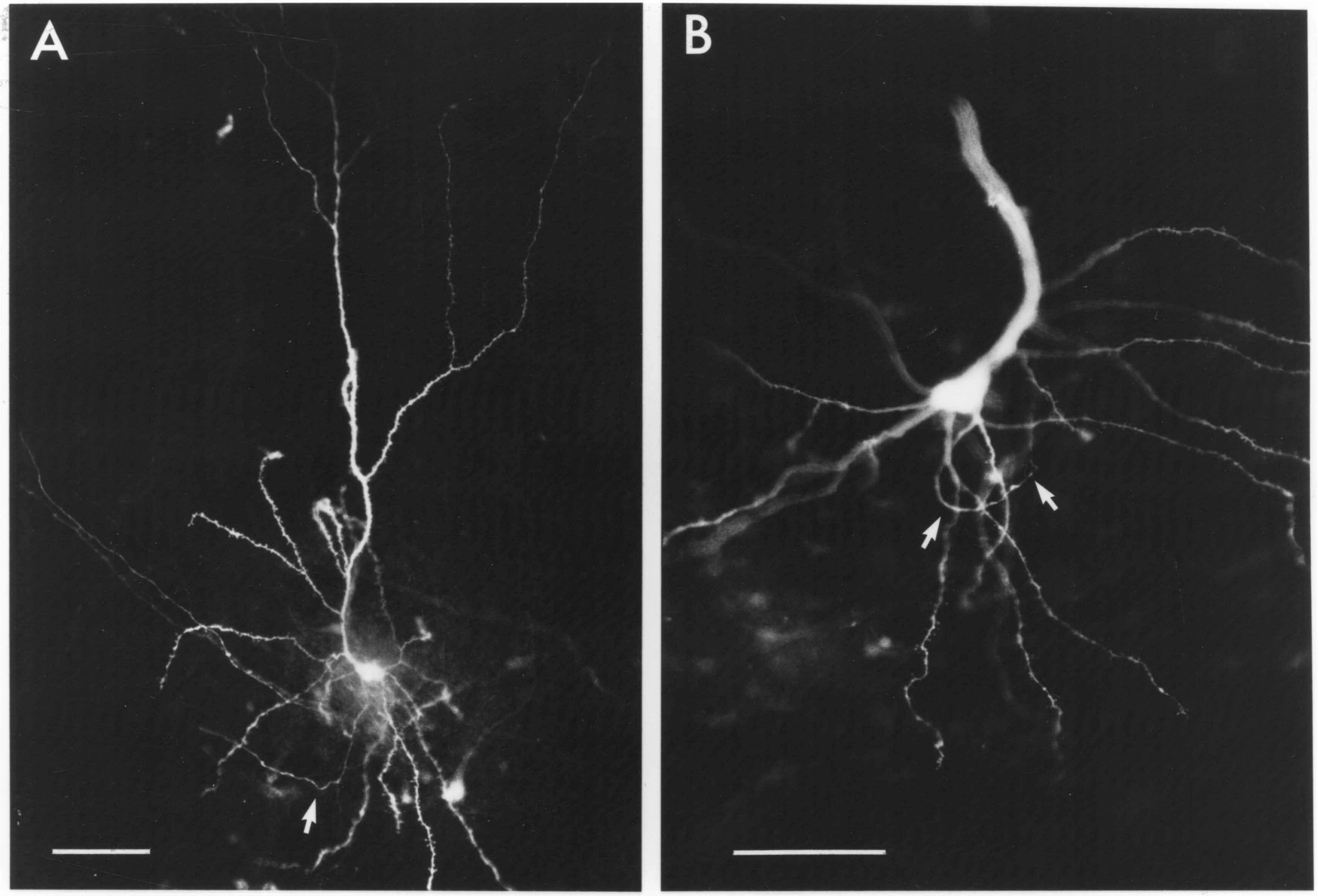
A
B

Figure 39. Drawing of the intrinsic pyramidal cell shown in Fig. 38a. The size and shape of the basal dendrites, the spine distribution on the apical dendrites, and the morphology and distribution of the axon collaterals resemble those of LGN projecting neurons. A very thin, unmyelinated process enters the white matter, but definitely ended where indicated. The thick ascending collaterals could not be followed to their final destination, although some terminals are clearly visible in layer V.

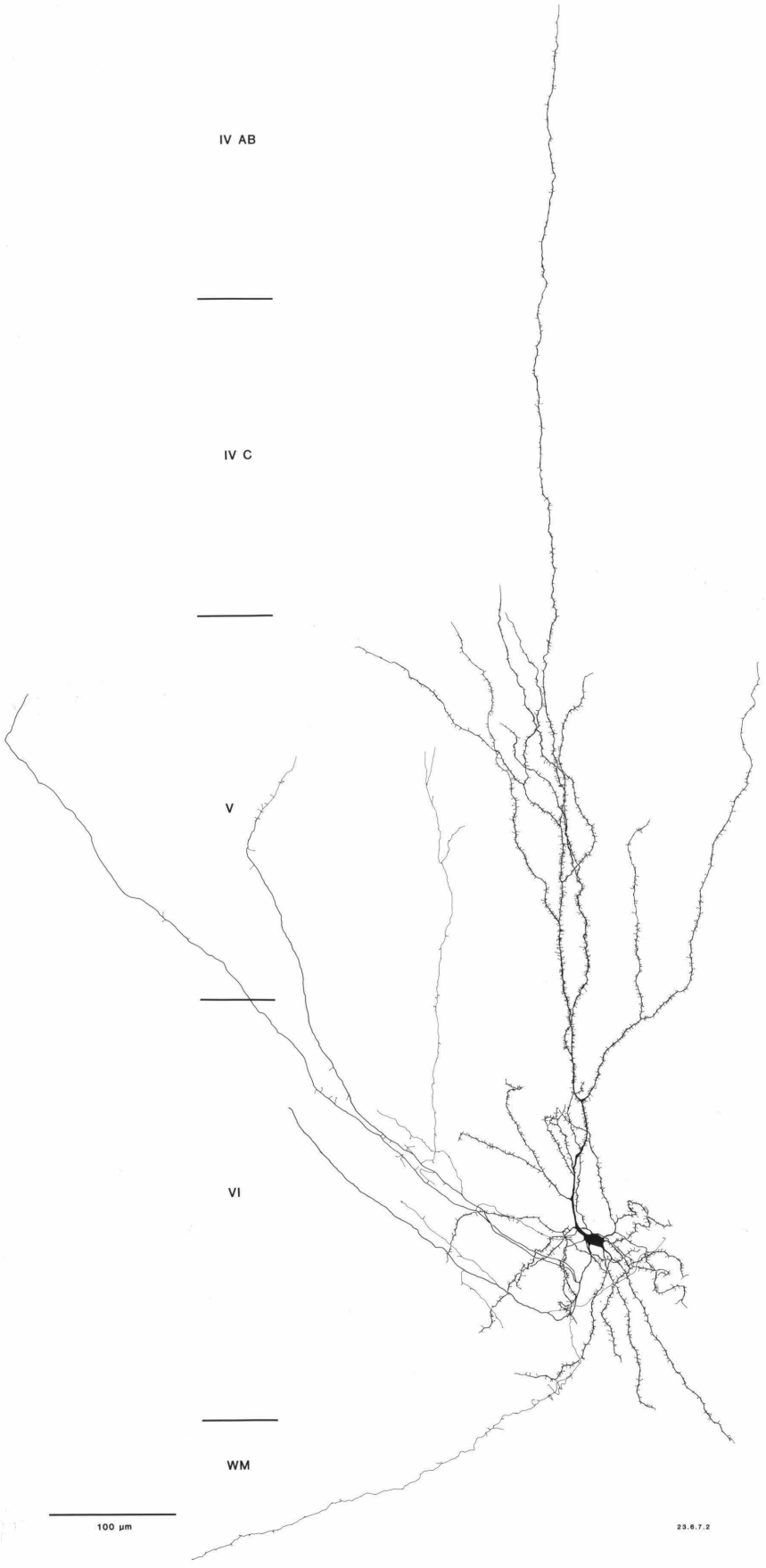
IV AB
IV C
V
VI
WM
100 µm
23.6.7.2

Figure 40. Intrinsic pyramidal cell with morphological characteristics resembling those of claustrum projecting neurons. Figure 41 is camera lucida drawing of this cell. Scale bar: 50 μm.

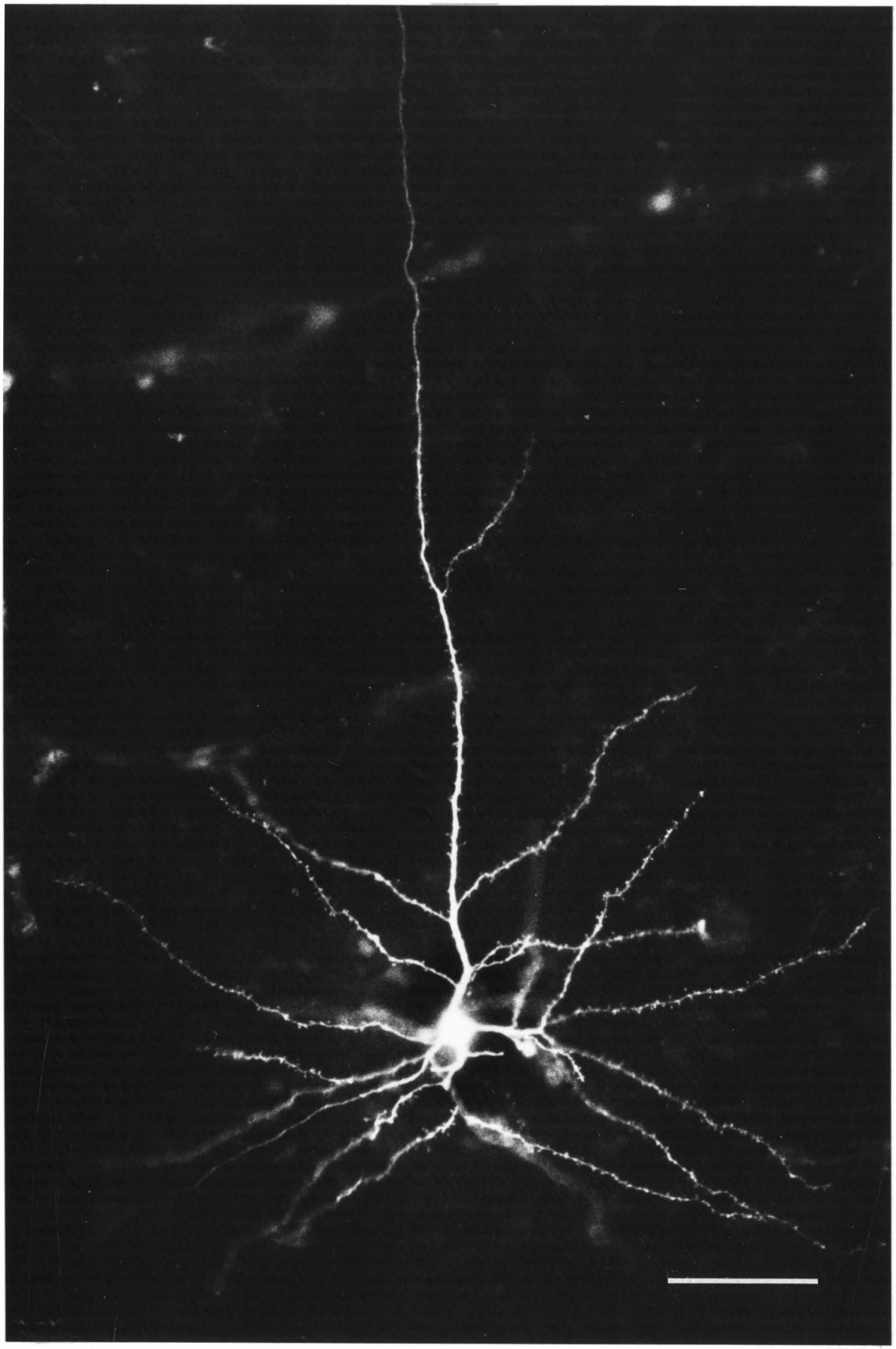

Figure 41. Drawing of the intrinsic pyramidal cell shown in Fig. 40. This cell has the asymmetric basal dendritic process, and long, thin, sparsely branched apical dendrite typical of claustrum projecting neurons (compare, for example, to Fig. 16). This is one of a very few cells whose apical dendrite terminated in layer I with a "spray" of branches. The axon initially heads in the direction of the white matter, but then turns to the right and travels horizontally, without entering the white matter, for over 1 mm (the axon traveled in the direction directly opposite to that of efferent axons that entered the white matter). The axon also shows features characteristic of claustrum projecting cells; in addition to the horizontal orientation of the processes, the axon sends up occasional short, vertically oriented subcollaterals. The overall axonal arbor of this cell is quite sparse, however.

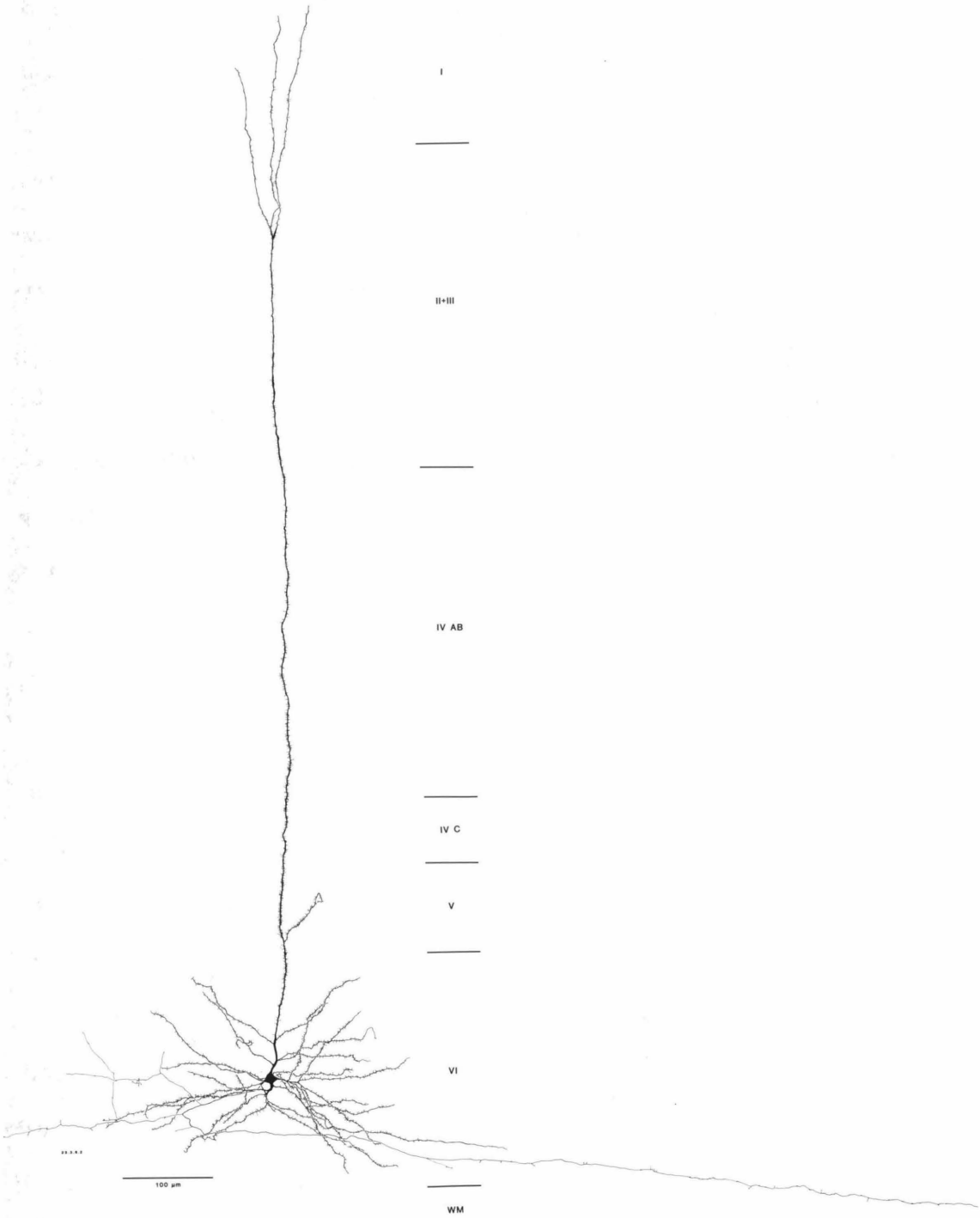
I
II+III
IV AB
IV C
V
VI
WM
100 µm

arbors, very similar to those of claustrum projecting neurons (Figs. 40 and 41). Such cells possessed 3-5 basal dendrites, with one considerably thicker than the rest, forming an asymmetric basal dendritic arbor. The thin apical dendrite reached layer I with minimal side branching and very short branches in layers VI and V. Both apical and basal dendritic processes had many spines. The thin intrinsic axons of these neurons ran horizontally within layer VI, and never rose above lower layer V. Although usually not as profuse as most claustrum projecting cells, the axon's horizontal extent seemed greater; in several cases a single process extended for over 1 mm.

Pyramidal cells without an efferent axon have been previously described (Gilbert and Wiesel 1983, O'Leary 1941, Sholl 1955). However, the use of the Golgi technique (except by Gilbert and Wiesel) in these studies makes the lack of an efferent axon ambiguous, for in some cases it might be due to failure of the process to impregnate. Also, neither the Golgi data, nor the in vivo intracellular work can provide a reasonable estimate for the frequency of such cells. In layer VI of the adult cat at least, they appear to be quite common. Based on the morphological resemblance of the intrinsic cells to known projection classes of pyramidal cells in the same layer, these cells might represent populations of neurons that originally projected either to the lateral geniculate or the claustrum, but which, during development, did not for some reason maintain connections to their respective post-synaptic targets (see **Discussion**).

DISCUSSION

LeVay and Sherk (1981a), on the basis of anterograde labeling within cortex following the injection of tritiated aspartate into the claustrum or LGN, first put forward the idea that claustrum and LGN projecting neurons might have

different patterns of intrinsic axonal connections. They noted, (as did Baughman and Gilbert 1980), that lateral geniculate injections produced, in addition to retrogradely labelled cell bodies within layer VI, a band of labelled terminals in layer IV, which they surmised originated from axonal collaterals of layer VI cells. After claustrum injections with tritiated aspartate, label, both within cell bodies and diffuse, was confined to layer VI. They interpreted this as implying a lack of ascending axons in claustrum projecting cells. Alternatively, the sensitivity of the retrograde aspartate technique might not have been sufficient to demonstrate a layer IV projection arising from a small population of neurons. However, the results presented here demonstrate that they were correct: claustrum projecting cells do not have axonal collaterals to layer IV. Their results, corraborate, therefore, on a population level, the results described here at the level of a sample of single identified neurons. Although the techniques employed by LeVay and Sherk did not allow them to visualize the complete dendritic arbors of claustrum projecting cells, their published drawings of somas and initial dendritic processes bulk-labelled after large peroxidase injections into the claustrum, clearly show the same cell types described here. Their Figure 5, for example, shows cells with two of the diagnostic features of claustrum projecting cells: the presence of one or two basal dendritic processes considerably thicker than the rest, and the marked asymmetry of the basal dendritic arborization. This again independently corroborates the identity of the cells described here.

The demonstration that neurons which project to the claustrum or LGN have such distinct differences in their patterns of dendrites and intrinsic axons has important implications for the kinds of information to which these cells have access, and the influences of these cells on the activity of other neurons within A17. The very widespread horizontal collaterals of claustrum projecting cells

suggests that the activity of one cell can influence other cells at a considerable distance. These collaterals contact unknown postsynaptic sites, making it imposssible to predict whether these collaterals have excitatory or inhibitory effects on, or possibly do not even connect with, other claustrum projecting neurons. The prediction of the sign of any post-synaptic effects is particularly difficult since electron-microscopic evidence shows that pyramidal cell collaterals can contact either dendritic spines, or the dendrites or somas of spine-free (and presumably inhibitory) neurons (LeVay 1973). However, the horizontal collaterals may coordinate in some way the activity of cells that form the single, highly ordered retinotopic map found in the claustrum (LeVay and Sherk 1981b). In all the experiments described here, coronal sections of A17 were used, and thus all horizontal collaterals of claustrum projecting cells ran primarily along the medial to lateral axis of the visual map. It is not known what the relative extent of such collaterals might be in the anterior-posterior direction. Based on the information obtained so far, it is not yet possible to explain the marked distortion of the claustrum map-in which the representation of the periphery is greatly expanded relative to A17-on the basis of observed axonal patterns of claustrum projecting cells. In monkey striate cortex, horizontal collaterals apparently strongly and specifically connect cytochrome oxidase "blobs" (Livingstone and Hubel, 1984); other functionally related cortical subsystems, such as the claustrum projection, may show similar connectional patterns. In any event, the sparse connections of LGN projecting cells within layer VI provides rather unambigious evidence that activity in any one of these cells must have little or no direct, monosynaptic effect on that cell's neighbors. On the other hand, the ascending collaterals to layer IV must have quite strong effects on at least some of the cells within that layer. Sherk and LeVay (1983) noted that after destruction of the claustrum, end stop inhibition was decreased

by roughly 20%, especially in layers IV, and II/III. They postulated that the ability of claustrum cells to respond to very long slits might underly an inhibitory circuit that generated end-stop inhibition. Since a fair amount of end-stopping persists even after destruction of the claustrum, it cannot be the sole source for generating this response property, and they considered it possible that the geniculo-cortical cells in layer VI, which also respond to long slits, might underly the remainder of the end-stopping. McGuire et al. (1983) have shown that the ascending axons of these cells contact dendrites of spine-free cells in layer IV, which would be consistent for such cells playing a role in the generation of end-stopping.

The relationship of cell morphology to afferent input

Both the LGN and claustrum send afferents to cortex, as well as receive input from the two neuron types described here. How do the structural features of these cells relate to the known pattern of their respective afferent inputs?

According to LeVay and Sherk (1981a) the claustrum projection to A17, assessed autoradiographically, distributes across all the cortical layers. The lower portion of layer VI, and layer IV show the densest labeling; layer V has markedly fewer terminals. Within layer V, a trough of claustrum afferent density, claustrum projecting cells have their apical dendritic branching; these branches absolutely stop at the V/IV border, where the afferents from the claustrum reach their peak. Conversely, at the lowest point of afferent density--in upper layer VI and layer V--the density of dendritic spines on the apical dendrite of these cells reaches its peak (Fig. 20). The basal dendrites, however, lie in a region of high claustrum afferent input, and do not extend into the upper part of layer VI, which has a low density of such input. The apical dendrites of claustrum projecting cells seem to follow one set of rules,

attempting to minimize the region of overlap between dendrites and claustral afferents, while the basal dendrites follow a different set of rules, and try to maximize such overlap.

The afferents to cortex from the LGN terminate principally in upper layer VI and throughout layer IV. In contrast to the claustrum projecting cells, the geniculate neuron apical dendrite structure does not seem to avoid layers in which the LGN afferents terminate; they have quite a few dendritic branches within layer IV. In addition, the apical dendrites have their highest concentrations of spines at the V/VI border, again an area of dense afferent innervation. This picture agrees well with that seen in monkey layer VI by Lund (1973). In that Golgi study, neurons identified as probably projecting to the LGN showed specific patterns of branching of their apical dendrites and intrinsic, recurrent collaterals back to the layers of primary afferent input from the various layers of the LGN.

Yet other work reveals neurons in other layers which, similar to the claustrum projecting cells, seem to avoid contacts within the layers of afferent termination. For instance layer V cells in both cat and monkey either have a greatly reduced spine density as their apical dendrite traverses layer IV (Lund 1973), or in the monkey, the apical dendrite becomes vestigal before or just after entering layer IV (Lund and Boothe 1975). Layer V, like the claustrum projecting cells in layer VI, sends a retinotopic projection to the superior colliculus (Gilbert and Kelly 1975, Palmer and Rosenquist 1974, Lund et al. 1975).

Cell morphology: possible relationships to feedforward and feedback projections

The differences in LGN and claustrum projecting cell's structure could be due to their projections to different efferent targets. However, an additional factor, perhaps even more significant, may be the different directions that they

send their respective information, either feedforward or feedback. The organization of visual cortical areas according to their position in feedforward and feedback loops has been studied extensively by Maunsell and Van Essen (1983a). Their definition of the direction of a projection rests on the anatomical relationships between two areas. Feedforward connections originate primarily from the upper (supragranular) cortical layers, with occasional small contributions from lower (infragranular) cortical laminae. These projections terminate principally in layer IV of the recipient area. Feedback projections originate predominantly from the infragranular layers and terminate in the supra- and infragranular layers of the recipient area, conspiciously avoiding layer IV. On a physiological level, an area that is higher in the hierarchy (that is, receives feedforward projections) has larger receptive fields at a given eccentricity, and tends to show greater selectivity in some response properties. They also recognized a third type of connectional pattern, intermediate between feedforward and feedback, which they termed lateral connections.

This scheme was explicitly constructed to explain patterns of connections between visual cortical areas in the macaque, and the authors caution that it may not be applicable to other species or to subcortical connections. Nevertheless, it serves as a useful starting point for analyzing the relationships between the morphology of cells in various laminae, and whether they send feedforward or feedback connections.

The claustrum is an unusual structure in that, although it is subcortical, it receives its input primarily from cortical areas, and sends its efferents exclusively to the cortical structures. It receives no direct inputs from visual thalamic relay nuclei, and thus in several ways resembles an extrastriate cortical area. By considering the patterns of projections to and from this structure, as well as the response properties within it, some educated guesses can be made

concerning its hierarchical position.

The afferents to the claustrum in A17 originate almost exclusively from layer VI, while layer III makes an almost negligible contribution. In the monkey this would be very unusual for a feedforward connection; in the cat as well, most of the well-defined feedforward connections originate from the supragranular layers of A17 (e.g. connections to areas 18 and 19). The projection from the clasutrum likewise has an unusual termination pattern: the densest projections are to layers IV and VI, although all layers recieve some input. While the layer VI projection would be expected for a feedback connection, the layer IV projection would not.

On a physiological level, claustrum cells have several characteristics which would indicate that they receive feedforward projections from A17. Their receptive fields are larger, at a given eccentricity, than those of layer VI cells. Other characteristics, such as binocularity, direction and velocity selectivity, suggest that individual claustrum cells may pool the input from several layer VI cells. The response properties of claustrum cells greatly resemble those seen in layer VI of A17: they have very elongated receptive fields, show linear response summation to slits of increasing length, and show marked orientation selectivity. Claustrum cells probably integrate the input from groups of input cells, since these cells are strongly binocular, whereas layer VI cells are strongly monocular; they have little direction selectivity, which is often strong in layer VI cells. Also, claustrum cells show response summation to slits of light even longer than those which generate maximal responses in layer VI (Sherk and LeVay 1981). Since the claustrum does not receive any visual input other than from cortical cells, disruption of the cortex would presumably eliminate responses in the claustrum. Ablation of the claustrum (by kainic acid injections) has rather mild effects on the response properties of cells in A17, reducing end-stop

inhibition in about 20% of the cells, but not destroying the overall responsiveness of any lamina (Sherk and LeVay 1983).

Based on the above considerations, it would seem somewhat artificial to afix a rigid hierarchical position to the claustrum. Although the laminar origins and terminations of projections are incorrect for the strict formulation of feedforward and feedback projections in macaque cortex, if the apparent physiological role of the projections is considered, it seems plausible that the projection to the claustrum from A17 has many of the characteristics of a feedforward projection, whereas the projection from the claustrum to A17 resembles a feedback connection.

In contrast, eliminating input to A17 by the application of local anesthetic to the LGN virtually silences layer VI (as well as layer IV) (Malpeli 1983). Interrupting the activity of A17 (by local cooling, for example) leaves the major response characteristics of LGN neurons intact (although subtle effects have been described (see **Introduction**), there is no concensus about how, or how strongly the A17 projection to the LGN influences the response properties of LGN neurons). Thus, on a formal (as well as intuitive) level, A17 has a feedback projection to the LGN.

Major conclusions about the underlying role of projection direction in defining neuronal structure obviously cannot be drawn from the examination of only two projections. However, other pieces of circumstantial evidence also suggest that it may provide an important determinant of at least the intrinsic axonal patterns of a given neuron. It is important to note that this suggestion is based entirely on observation, not on logical deduction about the different functions required of feedforward and feedback neurons. Stated explicitly, feedforward cells may have long horizontal intrinsic axonal collaterals, primarily within the lamina in which their cell body lies; feedback cells may have

restricted horizontal connections within the lamina, but extensive recurrent collaterals to other laminae. Within A17, no other extrinsic projections, besides the LGN projection, can be considered feedback. However, a group of pyramidal cells in layer Va of O'Leary (1941), which lie just superficial to the large pyramids of layer V, have many of the characteristics of feedback cells. Although they apparently lack efferent axons, these cells send a strong recurrent projection back to, and arborize extensively within, layer III, effectively bypassing layer IV. Within layer Va, however, these cells apparently have few horizontal processes, and thus resemble the pattern seen in geniculate projecting cells.

Virtually all other pyramidal cells in A17 participate in feedforward circuits--primarily to extrastriate areas from layers II and III and to subcortical areas in layer V. The studies of Gilbert and Wiesel (1979, 1981) on the structure of cells in these layers reveal that many of the cells described so far have extremely extensive horizontal collaterals--often traversing distances of greater than 2 mm.

It would be most interesting to examine, in contrast, the intrinsic axonal collaterals of cells in the upper layers of, for instance, area 18 that contribute to the feedback projection to A17, versus those that send feedfoward projections to area 19 (both feedfoward and feedback cells are found in layers II and III in A18) (Gilbert and Kelly 1975). Extracellular injections of HRP in either 17 or 18 unfortunately do not provide a clear answer to this particular question. While small HRP injections into area 17 produce patches of cell bodies as well as diffuse labelling in area 18 (Gilbert and Wiesel 1980), this approach cannot distinguish whether the diffuse label results from anterograde transport from 17, or portions of the axonal processes of the retrogradely labelled neurons. There have been no published Golgi studies on the morphology of cells within

extrastriate areas that would allow this question to be addressed. In one preliminary experiment, cells that projected to the LGN from areas 18 and 19 were double labeled by intracellular injection. The intrinsic axons of these cells, like those of A17 cells, showed minimal amounts of collateralization within layer VI, and had strong ascending collaterals to the upper layers. This, however, could again simply reflect a special case of shared morphological characteristics between cells that project to the same efferent target, albeit from different cortical areas. Nevertheless, this hypothesis of the directional dependence of intrinsic axon patterns is readily testable, using the approach described here for investigating the claustrum and LGN projecting cells.

Morphological variability of cell types projecting to the LGN

In the original formulation of this project, the goal was to compare the morphology of neurons projecting to two distinct efferent sites from the same position within a single cortical lamina. This somewhat simplified the real situation, for, on a variety of levels, the lateral geniculate nucleus is best considered not as a single unified structure, but rather as containing several distinct functional subsystems. Separate geniculate laminae subserve each of the two eyes, and perhaps most important, at least three functionally and anatomically distinct, parallel pathways are relayed through the LGN: specifically, the parallel X ("brisk sustained") Y, ("brisk transient") and W ("sluggish") afferents to cortex originating from the LGN (Lennie 1980). Anatomically, these subsystems terminate at different cortical levels, and the terminals and afferent axons have markedly different appearances (Ferster and LeVay 1977, Blasdel and Lund 1983). As described in **Results**, the characteristics of the axons of various types of geniculate projecting cells in layer VI show some morphological relationship to the characteristics of the distinct afferent

groups. In the monkey, where X and Y-like cells may be separated into parvi- and magnocellular layers of the geniculate (Hubel and Wiesel 1972), apparently distinct morphological cell types in layer VI project to either one or the other geniculate layers (Lund and Boothe 1975). Lund proposed a continuity of afferent information, from the recipient layer of A17 all the way to the feedback pathway from layer VI. Attention was drawn to the possibility that distinct morphological types of cells might collate different sorts of information to send to distinct efferent targets. In the cat the distinction between X,Y, and W cells cannot be made on the basis of geniculate laminae. X and Y feedback axons probably both go to laminae A and A1 (Updyke 1975), but may only contact cells involved in the X or Y circuits within those laminae. In sum, then, the morphological diversity of geniculate projecting cells may be consistent with the role of specific functional projections underlying the need for different cell types in cortex.

Intrinsic pyramidal cells in layer VI

A consistent, but unexpected finding during these experiments was the existence of significant numbers of pyramidal cells in layer VI lacking an efferent axon. The substantial numbers of such cells--about 20% of the total cells in layer VI--implies that these do not represent isolated "mistakes" or aberrant cells, but rather that they contribute significantly to the structure of, and presumably to the processing within, layer VI. These cells could originate via at least two distinct mechanisms: either they represent a class of neurons that never sent an axon into the white matter, or, alternatively, they represent cells that originally made efferent connections, but lost them during development. Indirect evidence from a number of studies on the development of neural connections in general, and those within cortex in particular, suggest the

latter possibility. At the neuromuscular junction, motorneurons originally innervate a considerably larger number of post-synaptic sites (muscle fibers) than they do in adult animals (reviewed in Van Essen 1982). The same phenomenon, observed in numerous developing neuronal systems including climbing fiber input into the cerebellum, and innervation of sympathetic ganglion cells, strongly suggests that early multiple innervation of post-synaptic sites is a general developmental rule (Cowan 1978). In the best studied case of the neuromuscular junction, multiple innervation is apparently reduced by retraction of processes of some motor neurons (Bixby 1981). In this system, however, if motor neurons are completely deprived of their efferent post-synaptic target, they die (reviewed in Cowan 1973).

The situation within cerebral cortex shows many similarities. Several experiments have demonstrated conclusively that in young animals, cortical cells make considerably more extensive efferent projections in the young animal than they do in the adult (Innocenti et al. 1980, O'Leary et al. 1981, Ivy and Killackey 1982). Changes in the extent of callosal projections illustrate this particularly well. In young kittens, cells which project across the corpus callosum are distributed extensively throughout A17, at a quite high density, in all cortical layers. In the adult, only the narrow strip of A17 representing the vertical meridian contains callosally projecting cells, confined primarily to layers II/III. However, in contrast to the situation at the neuromuscular junction, cortical cells that lose their callosal connections do not die, and clearly persist into adulthood (O'Leary et al. 1981). Some such cells do make other efferent connections (Ivy and Killackey 1982), but whether others may end up without efferent axons, is not known.

The significant proportion of intrinsic cells, as well as their resemblance (both in terms of axons and dendrites) to either geniculate or claustrum

projecting neurons, suggests that these cells may represent neurons which originally projected to one or the other site (or perhaps across the corpus callosum), but which retracted their axons during development. If this population does in fact represent a general developmental process in cortex, pyramidal cells without axons should be actually quite common in other cortical layers as well. In this regard it is interesting that Gilbert and Wiesel (1981) have described one such cell in layer II which despite having axon collaterals filled for over 4 mm, showed no evidence of an efferent axon. They also mention having encountered several other such cells. In Golgi preparations, Sholl (1955) classified neurons lacking an efferent axon; in his sample they generally represented about 3% of the cells in a given lamina. However, in Golgi studies it is difficult to tell whether an axon has simply failed to impregnate, or whether it in fact does not exist.

Whatever their origin, the role of intrinsic pyramidal cells in cortical processing is probably similar in some respects to other cells in the same layer that have an efferent axon. All the intrinsic pyramidal cells observed in slices had electrical activity indistinguishable from effererent projecting cells; thus the lack of an efferent connection does not impair their ability to generate action potentials. More directly, Gilbert and Wiesel showed, for the cell described above, normal receptive field properties, clearly demonstrating that such cells are well integrated into the surrounding circuitry.

Cell classification in cerebral cortex

Historically, classification of the myriad of cell types encountered in Golgi preparations of cerebral cortex proceeded, in the absence of functional information, along subjective, and frequently botanical, lines. Early anatomists considered the patterns of dendritic branches, dendritic spines, and axonal

collaterals as particularly significant (Cajal 1911, Lorente de Nó 1933, O'Leary 1941, Sholl 1954, 1955). Even at this level of analysis, cortical cells could be quite readily divided into three classes: the intrinsic axon cells, with spine free dendrites, the spiny stellate cells in the afferent recipient layers, and the efferent projecting, spiny pyramidal cells. A variety of independent criteria allow these fundamental distinctions, including distribution of axon terminals, the electron microscopic appearance of terminals, and differences in neurotransmitter (Levay 1973, Somogyi 1978, Peters and Fairén 1978, Ribak 1978, Baughman and Gilbert 1981). Within each of these broad classes, however, cells show considerable morphological variability. The work presented here specifically addresses the question of whether any consistent rules of cortical organization subdivide pyramidal cells into distinct, consistent cell classes, or whether the morphological variability observed in a given cortical layer results from sampling a continuum of cell types. The distinctions between various kinds of intrinsic interneurons may follow fundamentally different rules than those observed for pyramidal cells, and such questions will not be addressed here.

Perhaps only in the past 20 years, with the explosion of information about the functional organization of cortex, has anatomical work had a more objective set of criteria by which to classify cells. The impact of this knowledge on understanding the Golgi picture in cortex is well illustrated by the work of Lund in the macaque. Here the relationship between a neuron's laminar position, patterns of apical dendritic branching and intrinsic axonal arborization, and probable efferent connectivity, were related to the levels of termination of specific groups of cortical afferents. Retrograde tracing showed that neurons in the lower layers of layer VI apparently provided the feedback to the magnocellular layers of the LGN, whereas those in the upper layers seemed to project to the parvicellular layers. The Golgi picture of cells in the two parts of

layer VI was quite distinct: cells in the layer which tended to project to magnocellular LGN had apical dendritic branches primarily in layers Va and IVca, or exclusively within IVb or exclusively within Vb. In contrast, cells in the lamina which tended to project to parvicellular LGN had branches in VB and IIIa, or Va and IIIb. These two classes did not seem to simply represent the extremes of a morphological continuum; no neurons with intermediate patterns have been described. Certainly, the specific relationship of these classes to a set of functionally derived criteria--specifically patterns of afferent and efferent connectivity--makes them considerably less arbitrary than the various classifications used in previous Golgi work. The work of Sholl on the organization of cellular elements in cortex provides an interesting counterpoint to this approach. Like Lund, he attempted to classify cells on the patterns of distribution on axon collaterals and dendrites, but at that time no information existed about the significance of specific patterns--for instance, why a collateral to the upper part of layer IV may have different effects than one to the lower portion. As a result, his view of cortex lacked any specific sorts of interactions, processing took place not by specific circuits but by statistical consequences of random connections within limited areas.

Both the work of Lund described above, and the work described in this report, provide strong evidence for the existence of morphological classes of cells based on efferent projection patterns. However, how even well defined morphological classes relate to the physiology and response properties of cortical neurons remains obscure. Indeed, as Kelly and Van Essen, and Gilbert and Wiesel have shown, the standard set of receptive field properties distributes across even the broad morphological distinctions of spinefree, spiny stellate, and pyramidal cells. There are at least two possible explanations for this discrepancy: 1) that the kinds of physiological tests (orientation and direction selectivity, ocular

dominance, complex vs simple) are either not sensitive enough, or do not include some unknown important stimulus parameter, or 2) that many of the observed morphological differences do not exist solely to construct a cell's receptive field properties, underlying instead some other (unknown) function of a specific morphological cell class. In this regard it is somewhat disturbing that the morphological feature of pyramidal cells that frequently attracts the greatest attention--namely the shape of the apical dendrite--has a completely unknown function. In contrast, the structure of non-pyramidal cells has provided some insights into their possible function. Basket cells, for example, show responses to visual stimulation virtually identical to those of pyramidal cells (Martin et al. 1983), however, the structure of their axonal arbors--with well developed, horizontally running collaterals with numerous pericellular baskets--suggests that they may play a role in inhibiting pyramidal cells over a considerable horizontal extent (Marin-Padilla 1974, Jones 1975). As more is learned about the properties of areas to which groups of pyramidal cells project, and about how pyramidal cells relate to each other synaptically, both what information various cells extract from A17, and how the morphology of specific cell types underlies this process, may become clearer.

Comparison of brain slices with Golgi techniques

Until the introduction of intracellular staining of cortical neurons by Kelly and Van Essen (1974) and more recently by Gilbert and Weisel (1979, 1983) and Martin et al. (1983), the Golgi technique provided the only detailed pictures of the cellular architecture of cerebral cortex. Probably the most dramatic result of Gilbert and Wiesel's intracellular injections was the discovery of extremely extensive intrinsic axonal connections never seen in Golgi preparations. This provided one concrete example of what had been long suspected--namely that

the Golgi technique has important constraints on the extent and completeness of cell visualization. Indeed, in the adult cat, it has been virtually impossible, using Golgi techniques, to extensively visualize the axons of pyramidal cells (Lund et al. 1975).

Although the in vivo intracellular fills provide by far the greatest detail on the structure of any given cell, this resolution is obtained at the expense of the number of cells available for analysis, as well as an inability to choose which particular cells to study.

The use of brain slices for anatomical studies is not completely novel- several authors have published short accounts of intracellularly stained neurons in hippocampal slices (Schwartzkroin and Mathers 1978) and in hypothalamic areas (Kelly et al. 1979, MacVicar et al. 1982). In most cases, however, the staining primarily confirmed the general type of cell from which a physiological recording originated, e.g., pyramidal vs. granule cells in the hippocampus. No previous descriptive studies on the morphology of neurons in brain slices go much beyond simply relating cells to known Golgi cell types from the same area (but see Knowles and Schwartzkroin 1981).

The major advantages of slices over Golgi techniques for studying cellular architecture include: 1) fewer truncated processes due to the use of thicker slices, 2) excellent filling of axonal processes, even in adult animals, and 3) directed filling of specific cells in specific areas or laminae of cortex. A more detailed discussion of these points follows below.

The picture of layer VI neurons obtained in Golgi studies differs in several respects from that seen in slices. For LGN projecting cells, for instance, the previous Golgi descriptions of O'Leary (1941), Cajal (1911), and Lund et al. (1979) show a basically similar cell type to that described here. However, in the Golgi picture, the basal dendritic field is considerably sparser than that seen in slices;

the horizontal extent of the apical dendrites is much reduced as well. This indicates significant truncation of dendritic processes, even when the most complete Golgi stained cells were used. Sholl (1954) examined the number of basal dendritic arms of cortical pyramidal cells and reported a range of 4-10, with an average of about 6. A similar number was observed using slices, thus the sparser dendritic arbors of Golgi stained neurons probably did not result from a failure to impregnate some of the dendritic arms. Rather, the thickness of the sections used in Golgi studies (generally 100-200 μm, uncorrected for shrinkage), which is considerably thinner than the observed diameter of the dendritic field, results in an underestimation of the density of basal dendritic branches. This may also explain why the unusually elongated basal dendrites of claustrum projecting cells have not been described in cat. Also, no cells showing of the class I LGN-projection type--with the widespread dendritic side branches (such as the cells in Figs. 24 and 25)--have been previously mentioned in the Golgi literature.

A second major problem with the Golgi technique is the difficulty, in the cat at least, of obtaining any impregnations whatsoever of intrinsic axonal collaterals in adult animals (Lund et al. 1979); thus not surprisingly the vast majority of studies on the Golgi architecture of cat cortex have been actually on the brains of kittens of various ages (with the exception, apparently, of Sholl 1954). The visual cortex undergoes profound transformations during the "critical period" of 3-12 weeks postnatal (Hubel and Wiesel 1970, Shatz and Stryker 1978, LeVay et al. 1978); most Golgi sudies are done on animals younger than this (up to about 4 weeks old). The structure of the cells of young animals might significantly differ, in unknown ways, from that of older animals, since in other systems some substantial differences have been seen. For instance Guillery (1966) saw changes in the morphology of the various classes of LGN neurons

between young animals and adults; Lund et al. (1977) have observed changes in the number of dendritic spines on pyramidal cells of different ages. One persistent and somewhat puzzling difference between Golgi studies of layer VI cells and the results reported here concerns neurons whose apical dendrite arborizes within layer I. Both O'Leary (1941) and Lund et al. (1979) describe layer VI (in young kittens) as containing either exclusively (O'Leary) or primarily (Lund et al.) such neurons. In slices of adult cortex, the LGN projecting cells, which clearly form the bulk of the neurons in the lamina, never had an apical dendrite above layer III. Even in the case of claustrum projecting cells, only a few had the characteristic "spray" of processes in layer I; most simply ended in the upper portion of layer II or at the lower border of layer I. The only cell which showed a significant apical dendritic arbor in layer I was an intrinsic pyramidal cell of the claustrum projecting type (Fig. 39). It is extremely unlikely that this difference is due to a failure to fill such processes in virtually all the cells. In most cases (and certainly in all those drawn for figures) the actual end of the dendrite was visible: the process did not gradually fade out, but rather abruptly stopped at a certain point. In addition, in both published and personal communications, Gilbert and Wiesel (1979, 1983) have observed that in vivo LGN-projecting type cells have apical dendrites to layer III; claustrum projecting cell types have long thin apical dendrites which end without a "spray" either below layer I or at the I/II border. These pieces of evidence suggest either that 1) a considerable amount of reshaping and retracting of the dendritic field is occurring between 2.5 weeks of age and adulthood, involving specifically the elimination of connections to layer I, or 2) the Golgi technique selectively impregnates a rare cell type in layer VI, making it appear as the dominant cell type of the layer. In her study of the development of monkey visual cortex neurons, Lund et al.(1977) found no evidence for reshaping or pruning of apical

dendritic fields. However, since this study employed the Golgi technique, the results are subject to the same constraint raised in point (2) above. This final point, of course, has been a worrisome one for quite some time, since the basis on which a neuron becomes Golgi stained is completely obscure.

The controlled filling of cells, in contrast with the unknown basis of the Golgi stain, constitutes a major advantage of intracellular staining in slices: one can either chose to impale specific neurons (such as those in a particular part of a layer, or several neurons with a specified spatial relationship to one another), or, alternatively, random filling of cells is probably close to truly random, and therefore gives a fairly accurate estimate of the relative proportions of specific cell types. The evidence for this last point (with the caveat that very small cells may be under-represented) comes primarily from early experiments in which cells were filled in a fashion taken to be random. In those cases, the proportion of double labeled cells in a given experiment was remarkably close to that which would have been expected on the basis of truly random filling. This in turn led to the discovery that a significant proportion of layer VI cells were intrinsic pyramidal cells--a conclusion that would have been quite suspect using Golgi staining.

However, without some of the very elegant and incisive interpretations of Golgi stains, simply injecting cells in slices, without some reference to either Golgi or in vivo work, can be quite risky, since a whole new class of slice artifacts may exist. Also, for an overview of a given brain area, Golgi staining provides a much larger scope, allowing the simultaneous visualization of hundreds of cells in all configurations, and in all layers. Finally, Golgi staining may be demonstrably superior to intracellular staining in the completeness and number of small cells stained. Even in vitro, it is difficult to penetrate, hold, and adequately fill cells smaller than about 8 μm in diameter.

The problem of truncation of processes, particularly long axonal ones, remains even in well filled cells in slices. Slices, although superior in this respect to Golgi stains, nevertheless cannot compare to in vivo intracellular fills in the completeness of collateral staining. This was seen particularly clearly when the projection to layer IV originating from LGN-projecting neurons filled in vitro was compared to similar cells filled in vivo: the density of axon terminals, even in the best in vitro cases, was considerably less than seen in the best in vivo cases. Slices do have significant advantages in some respects over in vivo experiments, principally in the greater number of well filled cells that can be obtained in vitro versus in vivo; additionally, specific cell populations can be studied in vitro, which is almost impossible using in vivo intracellular injections.

These three techniques for studying the structure of single neurons have complementary strengths: the superb detail and physiological information available from in vivo intracellular work, the cellular overview possible from Golgi staining, and the ability to study defined groups of cells in great anatomical detail allowed by the in vitro approach.

Determinants of cell form in cortex

The question of cell classification in cortex relates intimately to the question of the mechanisms by which might generate distinct cell classes. One extreme view would be that genetic factors determine all the branching patterns of a cells axons and dendrites; the opposite view would be that all cell features differentiate in response to the environment in which the cell finds itself in cortex.

It is abundantly clear that most vertebrate and invertebrate neurons have a strong innate program to differentiate along a certain basic pattern. Thus for a

variety of vertebrate systems--including cortex (Dichter 1978, Kriegstein and Dichter 1983), and cerebellum (Gähwiler 1981)--fetal cells grown in culture usually aquire morphological patterns which resemble one of the cell types typical of the area from which the culture was derived. In cerebellar cultures in particular, the Purkinje cell, a homogeneous cell type (both in terms of dendritic morphology and efferent axon projections), is clearly recognizable in vitro. This has only been studied in a broad sense in cortex--i.e., whether a cell aquires a pyramidal morphology versus various kinds of spiny stellate or spine-free morphologies. Thus even cells disconnected from their normal pattern of inputs and outputs, differentiate into recognizable cell types. In a sense the in vivo work on reeler mice, whose cortical structure is completely abnormal, shows the same result: well defined pyramidal and non-pyramidal cells are easily recognizable in reeler cortex, even though they may assume abnormal orientations (Caviness 1977).

The effects of a cell's surroundings--in particular its specific patterns of inputs--apparently have morphologically more subtle effects. Features consistently effected by the amount or type of input a cell receives include the density and distribution of dendritic spines, and the number and distribution of tertiary dendritic branches (reviewed in Cowan 1979, Berry 1982). Certain features of the axonal arbors of cells--such as described here for intrinsic pyramidal cells--are probably a consequence of developmental, and not strictly innate processes. Geniculo-cortical afferents undergo significant morphological changes--either expanding or contracting the region of layer IV they cover--in response to changes in the activity level of the visual pathway (e.g. by monocular lid suture) (Shatz and Stryker 1978). It would be surprising if other cortical cells intrinsic axons--such as the layer VI cortico-geniculate cells feedback arborizations in layer IV--did not show similar, perhaps compensatory, changes as well.

Both claustrum projecting and LGN projecting cells occupy similar laminar positions, and therefore at least have potential access to many, if not all of the same environmental influences. Nonetheless they show non-graded, non-overlapping patterns of dendrites and axons. This strongly suggests innate differences between these cell types, and not differentiation from a common precursor.

The observation that claustrum and LGN projecting cells occupy overlapping horizontal positions in layer VI implies that some of each of these projection classes must have been generated and migrated to cortex at virtually identical times (Rakic 1974). This in turn suggests that birthdate does not in itself form a sufficient cue for telling an individual cortical cell where to send its efferent projection. There is evidence in the monkey that time of birth does play some role in organizing efferent projections: the first neurons to reach their final position in layer VI send out the first axons to the magnocellular portions of the LGN, the projection to the parvicellular layers originates later, from a second group of neurons in layer VI born after the first (Shatz and Rakic 1981). It remains a difficult problem to explain how a small group of neurons projecting to one site can find where to go when surrounded by at least ten times as many cells projecting somewhere else.

Since birthdate does not seem to provide specific enough cues for organizing the efferent projection of claustrum projecting cells, these neurons could rely on some common marker which allows them to sort themselves out from the plethora of LGN projecting cells. One such system-related cell surface marker has been described for the limbic system (Levitt 1984). Because the claustrum projection consists of relatively few cells, (probably fewer than 150,000 in area 17), and because they exhibit such uniform morphological characteristics, they could conceivably all be clonally derived from a very small

number of precursor cells. In this case 7-8 divisions of 5 clonal precursors could generate all the claustrum projecting cells in layer VI. A similar proposal has been advanced, with more direct evidence from studies of chimeric mice, for the relationships of Purkinje cells (another quite uniform cell type) in the cerebellum (Wetts and Herrup 1981). A clonal relationship between cells (Moody and Jacobsen 1983) might provide a mechanism which produces a morphologically uniform cell class which could make specific contacts with each other, as well as with their efferent target.

REFERENCES

Albus, K., and F. Donate-Oliver (1977) Cells of origin of the occipitopontine projection in the cat: Functional properties and intracortical location. Exp. Brain Res. 28: 167-174.

Baker, J. F., S. E. Petersen, W. T. Newsome, and J. M. Allman (1981) Visual response properties of neurons in four extrastriate visual areas of the owl monkey (Aotus trivirgatus): A quantitative comparison of medial, dorsomedial, dorsolateral, and middle temporal areas. J. Neurophysiol. 45: 397-416.

Barlow, H. B., R. M. Hill, and W. R. Levick (1964) Retinal ganglion cells responding selectively to direction and speed of image motion in the rabbit. J. Physiol. (Lond.) 173: 377-407.

Baughman, R. W., and C. D. Gilbert (1981) Aspartate and glutamate as possible neurotransmitters in the visual cortex. J. Neurosci. 1: 427-439.

Berry, M. (1982) Cellular differentiation: Development of dendritic arborizations under normal and experimentally altered conditions. Neurosci. Res. Prog. Bull. 20: 451-461.

Bishop, P. O., W. Kozak, and G. J. Vakkur (1962) Some quantitative aspects of the cat's eye: Axis and plane of reference, visual field coordinates and optics. J. Physiol. 163: 466-502.

Bixby, J. L. (1981) Ultrastructural observations on synapse elimination in neonatal rabbit skeletal muscle. J. Neurocytol. 10: 81-100.

Blasdel, G. G., and J. S. Lund (1983) Termination of afferent axons in macaque striate cortex. J. Neurosci. 3: 1389-1413.

Cajal, S. R. (1911) Histologie du Systeme Nerveux de l'Homme et des Vertebres, 1972 ed., CSIC, Madrid.

Caviness, V. W. (1977) Reeler mutant mouse: A genetic experiment in developing mammalian cortex. Soc. Neurosci. Symp. 2: 27-46.

Cowan, W. M. (1973) Neuronal death as a regulative mechanism in the control of cell number in the nervous system. In Development and Aging in the Nervous System, M. Rockstein, ed., pp. 19-41, Academic Press, New York, NY.

Cowan, W. M. (1978) Aspects of neural development. Int. Rev. Physiol. 17: 149.

Cowan, W. M. (1979) Selection and control in neurogenesis. In The Neurosciences: Fourth Study Program, F. O. Schmitt and F. G. Worden, eds., pp. 59-79, MIT Press, Cambridge, MA.

Cowan, W. M., D. I. Gottlieb, A. E. Hendrickson, J. L. Price, and T. A. Woolsey (1972) The autoradiographic demonstration of axonal connections in the central nervous system. Brain Res. 37: 21-51.

Dichter, M. A. (1978) Rat cortical neurons in cell culture: culture methods, cell morphology, electrophysiology, and synapse formation. Brain Res. 149: 279-293.

Dingledine, R., J. Dodd, and J. S. Kelly (1980) The in vitro brain slice as a useful neurophysiological preparation for intracellular recording. J. Neurosci. Meth. 2: 323-362.

Ewert, J.-P. (1980) Neuroethology, Springer Verlag, New York, NY.

Ferster, D., and S. LeVay (1978) The axonal arborization of lateral geniculate neurons in the striate cortex of the cat. J. Comp. Neurol. 182: 923-944.

Ferster, D., and S. Lindström (1983) An intracellular analysis of geniculo-cortical and intracortical connectivity in area 17 of the cat. J. Physiol. 342: 181-216.

Gähwiler, B. H. (1981) Morphological differentiation of nerve cells in thin organotypic cultures derived from rat hippocampus and cerebellum. Proc.

R. Soc. Lond. B 211: 287-290.

Gilbert, C. D. (1977) Laminar differences in receptive field properties in cat primary visual cortex. J. Physiol. 268: 391-421.

Gilbert, C. D. (1983) Microcircuitry of the visual cortex. Ann. Rev. Neurosci. 6: 217-247.

Gilbert, C. D., and J. P. Kelly (1975) The projections of cells in different layers of the cat's visual cortex. J. Comp. Neurol. 163: 81-106.

Gilbert, C. D., and T. N. Wiesel (1979) Morphology and intracortical projections of functionally identified neurons in cat visual cortex. Nature 280: 120-125.

Gilbert, C. D., and T. N. Wiesel (1980) Interleaving projection bands in cortico-cortical connections. Soc. Neurosci. Abstr. 6: 315.

Gilbert, C. D., and T. N. Wiesel (1983) Clustered intrinsic connections in cat visual cortex. J. Neurosci. 3: 1116-1133.

Guillery, R. W. (1966) A study of Golgi preparations from the dorsal lateral geniculate nucleus of the adult cat. J. Comp. Neurol. 128: 21-50.

Guillery, R. W. (1967) Pattern of fiber degeneration in the dorsal lateral geniculate nucleus of the cat following lesions in the visual cortex. J. Comp. Neurol. 130: 197-222.

Gupta, R. K., B. M. Salzberg, A. Grinvald, L. B. Cohen, K. Kamino, S. Lesher, M. B. Boyle, A. S. Waggoner, and C. H. Wang (1981) Improvements in optical methods for measuring rapid changes in membrane potential. J. Membrane Biol. 58: 123-137.

Harvey, A. R. (1978) Characteristics of corticothalamic neurons in area 17 of the cat. Neurosci. Lett. 7: 177-181.

Hatton, G. I., A. B. Doran, A. K. Salm, and K. D. Tweedle (1980) Brain slice preparation: Hypothalamus. Brain Res. Bull. 5: 405-414.

Henry, G. H., A. R. Harvey, and J. S. Lund (1979) The afferent connections and laminar distribution of cells in the cat striate cortex. J. Comp. Neurol. 187: 725-744.

Hoffman, K.-P., and J. Stone (1971) Conduction velocity of afferents to cat visual cortex: A correlation with receptive field properties. Brain Res. 32: 460-466.

Hubel, D. H., and T. N. Wiesel (1961) Integrative action in the cat's lateral geniculate body. J. Physiol. 155: 385-398.

Hubel, D. H., and T. N. Wiesel (1962) Receptive fields, binocular interaction and functional architecture in the cat's visual cortex. J. Physiol. 160: 106-154.

Hubel, D. H., and T. N. Wiesel (1963) Shape and arrangement of columns in cat's striate cortex. J. Physiol. 165: 559-568.

Hubel, D. H., and T. N. Wiesel (1970) The period of susceptibility to the physiological effects of unilateral eye closure in kittens. J. Physiol. (Lond.) 206: 419-436.

Hubel, D. H., and T. N. Wiesel (1972) Laminar and columnar distribution of geniculo-cortical fibers in the macaque monkey. J. Comp. Neurol. 146: 421-450.

Hudspeth, A. J., and D. P. Corey (1978) Controlled bending of high-resistance glass micropipettes. Am. J. Physiol. 234: C56-C57.

Hull, T. F. (1968) Corticofugal influence in the macaque lateral geniculate nucleus. Vision Res. 8: 1285-1298.

Innocenti, G. M., and R. Caminiti (1980) Postnatal shaping of callosal connections from sensory areas. Exp. Brain Res. 38: 381-394.

Innocenti, G. M., L. Fiore, and R. Caminiti (1977) Exuberant projection into the corpus callosum from the visual cortex of newborn cats. Neurosci. Lett. 4: 237-242.

Ivy, G. O., and H. P. Killackey (1982) Ontogenetic changes in the projections of neocortical neurons. J. Neurosci. 2: 735-743.

Jones, E. G. (1975) Varieties and distribution of non-pyramidal cells in the somatic sensory cortex of the squirrel monkey. J. Comp. Neurol. 160: 205-268.

Kalil, R. E., and R. Chase (1970) Corticofugal influence on activity of lateral geniculate neurons in the cat. J. Neurophysiol. 33: 459-474.

Kawamura, K., and M. Chiba (1979) Cortical neurons projecting to the pontine nuclei in the cat. An experimental study with the horseradish peroxidase technique. Exp. Brain Res. 35: 269-285.

Kawamura, K., and T. Konno (1979) Various types of corticotectal neurons of cats as demonstrated by means of retrograde axonal transport of horseradish peroxidase. Exp. Brain Res. 35: 161-175.

Kawamura, K., and J. Naito (1980) Corticocortical neurons projecting to the medial and lateral banks of the middle suprasylvian sulcus in the cat: An experimental study with the horseradish peroxidase method. J. Comp. Neurol. 193: 1009-1022.

Kelly, J. P. and D. C. Van Essen (1974) Cell structure and function in the visual cortex of the cat. J. Physiol. 328: 515-547.

Kelly, M. J., U. Kuhnt, and W. Wuttke (1979) Morphological features of physiologically identified hypothalamic neurons as revealed by intracellular marking. Exp. Brain Res. 34: 107-116.

Knowles, W. D., and P. A. Schwartzkroin (1981) Axonal ramifications of hippocampal CH1 pyramidal cells. J. Neurosci. 1: 1236-1241.

Kriegstein, A. R. and M. A. Dichter (1983) Morphological classification of rat cortical neurons in cell culture. J. Neurosci. 3: 1634-1647.

Kuffler, S. W. (1953) Discharge patterns and functional organization of the

mammalian retina. J. Neurophysiol. 16: 37-68.

LaVail, J. H. (1975) Retrograde cell degeneration and retrograde transport techniques. In The Use of Axonal Tranport for Studies of Neuronal Connectivity, W. M. Cowan and M. Cuénod, eds., pp. 217-223, Elsevieer, Amsterdam.

Lennie, P. (1980) Parallel visual pathways: A review. Vis. Res. 20: 561-594.

LeVay, S. (1973) Synaptic patterns in the visual cortex of the cat and monkey. Electron microscopy of Golgi preparations. J. Comp. Neurol. 150: 53-86.

LeVay, S., M. P. Stryker, and C. J. Shatz (1978) Ocular dominance columns and their development in layer IV of the cat's visual cortex: A quantitative study. J. Comp. Neurol. 179: 223-244.

LeVay, S., and H. Sherk (1981a) The visual claustrum of the cat. I. Structure and connections. J. Neurosci. 1: 956-980.

Levay, S., and H. Sherk (1981b) The visual claustrum of the cat. II. The visual field map. J. Neurosci. 1: 981-992.

Levitt, P. (1984) A monoclonal antibody to limbic system neurons. Science 223: 299-301.

Leventhal, A. G., and H. V. B. Hirsch (1978) Receptive field properties of neurons in different laminae of visual cortex of the cat. J. Neurophysiol. 41: 948-962.

Levick, W. R. (1967) Receptive fields and trigger features of ganglion cells in the visual streak of the rabbit's retina. J. Physiol. (Lond.) 188: 285-307.

Livingstone, M. S., and D. H. Hubel (1984) Anatomy and physiology of a color system in the primate visual cortex. J. Neurosci. 4: 309-356.

Llinas, R., and R. Hess (1976) Tetrodotoxin-resistant dendritic spikes in avian Purkinje cells. Proc. Natl. Acad. Sci. USA 73: 2520-2523.

Llinas, R., and M. Sugimori (1980) Electrophysiological properties of in vitro

Purkinje cell dendrites in mammalian cerebellar slices. J. Physiol. (Lond.) 305: 197-213.

Lorente de Nó, R. (1933) Studies on the structure of the cerebral cortex. J. Psychol. Neurol. 45: 382-438.

Lund, J. S. (1973) Organization of neurons in the visual cortex, area 17, of the monkey (Macaca mulatta). J. Comp. Neurol. 147 455-496.

Lund, J. S. (1981) Intrinsic organization of the primate visual cortex, area 17, as seen in golgi preparations. In The Organization of Cerebral Cortex, F. O. Schmitt, F. G. Worden, G. Adelman, and S. G. Dennis, eds., pp. 325-345, MIT Press, Cambridge.

Lund, J. S., and R. G. Boothe (1975) Interlaminar connections and pyramidal neuron organization in the visual cortex, area 17, of the Macaque monkey. J. Comp. Neurol. 159: 305-334.

Lund, J. S., R. G. Boothe, and R. D. Lund (1977) Development of neurons in the visual cortex (area 17) of the monkey (Macaca nemestrina): A Golgi study from fetal day 127 to postnatal maturity. J. Comp. Neurol. 176: 149-188.

Lund, J. S., G. H. Henry, C. I. Macqueer, and A. R. Harvey (1979) Anatomical organization of the primary visual cortex (area 17) of the cat. A comparison with area 17 of the Macaque monkey. J. Comp. Neurol. 184: 599-618.

Maciewicz, R. J. (1974) Afferents to the lateral suprasylvian gyrus of the cat traced with horseradish peroxidase. Brain Res. 78: 139-143.

MacVicar, B. A., R. D. Andrew, F. E. Dudek, and G. Hatton (1982) Synaptic inputs and action potentials of magnocellular neuropeptidergic cells. Intracellular recording and staining in slices of rat hypothalamus. Brain Res. Bull. 8: 87-93.

Magalhaes-Castro, H. H., P. E. S. Saraiva, and B. Magalhaes-Castro (1975)

Identification of corticotectal cells of the visual cortex of the cat by means of horseradish peroxidase. Brain Res. 83: 474-479.

Malpeli, J. G., P. H. Shiller, and C. L. Colby (1981) Response properties of single cells in monkey striate cortex during reversible inactivation of individual lateral geniculate laminae. J. Neurophysiol. 46: 1102-1119.

Malpeli, J. G. (1983) Activity of cells in area 17 of the cat in absence of input from layer A of lateral geniculate nucleus. J. Neurophysiol. 49: 595-610.

Marin-Padilla, M. (1974) Three-dimensional reconstruction of the pericellular nests (baskets) of the motor (area 4) and visual (area 17) areas of the human cerebral cortex. A Golgi study. Z. Anat. Entwicklungsgesch. 144: 123-135.

Martin, K. A. C., D. Somogyi, and D. Whitteridge (1983) Physiological and morphological properties of identified basket cells in the cat's visual cortex. Exp. Brain Res. 50: 193-200.

Masukawa, L. M., and D. A. Prince (1984) Synaptic control of excitability in isolated dendrites of hippocampal neurons. J. Neurosci. 4: 217-227.

Maunsell, J. H. R., and D. C. Van Essen (1983a) Functional properties of neurons in middle temporal visual area of the Macaque monkey. I. Selectivity for stimulus direction, speed, and orientation. J. Neurophysiol. 49: 1127-1147.

Maunsell, J. H. R., and D. C. Van Essen (1983b) Functional properties of neurons in middle temporal visual area of the Macaque monkey. II. Binocular interactions and sensitivity to binocular disparity. J. Neurophysiol. 49: 1148-1167.

Maunsell, J. H. R., and D. C. Van Essen (1983c) The connections of the middle temporal visual area (MT) and their relationship to a cortical hierarchy in the macaque monkey. J. Neurosci. 3: 2563-2586.

McGuire, B. A., J. P. Hornung, C. D. Gilbert, and T. N. Wiesel (1983) Layer 6

cells primarily contact smooth and sparsely spiny neurons in layer 4 of cat striate cortex. Soc. Neurosci. Abst. 9: 617.

Miller, J. P., and A. I. Selverston (1979) Rapid killing of single neurons by irradiation of intracellularly injected dye. Science 206: 702-704.

Moody, S. A., and M. Jacobson (1983) Compartmental relationships between anuran primary spinal motorneurons and somitic muscle fibers that they first innervate. J. Neurosci. 3: 1670-1682.

O'Leary, D. D. M., B. B. Stanfield, and W. M. Cowan (1981) Evidence that the early postnatal restriction of the cells of origin of the callosal projection is due to the elimination of axonal collaterals rather than to the death of neurons. Dev. Brain Res. 1: 607-617.

Otsuka, R., and H. Hassler (1962) Uber aufbau und Gliederung der corticalen Sehsphare bei der Katze. Arch. Psych. Nevenkr. 203: 212-234.

Palmer, L. A., and A. C. Rosenquist (1974) Visual receptive fields of single striate cortical units projecting to the superior colliculus in the cat. Brain Res. 67: 27-42.

Peters, A., and A. Fairén (1978) Smooth and sparsely-spined stellate cells in the visual cortex of the rat: A study using a combined Golgi-electron microscope technique. J. Comp. Neurol. 181: 129-172.

Rakic, D. (1974) Neurons in rhesus monkey visual cortex: Systematic relation between time of origin and eventual disposition. Science 183: 425-427.

Ribak, C. E. (1978) Aspinous and sparsely-spinous stellate neurons in the rat's visual cortex contain glutamic acid decarboxylase. J. Neurocytol. 7: 461-478.

Rodieck, R. W. (1979) Visual pathways. Ann. Rev. Neurosci. 2: 193-225.

Sanderson, K. J. (1971) The projection of the visual field to the lateral geniculate and medial interlaminar nuclei in the cat. J. Comp. Neurol. 143: 101-118.

Schmielau, F., and W. Singer (1977) The role of the visual cortex for binocular interactions in the cat lateral geniculate nucleus. Brain Res. 120: 354-361.

Schwartzkroin, P. A. (1975) Characteristics of CA1 neurons recorded intracellularly in the hippocampal in vitro slice preparation. Brain Res. 85: 423-436.

Schwartzkroin, P. A., and L. H. Mathers (1978) Physiological and morphological identification of a nonpyramidal hippocampal cell type. Brain Res. 157: 1-10.

Shatz, C. J., and M. P. Stryker (1978) Ocular dominance in layer IV of the cat's visual cortex and the effects of monocular deprivation. J. Physiol. (Lond.) 281: 267-283.

Shatz, C. J., and P. Rakic (1981) The genesis of efferent connections from the visual cortex of the fetal rhesus monkey. J. Comp. Neurol. 196: 287-307.

Sherk, H., and S. LeVay (1981) The visual claustrum of the cat. III. Receptive field properties. J. Neurosci. 1: 993-1002.

Sherk, H., and S. LeVay (1983) Contribution of the cortico-claustral loop to receptive field properties in area 17 of the cat. J. Neurosci. 3: 2121-2127.

Sholl, D. A. (1955) The organization of the visual cortex in the cat. J. Anat. 89: 33-46.

Singer, W. (1970) Inhibitory binocular interaction in the lateral geniculate body of the cat. Brain Res. 18: 165-170.

Singer, W., F. Tretter, and M. Cynader (1975) Organization of cat striate cortex: A correlation of receptive field properties with afferent and efferent connections. J. Neurophysiol. 38: 1080-1098.

Somogyi, P. (1978) The study of Golgi stained cells and of experimental degeneration under the electron microscope: A direct method for the identification in the visual cortex of three successive links in a neuron

chain. Neuroscience 3: 167-180.

Stewart, W. W. (1978) Functional connections between cells as revealed by dye-coupling with a highly fluorescent Naphthalimide tracer. Cell 14: 741-759.

Tombol, T., F. Hajdu, and G. Somogyi (1975) Identification of the golgi picture of the layer VI cortico-geniculate projection neurons. Exp. Brain Res. 24: 107-110.

Toyama, K., K. Matsunami, T. Ohno, and S. Tokashiki (1974) An intracellular study of neuronal organization in the visual cortex. Exp. Brain Res. 21: 45-66.

Tsumoto, T., O. D. Creutzfeldt, and C. R. Legendy (1978) Functional organization of the corticofugal system from visual cortex to lateral geniculate nucleus in the cat. Exp. Brain Res. 32: 345-364.

Updyke, B. V. (1975) The patterns of projection of cortical areas 17, 18, and 19 onto the laminae of the dorsal lateral geniculate nucleus in the cat. J. Comp. Neurol. 163: 377-396.

Van Essen, D. C. (1979) Visual areas of the mammalian cerebral cortex. Ann. Rev. Neurosci. 2: 227-263.

Van Essen, D. C. (1982) Neuromuscular synapse elimination: Structural, functional, and mechanistic aspects. In Neuronal Development, N. C. Spitzer, ed., pp. 333-376, Plenum, New York.

Wetts, R., and K. Herrup (1981) Cerebellar Purkinje cells originate from a small number of progenitors committed early in development. Soc. Neurosci. Abstr. 7: 544.

Wong, R. K. S., D. A. Prince, and A. I. Basbaum (1979) Intradendritic recordings from hippocampal neurons. Proc. Nat. Acad. Sci. USA 76: 986-990.

Zeki, S. M. (1974) Functional organization of a visual area in the posterior bank of the superior temporal sulcus of the rhesus monkey. J. Physiol. (Lond.) 236: 549-573.

CHAPTER II

Development and Attributes of Fluorescent Latex Microspheres as a Retrograde Tracer in the Central Nervous System

(manuscript by L.C. Katz, A. Burkhalter, and W.J. Dreyer)

Fluorescent latex microspheres: a retrograde neuronal marker for in vivo and in vitro studies of cortex

L.C. Katz[1], A. Burkhalter[2] and W.J. Dreyer, Div. of Biology, 216-76, California Institute of Technology, Pasadena, CA 91125

[1] To whom correspondence should be addressed

[2] Present address: Dept. of Neurobiology, Harvard Medical School, Boston, MA 02115

The use of retrograde axonal transport of various substances (e.g. enzymes, lectins, synthetic fluorescent compounds) has yielded a wealth of information on the organization of neuronal pathways. Each type of retrograde tracer has its own set of attributes which define the scope of problems it can address[1-3]. We describe here a new class of retrograde tracer, rhodamine-labeled fluorescent latex microspheres (0.02-0.2 μm diameter), which have distinct advantages over other available tracers for in vivo and in vitro applications. When injected into brain tissue, these microspheres show little diffusion and consequently produce small, sharply defined injection sites. Once transported back to neuronal somata, the label persists for at least 10 weeks in vivo and 1 year after fixation. Microspheres have no obvious cyto- or phototoxicity as assessed by intracellular recording and staining of retrogradely labeled cells in a cortical brain slice preparation. This approach was further employed to visualize and compare, in cat visual cortex slices, neurons with different projection patterns, revealing significant differences in patterns of intrinsic axons and dendrites. These properties of microspheres open new avenues for anatomical and physiological studies of identified projection neurons in slices as well as in dissociated cell cultures.

The methodology for obtaining retrograde labeling was studied by injections into the visual cortex (area 17, 40 cases) and corpus callosum (3 cases) of adult rats. The first 20 rats were used to establish parameters such as the concentration and volume of bead suspensions, bead size, survival time, and histological procedures. The 23 remaining rats were used to ascertain the effective injection site and test for uptake by fibers, pathway selectivity, long term survival effects and toxicity. Using a standardized protocol (see Fig. 1 legend) 21 of the 23 rats injected showed retrograde labeling.

Injection sites, 50-200 μm in diameter (Fig. 1a), remained similar in size

after 6 hours or 10 weeks of post-injection survival time. Their restricted extent probably results from the relatively large size (on a molecular scale) of the microspheres, and the hydrophobic nature of plastic polymers. Semi-thin sections of the injection site revealed apparently healthy tissue and normal looking neurons; the only signs of injury were numerous bead-filled macrophages invading the electrode track.

Injections into area 17 (A17) resulted in retrograde labeling locally within A17, in cortical areas outside A17, and subcortically. We measured the extent of retrograde labeling in the lateral geniculate nucleus (LGN) to estimate the effective site of bead uptake. Injections into the peripheral representation of the upper visual field typically produced a cluster (0.15-0.3 mm across) of labeled LGN neurons. The part of the visual field represented by such a cluster corresponds with the area included in the cortical injection site[4,5], thus the injection site boundaries delineate the effective site of uptake.

Retrograde transport was obtained after 12-hour survival times, improved over 48 hours, and remained completely unchanged even 10 weeks post-injection.

The results of injections in A17, typically including layer IV and parts of layer II/III, were compared with published HRP labeling, a non-pathway selective tracer[3]. The known connections of rat A17[7] were all labeled, suggesting that microsphere uptake and transport is not selective for specific neuronal pathways. These injections also labeled a previously undescribed set of intrinsic connections within A17. When the injection site was about 150 μm in diameter, labeling was seen immediately surrounding the injection site; in layer V, retrogradely labeled cells were spread over an area about five times the diameter of the injection site. Upper layer VI was generally free of labeling. In sharp contrast to this, cells in lower layer VI were found in an area about ten times the diameter of the injection site (Fig. 1b). The lateral extent of labeled

cells in layer V and lower layer VI indicates that these neurons have widespread lateral axonal connections (Burkhalter and Katz, unpublished observations), consistent with the morphology of some layer V and VI cells in cat A17[6]. Label in the extrastriate visual areas 18a and 18b included layers II-VI. Subcortical labeling was observed in the ipsilateral LGN (Fig. 1d) and in the lateral posterior thalamic nucleus. Microspheres are transported by broken axons as well. Injections into the corpus callosum resulted in many densely labeled pyramidal cells in layers II/III, V, and VI throughout the cortex (Fig 1e). In one experiment, instead of injecting the corpus callosum, 4 μl of microspheres were placed on top of it, which produced no retrograde labeling. This suggests that while severed fibers take up and transport microspheres, unbroken fibers of passage do not.

In all labeled neurons, label, confined to the cytoplasm, filled the soma and the proximal dendrites (Fig. 1c,d,f) with a granular fluorescence, leaving nuclei unlabeled.

All structures which contained retrogradely labeled cell bodies are reciprocally connected to A17[7,8], but close examination failed to reveal any evidence of anterograde labeling. The same negative result was found in the superior colliculus, a known target of layer V pyramidal cells[9]. Thus, at the level of the light microscope, microspheres are an exclusively retrograde tracer.

Retrograde labeling of cat A17 pyramidal cells, combined with an in vitro brain slice preparation was used to study the morphology and distribution of the dendritic and axonal arbors of LGN[10] and claustrum[11] projecting cells co-localized within layer VI. Three days after injections of either the LGN or claustrum, slices of area 17 were prepared and microsphere labeled cells were intracellularly injected with lucifer yellow (Fig. 1 legend). Fifty LGN projecting cells (in 4 cats) and 30 claustrum projecting cells (3 cats) were analyzed. All the double labeled neurons showed normal resting, synaptic, and action potentials

whose size (x=45 ± 5 mV versus 42 ± 5mV) and time course was indistinguishable from unlabeled neurons. Morphologically, the double labeled cells showed no evidence of degeneration in axons, dendrites, or dendritic spines (Fig 1f). Thus, microspheres did not have obvious toxic effects, and intermittent illumination with rhodamine excitation wavelengths in vitro for several minutes did not seem harmful. Comparison of these two efferent projection classes revealed striking differences in the laminar distribution of dendritic and intrinsic axonal arbors (Fig. 2). Claustrum projecting cells have roughly half the number of basal dendritic arms (3-5) compared to LGN projecting cells (6-8). The apical dendrites of claustral cells reach to layer I with branches in layers VI and V only; LGN projecting cells branch in VI, V, and IV, but do not reach above layer III. Finally, all claustral projecting cells had fine, horizontally directed axonal collaterals that extended for up to 1 mm in layer VI. In contrast, LGN projecting neurons had very few axon collaterals within layer VI, but thick, ascending processes which terminated in layer IV. These two classes therefore not only receive different afferent inputs via different dendritic patterns, but their non-overlapping intrinsic axon patterns indicate participation in distinct circuits within A17, which may be involved in the extraction of feedback (to the LGN) and feedforward signals (to the claustrum).

The mechanism(s) by which microspheres get taken up and transported are unknown. However, not all latex microspheres are retrogradely transported. Experiments with coumarin labeled carboxy-activated (0.05 μm diameter) or plain polystyrene (0.1 μm diameter) microspheres (Polysciences) produced no observable labeling; neither did larger diameter microspheres (>0.2 μm) of the type described herein. Thus, both the size and surface properties[12] may play a role. Latex microspheres can bind many antibodies non-covalently (which is the basis of most latex particle agglutination tests[13]); possibly microspheres below a

certain size can enter synaptic clefts, and interactions between non-specific synaptic determinants and reactive groups on the bead's surface could trigger an endocytotic event[14] (endocytosis of latex particles by many cells, including amoebae[15] and platelets[16] is well-known). Endocytotic vesicles containing microspheres may then be transported by fast retrograde transport[17]. The uptake by broken fibers may be explained by the formation of growth cones at the proximal ends of severed axons[18], followed by internalization and subsequent retrograde transport of microspheres bound to membrane components[19]. Microspheres are probably transported packed in vesicles, since naked latex microspheres with similar negative charge move only in the anterograde direction when injected directly into axons[12]. This, however, does not rule out vesicle bound anterograde transport of beads, which may have remained undetected[20].

The resistance of these rhodamine-labeled microspheres to fading under illumination, and their non-phototoxicity within cells are probably related, since the relationship between bleaching time and killing time is usually linear[21]. Both photodynamic damage and bleaching depend on the presence of molecular oxygen[22] and probably results from the formation of free radicals. Hydrophobic polymers (such as styrene), by restricting the access of molecular oxygen to the rhodamine dye in the interior of the microspheres, could greatly attenuate the formation, and resultant phototoxicity of destructive free radicals.

These microspheres exhibit a variety of characteristics available in very few tracers. The highly restricted injection sites, the compatibility with all known retrograde and anterograde tracers and with immunocytochemical procedures (Burkhalter, Baughman and Katz, in prep.) makes microspheres particularly useful for the study of local circuitry within or between brain areas. The exceptionally long stability of this label makes it attractive for

developmental studies on the reshaping of patterns of axonal connections and as a marker in transplantation studies. The most outstanding property of this tracer, however, is that the viability of neurons is unaffected by transported microspheres. Fluorescent microspheres can therefore be used for in vitro studies of identified projection neurons, and their role in cortical circuits. Preliminary experiments indicate that bead labeling can also be used as a marker for dissociated neurons in culture which were sorted in a fluorescence activated cell sorter (Huettner and Baughman, personal communication).

Although numerous approaches exist for identifying neuronal cell classes, very few of those presently available can be used to study living cells. Recently a specific cell surface marker has been used to study, in vitro, the physiology of identified neurons in culture[23]. The approach described here may provide an attractive alternative for the visualization and physiological study of projection neurons.

We are grateful to Drs. M. Konishi and D. Van Essen for their lab facilities and support, and to Drs. J. Nerbonne and J.P. Revel for electron microscopic analysis of the microspheres. This work was supported by grants from the Caltech President's Venture Fund (to M. Konishi) and the Swiss National Foundation (A.B.), and an NSF predoctoral Fellowship (L.C.K.).

Figure Legends

Figure 1. Retrograde labeling by fluorescent rhodamine latex microspheres. A. Injection site, less than 100 μm diameter, produced by injection of 0.02-0.05 μl of microsphere suspension into layer IV of rat visual cortex. B. A patch of cells in layer VI in area 17, at the grey/white matter border, labeled after an injection approximately 400 μm away that included layers III and IV. C. Labeling of layer V pyramidal cells in area 18b after area 17 injection. Note labeling of apical and basal dendrites, low background, and distinctive granular appearance of label. D. Lateral geniculate nucleus labeling after an area 17 injection. E. Dense retrograde labeling of pyramidal cells in layers II/III after corpus callosum injection, indicating transport by broken axons. F. LGN projecting neuron in layer VI of A17 from a cat in vitro cortical brain slice preparation, retrogradely labeled with microspheres and intracellularly injected with lucifer yellow; the soma, dendrites and dendritic spines appear normal. Inset: Single exposure micrograph of microsphere labeled soma. Scale bars: A, 100 μm; B,C,D,F, 20 μm; E, 50 μm.

Methods: An aqueous suspension of rhodamine-labeled fluorescent microspheres, was obtained from International Diagnostics Technology, Palo Alto, CA (Dr. Boyse Burge, Director of Research). Anesthetized rats were injected with 0.02 to 0.1 μl of bead suspension using a glass pipettes with 30-50 μm tip diameter. After survival times of 24 to 72 hours, rats were reanesthetized and perfused with phosphate buffer (0.1 M) followed by 4% paraformaldehyde in 0.1 M phosphate buffer (pH 7.4) (glutaraldehyde can be used as a fixative, however the resulting higher background may make bead labeling more difficult to discern). After the brains sank in 30% sucrose in buffer, 30 μm sections were cut on a

freezing microtome, collected in phosphate buffer, mounted on gelatinized slides and either air dried or inspected wet. Brief dehydration (30 sec, 100% ethanol, after air drying), followed by clearing in xylene (60 sec) and mounting in Fluoromount (Gurr) or Krystalon (Harleco) often improved the visibility of label significantly. However, longer exposures to ethanol, and in particular to xylenes, causes serious deterioration of the bead fluorescence. Observations were made using a rhodamine filter combination (Zeiss filters, exciter BP 510-560, beam splitter FT 580, barrier LP 590) on an epifluorescence equipped microscope. Labeled neurons are readily visible in sections prepared over a year ago, stored either dry in the dark or unmounted in 4% formaldehyde in phosphate buffer at $4^{o}C$.

Cat cortical slices (400 μm thick, coronal sections) were prepared and maintained using essentially standard hippocampal slice techniques[24]. For intracellular recording and staining, slices were transferred to a chamber on the stage of an epifluorescence equipped compound microscope. Microsphere labeled cell bodies can be seen in living tissue even at low magnifications (100X or 160X). Cells in layer VI were impaled with micropipettes filled with 20% Lucifer yellow (Aldrich) in 0.1 M LiCl (final resistance 100-150 MΩ). Neurons with stable resting potentials and action potentials of at least 35 mV amplitude were filled with dye by passing hyperpolarizing current pulses (3 nA, 200 msec, 4 Hz, 1-10 minutes). Slices were fixed in phosphate buffered 10% formalin for at least two hours and processed as described for brain sections (except that the sections were 60 μm thick).

Figure 2. Camera lucida drawings of claustrum (A) and lateral geniculate nucleus (B) projecting neurons in cat area 17, obtained as described in the Fig. 1

legend and in the text. The numerals refer to laminar boundaries. Claustrum projecting cells had a thick, often asymmetric basal dendrite, in contrast with the compact, symmetric arbor of LGN projecting cells. The apical dendritic side branches of these two projection classes have terminate within different laminae. Most conspicuously the claustrum projecting cells, as in (A), had thin, horizontally directed intrinsic axonal collaterals, which remained within layer VI. The LGN projecting cells, as in (B), had few horizontal collaterals in VI, but sent thick ascending collaterals to layer IV, in which they terminated.

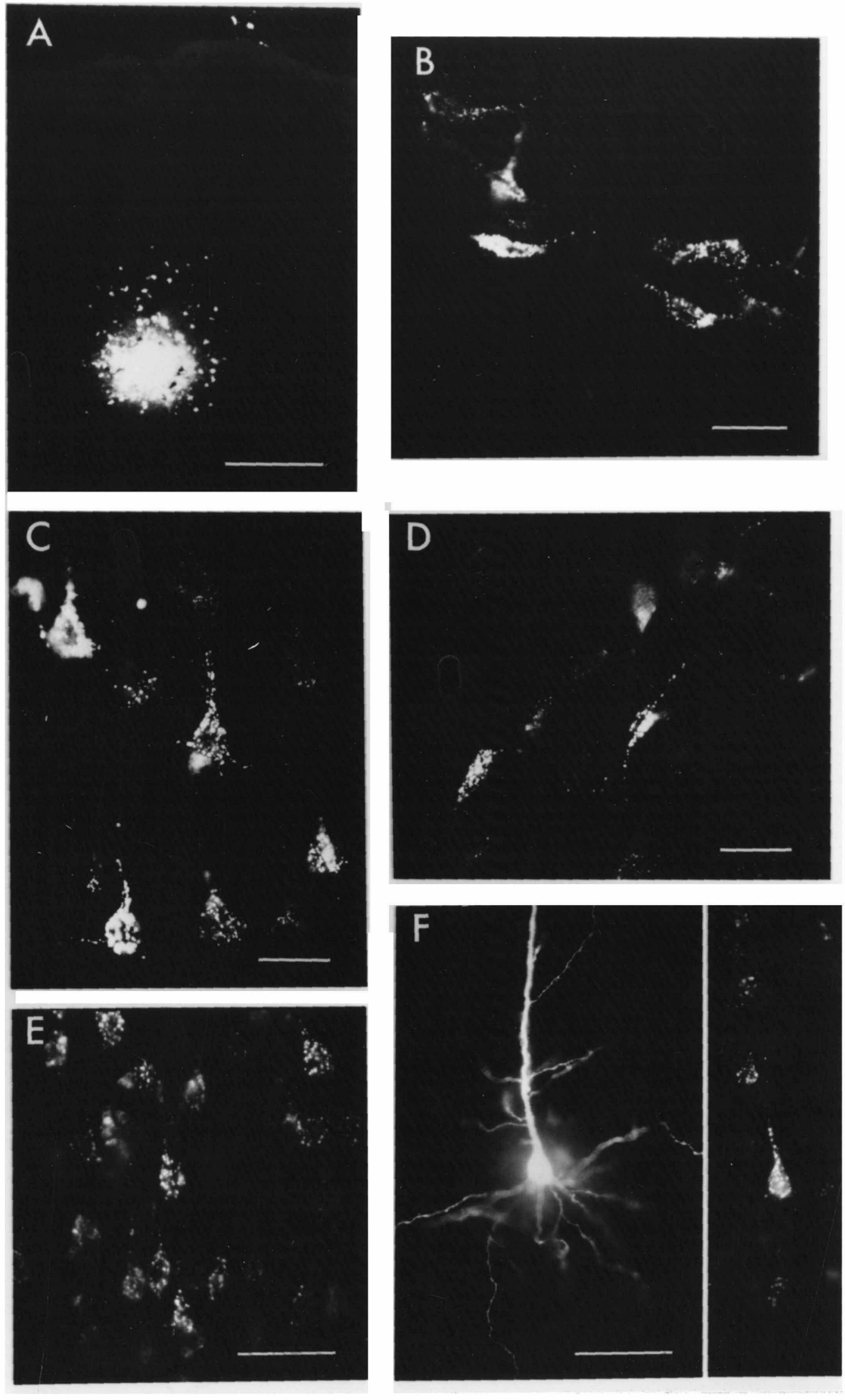
A
B
C
D
E
F

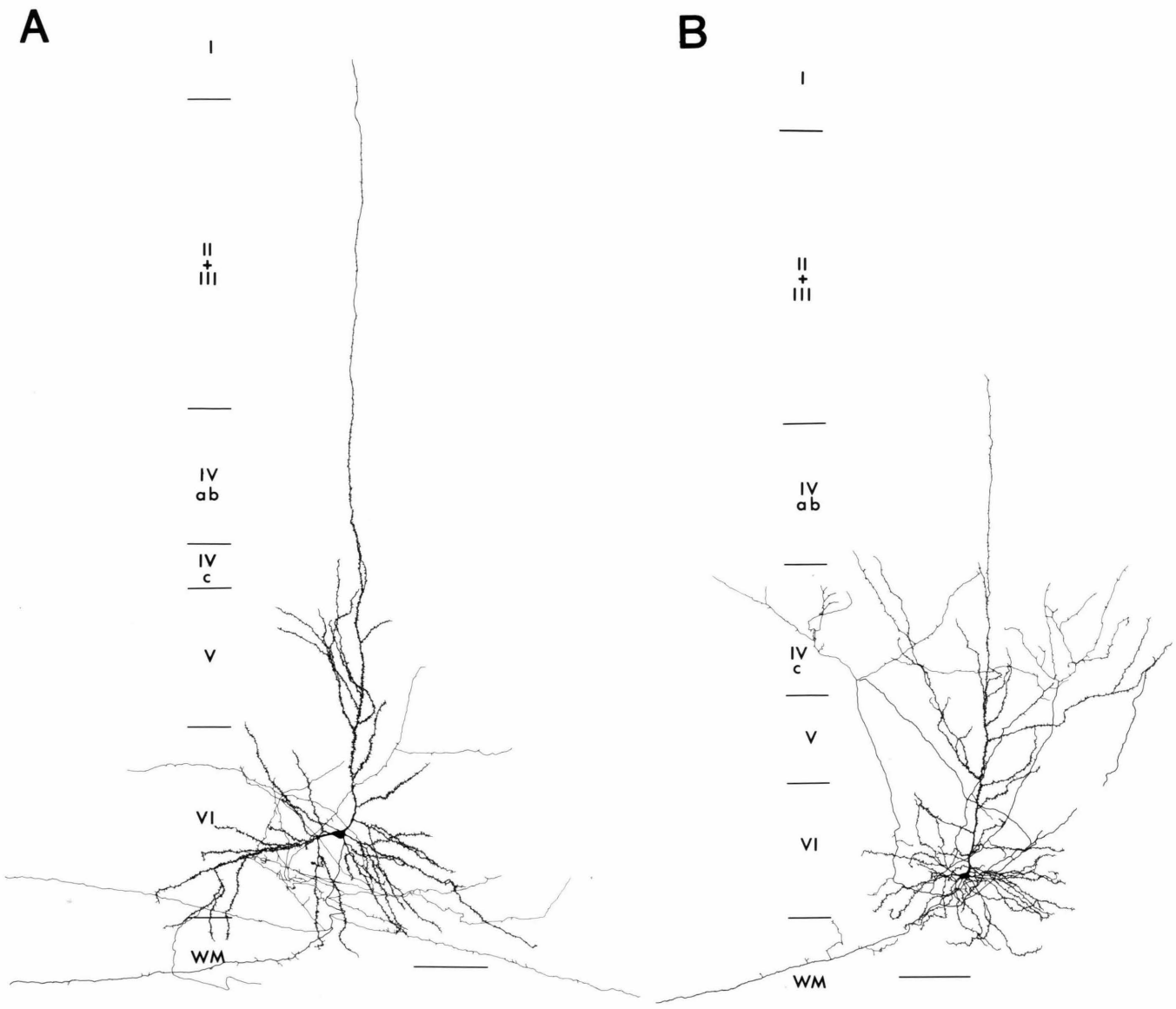
A
I
II
+
III
IV
ab
IV
c
V
VI
WM
B
I
II
+
III
IV
ab
IV
c
V
VI
WM

References

1. Jones, E.G. & Hartman, B.K. in Ann. Rev. Neurosci. (Annual Reviews, Palo Alto, 1978).
2. Aschoff, A. & Hollander, H. J. Neurosci. Meth. 6:179-197 (1982).
3. Mesulam, M-M. ed. Tracing Neural Connections with Horseradish Peroxidase (Wiley-Interscience, New York, 1982).
4. Montero, V.M., Brugge, J.F., & Beitel, R.E. J. Neurophysiol. 31:221-236 (1968).
5. Montero, V.M., Rojas, A., & Torrealba, F. Brain Res. 53:197-201 (1979).
6. Gilbert, C.D. & Wiesel, T.N. J. Neurosci. 3:1116-1133 (1983).
7. Miller, M.W. & Vogt, B.A. J. Comp. Neurol. (in the press).
8. Lent, R. J. Comp. Neurol. 206:227-242 (1982).
9. Sefton, A.J., Mackay-Sim, A., Baur, L.A., & Cottee, L.J. Brain Res. 215:1-13 (1981).
10. Gilbert, C.D. & Kelly, J.P. J. Comp. Neurol. 163:81-106 (1975).
11. LeVay, S. & Sherk, H. J. Neurosci. 1:956-980 (1981).
12. Adams, R.J. & Bray, D. Nature 303:718-720 (1983).
13. Milgrom, F., & Golstein, R. Vox Sang. 7:86-88 (1962).
14. Gonatas, N.K., Kim, S.U., Stieber, A., & Avrameas, S. J. Cell Biol. 73:1-13 (1972).
15. Korn, E.D., & Weisman, R.A. J. Cell Biol. 34:219-227 (1967).
16. Movat, H.Z., Weiser, W.J., Glynn, M.F., & Mustard, J.F. J. Cell Biol. 27:531-543 (1965).
17. Schwab, M.E. & Thoenen, H. J. Cell Biol. 77:1-13 (1978).
18. Aguayo, A.J., Benfy, M. & David, S. Birth Defects 19:327-340 (1983).
19. Carbonnetto, S. & Argon, Y. Dev. Biol. 80:364-378 (1980).

20. Brady, S.T. & Lasek, R.J. Science 218:1127-1131 (1982).

21. Gupta, R.K., Salzberg, B.M., Grinvald, A., Cohen, L.B., Kamino, K., Lesher, S., Boyle, M.B., Waggoner, A.S., & Wang, C.H. J. Membrane Biol. 58:123-137 (1981).

22. Salzberg, B.M. in Current Methods in Cellular Neurobiology vol. III, Barker, J.C. & McKelvig, J.F. eds. pp. 139-187 (1983).

23. Kettenmann, H., Weinrich, M., & Schachner, M. Neurosci. Lett. 41:85-90 (1983).

24. Dingledine, R., Dodd, J., & Kelly, J.S. J. Neurosci. Meth. 2:323-362 (1980).

APPENDIX

Auditory Responses in the Zebra Finch's Motor System for Song

(publication by L. C. Katz and M. E. Gurney)

Brain Research, 211 (1981) 192–197
Elsevier/North-Holland Biomedical Press

Auditory responses in the zebra finch's motor system for song

LAWRENCE C. KATZ and MARK E. GURNEY*

Division of Biology 216-76, California Institute of Technology, Pasadena, California 91125 (U.S.A.)

(Accepted May 14th, 1981)

Key words: songbird — hyperstriatum ventrale pars caudale — auditory — intracellular recording — intracellular HRP-staining

Vocal learning in songbirds is critically dependent on auditory information. Intracellular electrophysiological recordings, combined with horseradish peroxidase staining of single cells has revealed neurons within one central nervous system vocal control nucleus, hyperstriatum ventrale, pars caudale (HVc) that show responses to auditory stimuli. Auditory and non-auditory neurons fall into distinct morphological classes, based on soma size, dendritic field structure, and efferent projections. The neurons described may play a role in conveying auditory information into the vocal control system.

The development and maintenance of song in oscine birds shows two components: auditory acquisition of a song model, and vocal learning of the motor program for song[3]. Because vocal learning depends upon the bird using auditory feedback to match his own vocal output against his memory of the song model[3], auditory information must be accessible to the motor system controlling song. The vocal control system includes at least three telencephalic nuclei: the hyperstriatum ventrale, pars caudale (HVc), the nucleus robustus archistriatalis (RA), and Area X. HVc is afferent to RA, which in turn projects onto the motor neurons of the hypoglossal nucleus which innervate the syrinx, the avian vocal organ. Lesion of either HVc or RA produces a deficit in song[6]. We now report the discovery of neurons within HVc of the zebra finch (*Poephilia guttata*) which respond to auditory stimuli, as demonstrated by using intracellular recording and horseradish peroxidase (HRP) staining of single neurons.

Microelectrodes were pulled from 1.2 mm capillary tubing (Omega–Dot, Frederich Haer Co.), backfilled 18–24 h before an experiment with 8 % horseradish peroxidase (w/v, Boehringer–Mannheim grade I) in 0.5 M KCl buffered with Tris (0.1 M) to pH 7.4, and had resistances of 150–200 MΩ. Adult male zebra finches were anesthetized with 0.10 to 0.13 ml of 20% (w/v) urethane (Sigma) and held in a stereotaxic apparatus which was equipped with hollow ear bars for conveying the auditory stimuli to the bird's ears. The electrode was manually advanced using a

*Present address: Department of Pharmacological and Physiological Sciences, University of Chicago, Chicago, Ill. 60637, U.S.A.

Narishige microdrive (model SM-20) and penetration of neurons was facilitated by applying a series of square voltage pulses (40 V, 200 ms duration, 4 Hz) to the electrode. Successfully penetrated cells showed stable resting potentials of —30 to —60 mV, and action potentials of 30–80 mV with a half-height duration of approximately 2 ms. Approximately one minute after penetration such cells were presented with auditory stimuli consisting of noise or tone bursts of 30–50 dB SPL and 400 ms duration at a rate of one per second. Cells were held anywhere from 5–40 min, and data were collected throughout this time. Data collection ceased when a cell was either abruptly lost, or began to show signs of deterioration (i.e. decreased action potential height, greatly lengthened spike duration, or noticeable loss of resting potential). Usually only one cell per electrode track was filled with HRP by passing trapezoidal 5-nA current pulses (200 msec duration at 4 Hz) for 5–15 min. At the end of the experiment, the bird was perfused with phosphate buffer (0.13 M) followed by fixative (1.25% glutaraldehyde, 1% formaldehyde in 0.13 M phosphate buffer). The brain was

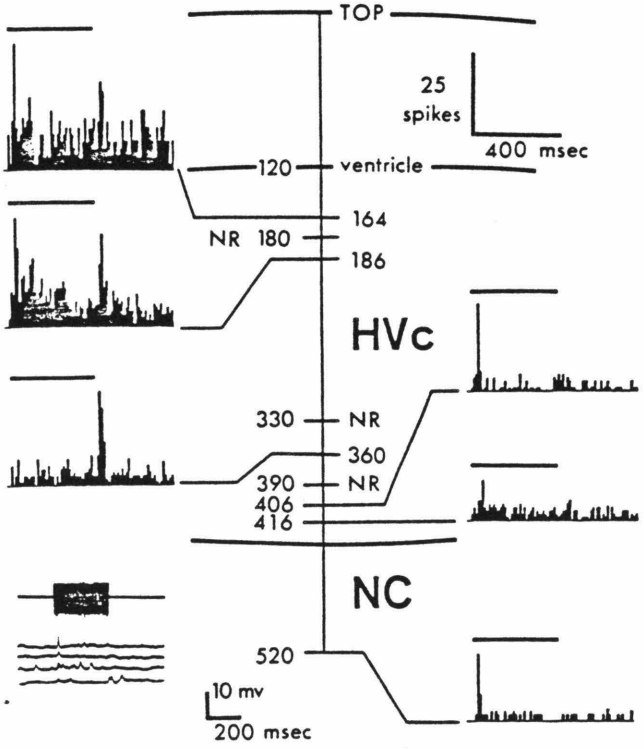

Fig. 1. Neuronal responses along an electrode penetration through HVc. All of the auditory neurons encountered on this track were phasically excited by the onset and or offset of the noise burst. Post-stimulus-time histograms (10-ms bins, 100 stimulus presentations) of action potentials for each of the intracellularly recorded neurons are shown together with a black bar which indicates the onset and duration of the noise burst (400-ms duration, 30–50 dB SPL intensity). TOP indicates the surface of brain, and the depth of each neuron encountered on the track is given in micrometers. Abbreviations: HVc, hyperstriatum ventrale, pars caudale; NC, neostriatum caudale; NR, no auditory response. Inset at lower left shows recordings obtained from the HVc neuron encountered at a depth of 416 μm. The top trace shows the noise burst, and beneath it are intracellular records of activity during four consecutive stimulus presentations.

removed from the skull and sagittal, 100 μm sections were cut using a vibratome (Oxford). HRP reaction product was demonstrated using the protocol of Mesulam[5].

Our results are based on experiments in 22 adult males, in which we tested 112 neurons for responses to auditory stimuli. Reconstruction of electrode tracks by using the HRP-filled cells as markers of depth revealed that 59 of these neurons were located within HVc. The borders of HVc were easily discernible using either darkfield or polarized light illumination, thus the location of HRP-filledc ells relative to the nucleus could be unambiguously determined. 36 (61 %) of the HVc neurons responded to noise, while 23 neurons (39 %) showed no alteration in either their synaptic activity or their firing rate which correlated to the presentation of the noise bursts. We did not notice any change in response properties of cells over the time during which we were recording data. Responses obtained along one electrode penetration are shown in Fig. 1. Most auditory HVc neurons showed excitation or inhibition apparently correlated with the onset and/or the offset of the noise burst; a few showed a sustained response correlated with the duration of the stimulus. (However, we cannot at this point be certain that sound onset and offset were the actual cues to which the HVc neurons were responding). For example, the two neurons encountered on this track at depths of 164 μm and 186 μm from the brain's surface were phasically excited by both the onset and the offset of the noise burst. Deeper in the same track, at a depth of 360 μm, lay a neuron which was phasically excited by only the stimulus offset. The two auditory neurons deepest in HVc responded only to the stimulus onset. Few neurons fired action potentials in response to each stimulus presentation, as illustrated by the raster plot of consecutive intracellular records in the inset of Fig. 1. This neuron (depth 416 μm) showed an excitatory postsynaptic potential (EPSP) which was timelocked to every stimulus presentation, yet only a minority of these generated action potentials. In general the spontaneous firing rate of auditory HVc neurons was less than 5 spikes/s. This was observed when the bird was anesthetized with either urethane (0.10 ml) or with Equithesin (0.035 ml, Jensen–Salsbery Laboratories) used in some of our preliminary experiments. Leppelsack and Vogt, who studied the responses to species-specific vocalizations by auditory neurons within Field L of awake starlings, found that a low rate of spontaneous activity was correlated with a high degree of selectivity for specific elements within the starlings' vocal repertoire[4]. When we compared the effectiveness of noise to tone bursts between 1 and 4 kHz, at 0.5-kHz steps (this covers most of the zebra finch's audibility range) we failed to find neurons which preferred tone bursts to noise. In many cases, tone bursts were completely ineffective at driving the neurons. The latencies of the excitatory responses to onset of the stimulus were generally 25–40 ms; excitatory responses to stimulus offset had somewhat longer latencies of 35–50 ms. We had the distinct impression that the response patterns (i.e. on/off profiles, latencies) of neurons encountered within 20–30 μm of one another resembled each other more than those of other neurons on the same electrode track. For pairs of cells within 25 μm of one another, 6 had similar response properties, while 4 had different; for pairs more than 25 μm apart, 8 had similar responses, 18 had different. Such a clustering of neurons with similar responses is evident in Fig. 1.

.HVc has two projections, one rostrally to Area X, the other caudally to nucleus

RA. Results obtained thus far indicate that HVc auditory neurons project to Area X, and that the RA projecting HVc cells do not show auditory responses. Of the 36 auditory neurons encountered in HVc, we filled 12 with HRP. Of these, 9 showed sufficient axonal filling to allow us to trace their axons beyond the rostral border of

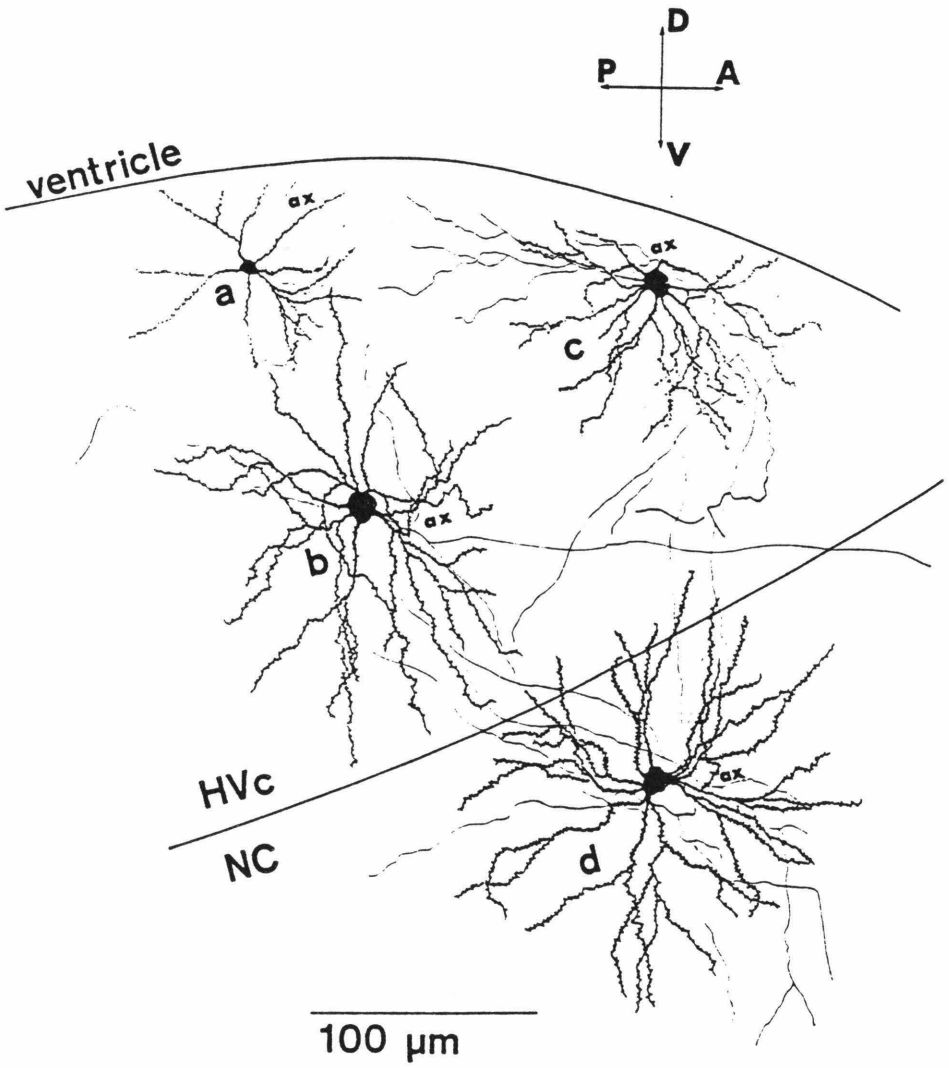

Fig. 2. Light microscopic drawings of horseradish peroxidase-stained neurons. Neuron b is representative of neurons which responded to noise bursts. Its axon could be traced beyond the rostral border of HVc and into the lamina hyperstriatica which carries the projection of HVc to Area X. The neurons labeled a and c did not respond to auditory stimuli. The axon of neuron a could be traced until it exited the caudal border of HVc and entered the tractus dorsalis archistriatalis which carries the projection of HVc to RA. Neurons a and b are each representative of distinct cell types within HVc and are distinguished physiologically by their response (or lack of response) to auditory stimuli, and morphologically on the basis of somatal diameter, dendritic field structure, and dendritic field diameter. Neuron c, like two other neurons which failed to respond to auditory stimuli, possessed a dendritic morphology similar to that of the auditory HVc neurons. The axon of one of these three non-responding neurons could also be traced beyond the rostral border of HVc and into the fiber tract carrying the projection to Area X. The neuron labeled d was located in the NC beneath HVc and responded to auditory stimuli. Its axon arborized dorsally into HVc as well as ventrally into the NC. The distal portions of some of its dorsal dendrites penetrated the lamina hyperstriatica and entered the ventral border of HVc.

HVc and into the fiber tract (lamina hyperstriatica) which carries the projection of HVc to Area X. In two exceptional cases, filled axons could be traced the entire 5-mm distance from HVc to Area X. In addition, the axons of all the Area X-projecting HVc neurons gave off many collaterals which arborized within HVc. Their dendritic morphologies were also similar: dendritic arms were heavily endowed with spines, and branching was strictly dichotomous. Somatal diameters of these neurons ranged from 10 to 15 μm; dendritic fields had diameters of 150–200 μm.

The HVc neurons which did not respond to either noise or tones fell into two classes: RA-projecting HVc neurons and Area X-projecting HVc neurons. The axons of 4 were followed until they exited the caudal border of HVc and entered the fiber tract (tractus dorsoarchistriatalis) carrying the projection of HVc to RA, while 3 had axons which exited HVc rostrally and appeared to project to Area X. The four neurons whose axons went to RA resembled each other in that they all had a somatal diameter of 6–8 μm and supported a sparse dendritic arborization 80–120 μm in diameter. The morphology of these neurons was clearly different from that of the auditory HVc neurons which project to Area X. The other three non-responding neurons, which projected to Area X, had somatal diameters and dendritic arborizations which closely resembled those of the auditory Area X projecting cells. Since we cannot be certain that noise or tone bursts were appropriate auditory stimuli for them, it may be that these neurons were also auditory. Alternatively, there may be two classes of HVc neurons which project to Area X: auditory and non-auditory.

Two additional auditory neurons we filled were within the neostriatum caudale (NC) immediately beneath HVc. This area corresponds to the neostriatal shelf, ventral to HVc, which Kelley and Nottebohm[2] report receives a projection from Field L in canaries. Axonal collaterals from these two cells arborized dorsally into HVc as well as ventrally into Field L. The response properties of one of these neurons (encountered at a depth of 520 μm) is shown in Fig. 1. Its response pattern closely resembles that typical of many HVc neurons. Three such NC cells were recorded. All preferred noise to tone bursts.

The discovery of neurons showing auditory responses in a part of the songbird vocal control system creates the opportunity for conjecture about the possible function of these neurons. Before such conjecture is possible, it will be necessary to ascertain the source of this auditory input. HVc has numerous afferents of unknown function (i.e. Uva and NIF[7]) in addition to neostriatal shelf area. While it appears that some auditory information reaches HVc via the shelf, we do not know if this is the only or one of many, such inputs. Furthermore, while the shelf receives inputs via the 'classical' auditory pathway (i.e. from Field L)[2], the possibility that it receives input from other brain regions cannot be excluded.

The long latencies and low firing rates seen in HVc auditory responses raise the possibility that the response might be some sort of non-specific multi-modal response, for example, a startle response. We strongly believe that this is not the case, since (1) it seems unlikely that only noise, and not tone bursts would be effective in producing the responses, and (2) a startle response would be expected to habituate quickly; our

responses remained unchanged (in terms of EPSP size, or spike frequency) for hundreds of stimulus repetitions presented once a second.

It must be mentioned that Zaretsky[8] claimed to have recorded auditory responses within HVc of zebra finches and canaries. We do not take this claim seriously, however, as he presents no decent histologic evidence for recording within HVc and the auditory responses he claims to have observed are at such great variance from ours that we think it extremely unlikely that he was actually looking at HVc.

Electrical stimulation in HVc elicits electromyographic responses in the syrinx[1], thus implicating the HVc neurons which project to RA as participating in the motor pathway for song. At some level in the brain, the motor program for song must be stored, and at some point reference to auditory feedback is used to modify the motor output (since learning of song requires auditory feedback). Interfaces between auditory pathway(s) and the descending motor pathway for song define the levels in the brain at which the motor output can be modified. An interface may exist in HVc, if the axonal collaterals of the auditory neurons within HVc synapse onto the HVc motor neurons which project in turn to RA.

We thank Dr. M. Konishi for providing research facilities and for calibrating our sound delivery system, and Drs. A. J. Hudspeth, M. Konishi, A. Moiseff, F. Nottebohm and D. Van Essen for their many useful comments on this work.

L.C.K. is supported by a National Science Foundation Graduate Fellowship, M.E.G. by a National Research Service Award (HD05940-01).

1 Arnold, A. P., Anatomical and electrophysiological studies of sexual dimorphism in a passerine vocal control system, *Proc. XVII Int. Cong. Ornith.*, Berlin, in press.

2 Kelley, D. B. and Nottebohm, F., Projections of a telencephalic auditory nucleus — Field L — in the canary, *J. comp. Neurol.*, 183 (1979) 455–470.

3 Konishi, M., The role of auditory feedback in the control of vocalization in the white crowned sparrow, *Z. Tierpsychol.*, 22 (1965) 770–783.

4 Leppelsack, H. J. and Vogt, M., Responses of auditory neurons in the forebrain of a songbird to stimulation with species-specific sounds, *J. comp. Physiol.*, 107 (1976) 263–274.

5 Mesulam, M-M, Tetramethyl benzidine for horseradish peroxidase neurohistochemistry: a non-carcinogenic blue reaction-product with superior sensitivity for visualizing neural afferents and efferents, *J. Histochem. Cytochem.*, 26 (1978) 106–117.

6 Nottebohm, F., Stokes, T. M. and Leonard, C. A., Central control of song in the canary *Serinus canarius*, *J. comp. Neurol.*, 165 (1976) 457–486.

7 Nottebohm, F., Brain pathways for vocal learning in birds: a review of the first 10 years, *Progress in Psychobiology and Physiological Psychology*, Vol. 9 (1980) 85–124.

8 Zaretsky, M. D., A new auditory area of the songbird forebrain: a connection between auditory and song control centers, *Exp. Brain Res.*, 32 (1978) 267–273.